ChemPubSoc Europe

DOI: 10.1002/slct.201500044

Chemistry SELECT Full Papers

Organic & Supramolecular Chemistry

An old dog with new tricks: Schiff bases for liquid crystals materials based on isoxazolines and isoxazoles.

Luma Fritsch and Aloir A. Merlo*[a]

Schiff bases are in action again showing an exuberant mesophase range despite their chemical and thermal weakness. Two series of Schiff bases (SB), based on isoxazolines **9a–f** and isoxazoles **10a–f**, are described. **9a–f** were synthesized by a [3+2] cycloaddition 1,3-dipolar of arylnitrile oxide from *p*-nitrobenzaldehyde (**1**) and alkenes. And, subsequently oxidized to **10a–f** by MnO_2. The isoxazolines and isoxazoles thus obtained were reduced to aniline derivatives and condensed with appropriated arylaldehydes. The SBs series isoxazolines **9a–f** presented a narrow mesophase range, while SBs series isoxazoles **10a–f** showed a large mesophase range. Nematic mesophase was observed for SBs with short and non-polar groups, while SmA and SmC mesophase for SBs with long and more polar terminal groups. The stability of the SBs is also dependent on the clearing temperature. For **10a–f** with high clearing temperature, decomposition induced by heat was observed during the first cycle of heating and in solutions of $CDCl_3$. Series **9a–f** was more resistant to the thermal decomposition.

Introduction

Schiff Bases (SBs) are well-known organic compounds that have been documented for a long time.[1] SBs belong to a group of organic compounds named imines, and their discovery was made by Ugo (Hugo) J. Schiff, one of the founders of modern chemistry.[2] SBs play an important role in many fields of chemistry and related areas. Their importance has extended over many branches of science, including organic synthesis, analytical chemistry, coordination chemistry, biological processes, etc. In liquid crystals (LC) science, SBs have been studied from an academic point of view and for their technological applications. SBs were artists of the history of the discovery and application in LC electro-optic displays (Figure 1). In 1968, George Heilmeier (Radio Corporation of America – RCA) reported for the first time ever the use of SBs in electro-optic displays based on the principle of dynamic scattering mode (DSM). He developed the first liquid crystal display using Schiff base MBBA, with negative dielectric anisotropy.[3] He received the Kyoto Award in 2005 for his discovery. SBs were also again protagonist in a new discovery in the LC field in the early 70's. In 1975, Robert B. Meyer, an American physicist, predicted that a smectic C phase could be ferroelectric if composed of chiral molecules in a tilted smectic mesophase.[4] Meyer et al were able to prove through symmetry criteria that chiral SBs (DOBAMBC) display ferroelectric properties, and later, Clark and Lagerwall developed a display with special architecture, the so-called *bookshelf geometry*, yielding bistable electro-optic effects with several orders of magnitude compared to switching times of several milliseconds in twisted nematic (TN) cells.[5] This achievement opened new opportunities to synthesize and use chiral SmC LC in displays with fast response time to external electric stimulus.[6]

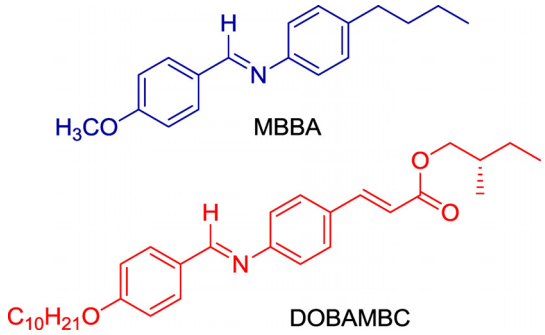

Figure 1. Old and famous Schiff bases in the history[4b] of liquid crystals.

SBs are still present nowadays and fascinate us because of their ability to self-organize and self-assembly. Banana-shaped LC or bent-core LC[7] is a new landmark of LC science where many derived banana LCs form SBs display new and exotic mesophases.[8]

The main drawback of SBs is their inherent chemical, thermal and photo-physical instability, which reduces their potential applications in electro-optic displays.[9] In this way, SBs remains a challenge for chemists in how to prepare new SBs that are stable under the conditions mentioned above. This prompted us to disclose our preliminary results in the preparation of new SB LCs containing isoxazoline and isoxazole rings. The molecular shape of the SBs presented may be regarded as calamitic liquid crystal despite of the bending of the central 5-membered heterocyclic.[9,10] The installation of an isoxazoline or isoxazole ring combined with an imine group into a mesogenic core provides a lateral dipole located on nitrogen atoms and a

[a] *MSc L. Fritsch , Prof. A. A. Merlo*
Chemistry Institute, Universidade Federal do Rio Grande do Sul (UFRGS)
Av. Bento Gonçalves 9500, CEP 91501970, Porto Alegre, Brazil
www.iq.ufrgs.br/lasomi
E-mail: aloir.merlo@ufrgs.br

Supporting information for this article is available on the WWW under http://dx.doi.org/10.1002/slct.201500044

bend of their long molecular axes.[11] Our previous synthesis work related to the design of new molecular architecture has shown that isoxazolines and isoxazoles serve as platforms for new liquid-crystalline materials.[12] In this work, our approach is addressed to straighforward synthesis of key intermediate arylamine derived from 3,5-disubstituted isoxazolines and 3,5-disubstituted isoxazoles and them to transform into a new series of Schiff base LC compounds.

Results and Discussion

The synthetic route to prepare Schiff bases is outlined in Schemes 1, 2, 3, and 4. The starting materials for all final compounds are commercial aldehyde **1** and *p*-substituted styrenes **3a–c.** The critical step is the preparation of intermediates **4a–c**, which were synthesized by [3 + 2] 1,3-dipolar cycloaddition between 1,3 dipole nitrile oxide and alkenes. Thus, isoxazolines **4a–c** are key intermediates for accessing new anilines to be exploited in the field of liquid crystals. In this work, oxime **2** is the precursor for reactive nitrile oxide obtained by oxidation using an aqueous solution of sodium hypochlorite (NaOCl, 5%).[13] The reactive 1,3 dipole was added to styrenes **3a–c** to give isoxazoles **4a–c** in good yields. Usually, isoxazolines are produced by oxidation using NCS as the oxidant[14] instead of an aqueous solution of NaOCl. The synthesis is outlined in Scheme 1. After

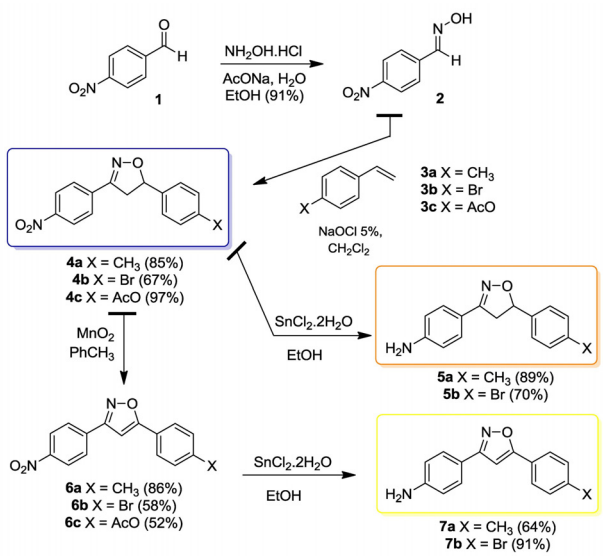

Scheme 1. Synthesis of the precursors isoxazolines **5a–b** and isoxazoles **7a–b.**

accomplishing the synthesis of **4a–c**, two more steps were needed: (i) reduction of the nitro group by tin(II)chloride dehydrate,[15] and (ii) oxidation of isoxazoline to isoxazole mediated by manganese dioxide[16], applied so that we could access 4,5-dihydroisoxazolylanilines **5a–c** and isoxazolylanilines **7a–c.** Despite the non-planar shape of the isoxazolines, compounds **5a–c** might be a component of liquid crystals as we have checked in previous works on similar isoxazolines.[12,17]

Scheme 2 describes the synthesis of linear alkylated isoxazoline **5d** and isoxazole **7d** by hydrolysis of the acetate

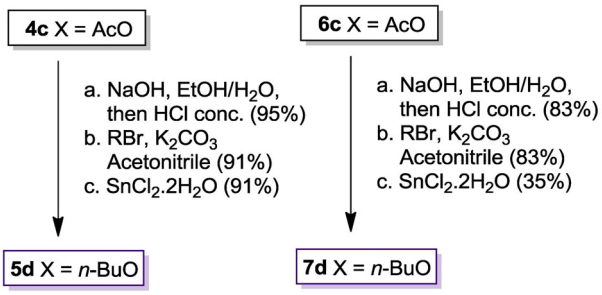

Scheme 2. Synthesis of linear alkylated isoxazoline **5d** and isoxazole **7d.**

group under basic conditions followed by alkylation with *n*-butyl bromide. The subsequent reduction step, as mentioned with the other intermediates described in Scheme 1, gave the intermediate **5d** with a yield of 91% and **7d** in low yield (35%).

The preparation of Schiff bases is described in Schemes 3 and 4. In Scheme 3, the series of Schiff bases **9a–d** and **10a–d**

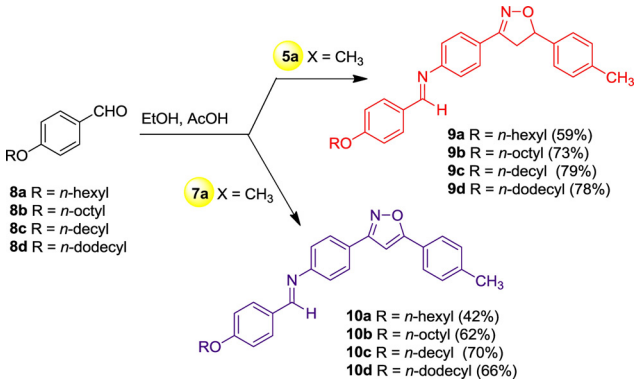

Scheme 3. Schiff bases **9a–d** and **10a–d**series preparation.

containing the less polar group methyl (CH_3–) are shown and were synthesized by condensation reaction of selected aldehydes **8a–d**[18] with anilines **5a** and **7a**, respectively. The Schiff bases were isolated as a solid powder after two or more crystallizations in ethanol, followed by filtration of the imine solution in DCM by Millipore filters. The yields of final imines are dependent on how many cycles of filtration were done to remove dusts, papers fibers, etc from the solution.

Four more polar Schiff bases containing bromine (Br–) **9e–f** and *n*-butyloxy (*n*-BuO–) **10e–f**, groups were also synthesized as described in Scheme 4. Anilines **5b**, **5d**, **7b** and **7d** were condensated with aldehyde **8b** to give Schiff bases **9e**, **9f**, **10e** and **10f**, respectively. Isolation and purification of the final compounds were done the same way as described above.

The major problem associated to the Schiff bases is their unstable behaviour under solution and when they undergo thermal and photochemical analysis.[19] In this study, all data

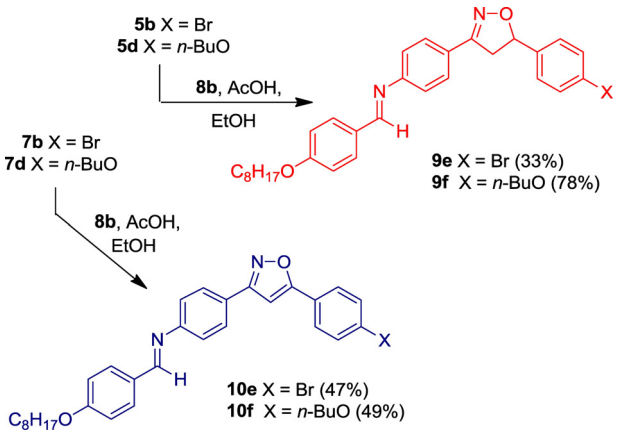

Scheme 4. Schiff bases **9e–f** and **10e–f** series preparation.

which is the result of the partial hydrolysis of the samples when left at room temperature for a long period of the time.

All synthesized Schiff bases displayed enantiotropic liquid crystalline behaviour. Transitional properties were acquired by Differential Scanning Calorimetry (DSC) and mesophase textures were analyzed by Polarized-light Optical Microscopy (POM). Data obtained from DSC and POM was found to be very similar in this study. For all isoxazolines, the DSC data was collected during the second heating cycle. However, DSC data of all isoxazole data was acquire during the first cycle upon heating. As evidenced by changes in the DSC profile during the first cycle upon cooling, and by visual observation of the samples under POM, they showed thermal decomposition during the first cycle of heating. To the isoxazoles series, the clearing temperature was obtained by DSC because the value is too high to be observed by POM.

Table 1. Phase transition temperatures (°C) and enthalpy (kcal/mol) for molecules **9a–f** and **10a–f.**

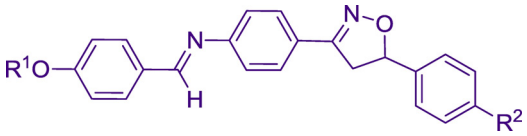

Entry	R^1	R^2	Cr_1		Cr_2		SmC		SmA		N		I
9a	C_6H_{13}	Me	•	143(8.70)	•	-	•	-	•	[135]*	•	159(0.10)	•
9b	C_8H_{17}	Me	•	132(3.60)	•	140(2.40)	•	-	•	149(0.20)	•	155(0.13)	•
9c	$C_{10}H_{21}$	Me	•	131(4.00)	•	138(2.10)	•	-	•	155(0.90)	•	-	•
9d	$C_{12}H_{25}$	Me	•	135(8.30)	•		•	-	•	154(1.60)	•	-	•
9e	C_8H_{17}	Br	•	161(8.60)	•	-	•	-	•	186(2.00)	•	-	•
9f	C_8H_{17}	*n*-BuO	•	138(5.80)	•	-	•	158(0.90)	•	-	•	-	•

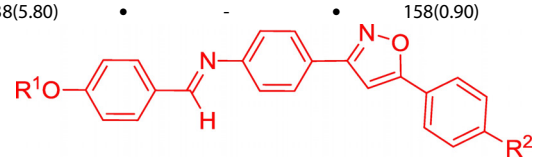

10a	C_6H_{13}	Me	•	143(7.60)	•	-	•	–	•	–	•	287(0.12)	•
10b	C_8H_{17}	Me	•	141(8.80)	•	-	•	–	•	–	•	278(0.17)	•
10c	$C_{10}H_{21}$	Me	•	125(5.60)	•	-	•	[140]*	•	–	•	253(0.11)	•
10d	$C_{12}H_{25}$	Me	•	107(11.40)	•	127(10.20)	•	178(0.10)	•	–	•	255(0.27)	•
10e	C_8H_{17}	Br	•	137(12.90)	•	-	•	-	•	301(1.20)	•	-	•
10f	C_8H_{17}	*n*-BuO	•	84(2.60)	•	122(4.00)	•	248(0.28)	•	-	•	-	•

Scan rate: 10 °C min^{-1} for all samples; Cr denotes Crystal phase; SmC=Smectic C phase; SmA=Smectic A phase and N=Nematic phase. *Monotropic SmA and SmC mesophase observed by POM on cooling are in brackets; The transition temperatures and enthalpy values were collected from a second heating scan to the isoxazolines-BS and the first cycle for the isoxazole-BS.

from NMR analyses were acquired from freshly prepared samples. Samples kept in solution for a long time have shown the well-known behaviour where solvolysis took place through analysis and interpretation of the their ^{1}H NMR spectrum solution in $CDCl_3$. Interestingly, imines which have an isoxazoline ring are less prone to hydrolysis in solution at room temperature than imines containing an isoxazole ring. Thermal degradation will be discussed in the liquid properties topics below. Figure 2 shows the partial ^{1}H NMR spectrum of **10c** in a solution of $CDCl_3$. A signal at 8.5 ppm is assigned to iminic hydrogen and at 10.0 ppm is attributed to benzaldehyde. Absence of this signal reveals that the samples are stable in a solution of $CDCl_3$. However, the signal at 10.0 ppm becomes visible and more intense to the spectrum recorded from time to time,

The transition temperatures, enthalpy values and mesophase sequences of Schiff bases **9a–f** and **10a–f** are presented in Table 1. A bar graphic is also presented for all Schiff bases in this study (Figure 3) to get a better view of their mesophase nature (distribution) as well as the temperature range of the mesophase for each Schiff base. A general overview is presented looking at data from Table 1 and the bar graphic in Figure 3. For all SBs, the temperatures at which the crystal melts to mesophase begin around 120 °C. For example, **10c** displays a transition of the crystal phase to liquid crystal mesophase at 125 °C, which is the smaller transition temperature to the crystal phase → mesophase observed in the two homologous ser-

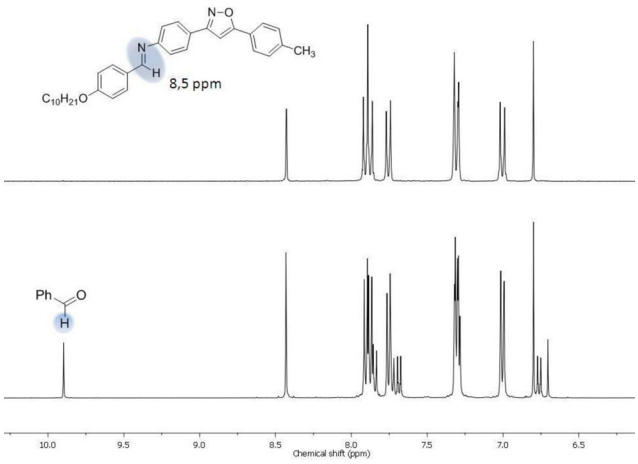

Figure 2. ^{1}H NMR spectrum solution in $CDCl_3$ (300 MHz) of Schiff base **10c** from fresh solution (top) and old solution (bottom).

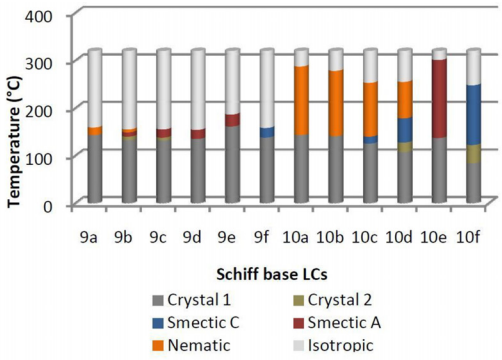

Figure 3. Bar graphics for Schiff base liquid crystals **9a–f** and **10a–f.**

ies. Total mesophase range for SBs containing an isoxazoline ring is smaller than SBs having an isoxazole ring, and the clearing temperatures of SBs **10a–f** are higher than those of SBs **9a–f.** The predominance of a nematic mesophase is observed for members with small alkyl chains and X=CH_3 group. Members with long alkyl chains favor the appearance of a layered mesophase (SmA and SmC). For SBs with a terminal polar group (X=Bromine) and with two alkyl chains as the terminal group, smectogenic behaviour is favored. For both series **9a–f** and **10a–f**, the nematic mesophase is present in the members with a small number of carbon atoms. Nematic behaviour disappears gradually with the increase of carbon atoms in the alkyl chain, while smectic mesophase emerges. Transition between crystal phases were observed for both series as evidenced by sharp and intense peaks as seen in DSC thermograms. The last two members **10e** and **10f** display typical smectogenic behaviour, as expected. The texture of the mesophase[20] was identified by microscopy studies on cooling from the isotropic liquid state of the samples.

Textures for SB **9a–d** are shown in Figure 4. Upon cooling from isotropic phase, **9a** enters into enantiotropic nematic phase with a bright schlieren texture, and a few seconds after, the homeotropic texture (black areas) appears quickly and remains while the mesophase persists. This means that the long molecular axes of the rod-shape of molecules are positioned perpendicular to the glass. Pressing the cover slips gently, we can induce the oscillation of the molecules, and visually the samples flash spontaneously. Upon cooling at 135 °C, a monotropic transition from nematic to smectic A is seen through POM. The texture is still homeotropic, but we can no longer see the flashes and the sample becomes more viscous. **9b** presents two more carbon atoms in the terminal alkyl chain and its mesomorphic profile is similar to that of **9a.** The transition to smectic A mesophase now appears at DSC traces, and the mesophase range is 9 °C. For **9c** and **9d**, nematic mesophase is absent and only smectic A is seen, with a mesophase range of 17 °C and 19 °C, respectively. Figure 4c and 4d show fan focal-conic and homeotropic textures of SmA mesophase. The next two SBs **9e** and **9f** present bromine and *n*-butoxy, respectively. For **9e**, orthogonal SmA mesophase was observed with fan focal-conic and homeotropic textures (black areas), while **9f** displayed a tilted SmC mesophase with broken focal conic texture and Schlieren texture (gray color) upon cooling.

Thermal data from the second series of SBs **10a–f** in Table 1 reveals how efficient the isoxazole ring is in the formation and stability of the mesophases. In general, mesophase tendency of SBs **9a–f** and **10a–f** is similar, with a predominance of a nematic mesophase for the first members and a smectic mesophase for the last members. However, the range of mesophases of SBs containing an isoxazole ring is much bigger than SBs containing an isoxazoline ring. Transition temperature from crystal phase to mesophase is very close for both series, while clearing temperature is quite different. For example, the first members of series **9a** and **10a** enter nematic mesophase at 143 °C, and they enter an isotropic state at 159 °C and 287 °C, respectively. This means that the temperature range of the nematic mesophase is much wider for isoxazole SBs than isoxazoline SBs. For **10a**, the range is $\triangle T = 144$ °C, while for **9a** $\triangle T = 16$ °C, and consequently, mesophase for **10a–f** is more stable than for **9a–f.** Moving up to the superior members **10b, 10c** and **10d**, the nematic mesophase range tends to be smaller. In this way, $\triangle T_{N-I}$ is 144 °C, 137 °C, 128 °C and 77 °C, for **10a**, **10b**, **10c** and **10d**, respectively. To compensate for the shortening of the nematic mesophase range, smectic C mesophase appears for **10c** (monotropic) and enantiotropic for **10d** with $\triangle T_{SmC-N}$ of the 51 °C. It is interesting to note that the total mesophase ranges of **10c** and **10d** are the same (128 °C) if we take into account the transition from crystal phase 1 to isotropic phase. The same conclusion is also observed for smectogenic SBs **10e** and **10f** with 164 °C of the total mesophase range. Of course, the clearing temperature and transition from crystal 1 to mesophase are not the same.

Figure 5 display the micrographs of the textures of N and SmC mesophases for SBs **10c** and **10d.** When the sample of **10c** is cooled from its isotropic phase, the nematic phase appears, exhibiting a planar thread-like texture, which is characteristic of a liquid-crystalline nematic phase.[21] Upon cooling, droplets form, which grow and then coalesce to planar texture as shown in Figure 5a and 5b, indicating a nematic phase due to the parallel orientation of molecules to the glass substrate.

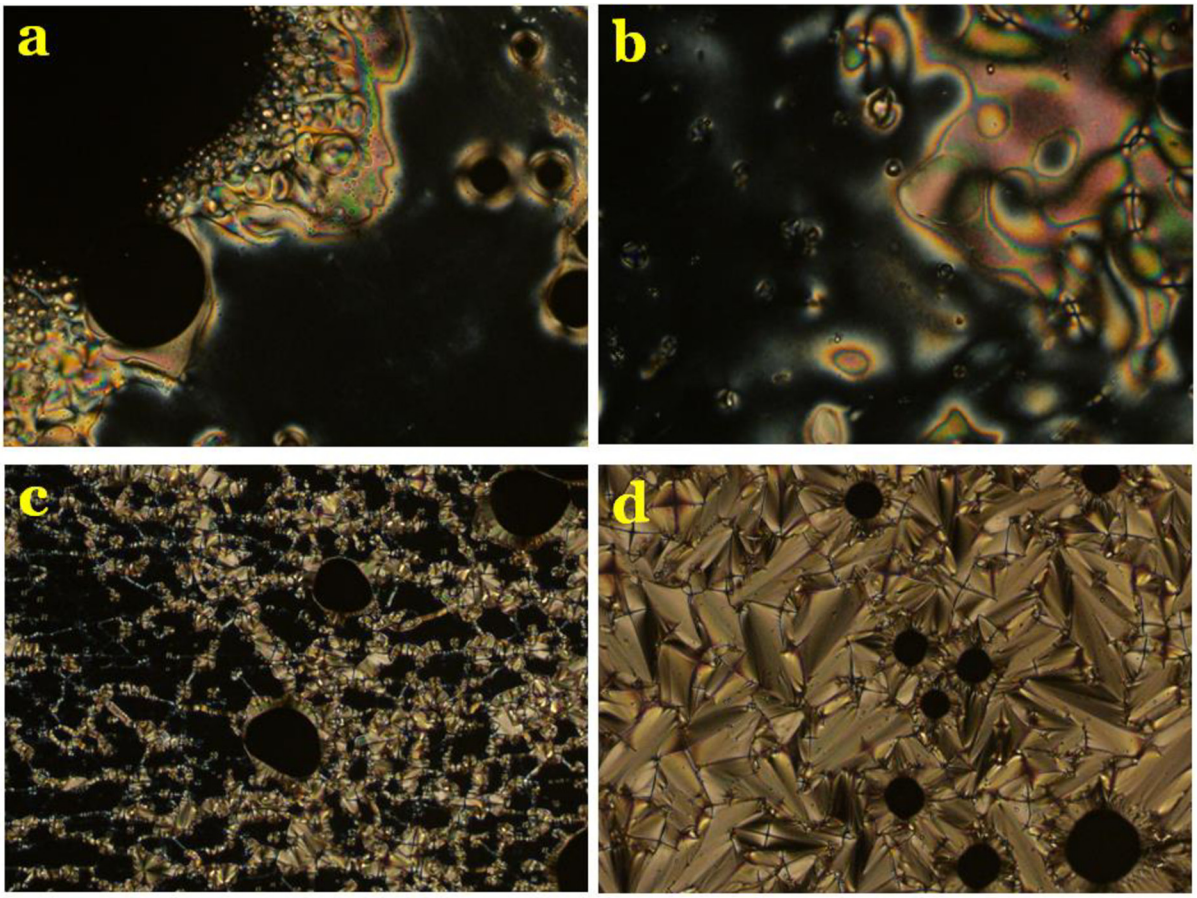

Figure 4. Representative optical textures for the mesophases behaviour of compounds (a) **9a** at 159 °C in the transition state from isotropic liquid to nematic; (b) **9b** at 155 °C in the transition state from isotropic liquid to nematic; (c) **9c** at 150 °C in the SmA mesophase and; (d) **9d** at 150 °C in the SmA mesophase.

Slowly reheating the sample again near the clearing temperature, the texture becomes highly colored as the phase becomes more fluid, and the fluctuation of the nematic phase director occurs, causing the scintillation effect – flash effects or sparks. This scintillation is rarely observed in any other mesophase. Upon cooling further, **10c** undergoes a two phase transition consecutively. Below the nematic transition temperature, **10c** displays a nematic-like texture (marbled texture, Figure 5b). The diagonal front line seen in Figure 5b during transition N to SmC separates two mesophases – SmC (left) and N (right) at 140 °C. The SmC mesophase is only observed upon cooling. No scintillation or flash effect is seen when the sample enters into monotropic (unstable) SmC mesophase. For **10d**, the transition between the N and SmC mesophases is visible in both the heating and cooling cycles, which means that mesophase stability is reached with the lengthening of the alkyl chain in the terminal group. Figure 5c and 5d show the planar thread-like texture of the nematic phase in the transition at 178 °C between SmC (top) and N (bottom) upon cooling. For SBs **10e–f**, upon cooling from isotropic state to mesophase, fan shaped texture and broken fan focal-conic texture were observed in the SmA and SmC mesophases, respectively.

The mesomorphic behaviours of **9a–f** and **10a–f** can understood in terms of the structural and electronic parameters present in SBs. Nematic mesophase was observed for SBs with methyl groups and the mesophase range decreases as the terminal alkoxy chain becomes longer. Nematic mesophase range is more pronounced for **10a–f.** The largest value is observed in **10a** and progressively diminishes as the number of carbon atoms increase in the alkyl chain. In general, **9a–f** are less mesogenic due to the non-planarity of the isoxazoline ring, while for **10a–f**, planarity is reached through the oxidation step. The torsional angle value for the phenyl ring and isoxazoline ring were determined by single crystal X-resolution of one intermediate obtained for us. The phenyl group is almost perpendicular to the isoxazoline ring with a torsional angle of 99° and, the angle between the isoxazoline and phenyl groups by carbon atom C5 is 119°.[22] Thus, the structural data does not favor mesophase formation in an isoxazoline system. However, by use of the elongating molecular strategy[11], it is possible to favor the molecular dimension length-to-breath ratio in LC system by the installation of more anisotropic groups.[23]

The flatness and co-planarity of the heterocyclic ring is well-known and documented, and the structural parameters are to be considered in the discussion of liquid crystals properties.[11,24] Despite the geometrical constrains of **9a–f**, imine groups impose on the final chemical structure additional orientational or positional order. Positional short-range order is gain along with

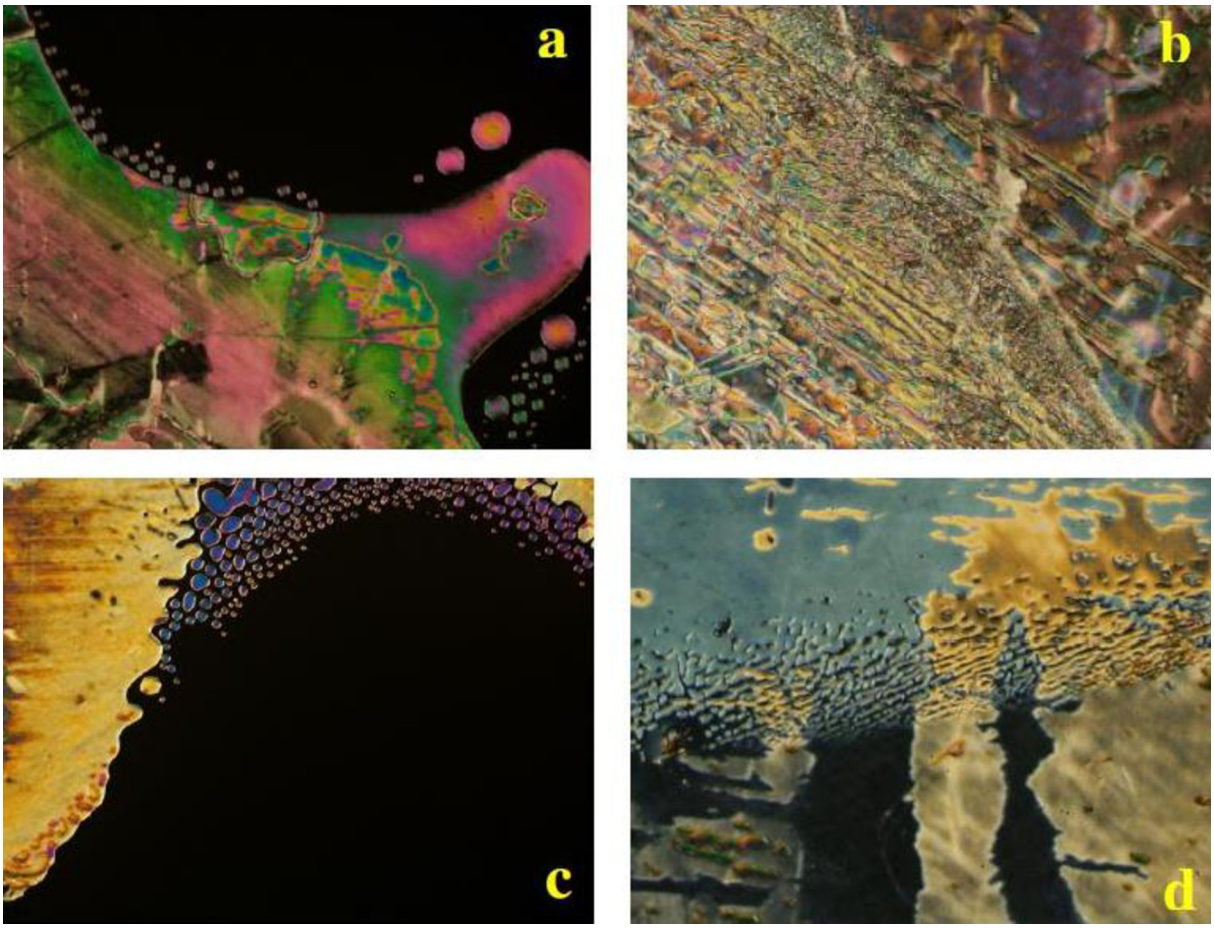

Figure 5. Representative optical textures for the mesophases behaviour of compounds **10c** at (a) 253 °C in the transition from isotropic liquid to nematic and at (b) 140 °C in the transition from nematic to SmC; **10d** at (c) 255 °C in the transition from isotropic liquid to nematic and at (d) 178 °C in the transition from nematic to SmC mesophase. Droplet formation on cooling an isotropic to Nematic phase is seen in (a) and (c).

orientational long-range order when we compare SBs derived from isoxazolines and isoxazoles. Strong π-stacking in the lattice is observed in crystal phase between two adjacent isoxazole rings.[25] Classical rod-shaped or bent-shaped LC is as elongated as possible through self-organization in the mesophase through intermolecular interaction or segregation effects. For SBs containing the isoxazole ring, the double π bond, at carbon atoms C4 and C5, the isoxazoline geometry changes from envelope to planar in the isoxazole ring. This leads to the conclusion that the molecules with isoxazole nuclei have bigger orientational long-range and positional short-range orders to explain the wide temperature range over which nematic and smectic phase are stable. Figure 6 describes the electron distributions in the canonical structures represented by long and short anisotropic cores. The resonance forms of SBs are more important to the core that contains the imine group. The extended conjugation over isoxazole and the imine group (left side, orange colour) is superior to the conjugation with the phenyl group (right side, blue colour). The SBs with methyl groups has a strong longitudinal dipole located on the isoxazole ring which favors the appearance of a nematic phase. For more polar groups located on the phenyl group, such as the bromine and alcoxy groups, the longitudinal dipole competes with the lateral dipole that comes from the 4-alcoxyphenyl group in the SBs with a smectic mesophase preference in detrimental to the nematic phase.

DSC traces of SBs **9d** and **10d** are shown in Figure 7. Schiff bases containing the isoxazoline and isoxazole rings undergo thermal heating and cooling cycles with distinct responses. For SB **9d**, it was possible (Figure 7, top) to note that they resist the many heating/cooling cycles. Upon heating, samples of **9a–f** melt to mesophase and with further heating they enter the isotropic phase. Upon cooling from the isotropic phase, they entry the corresponding mesophase, followed by transition to the crystal phase represented by the sharp peak at 118 °C, which corresponds to the crystallization temperature of the sample. Repetitive DSC cycles could be done with Schiff bases containing the isoxazoline ring without changes to the DSC profile. For SBs **10a–f**, DSC traces change drastically upon heating and cooling. Figure 7 (bottom) displays the thermogram of the heating and cooling cycle for **10d.** We can see that during the first heating cycle, the sample presents two sharp peaks related to the crystal phase transition and two small peaks located at 178 °C and 255 °C, related to the transition temperature between mesophase SmC and N, respectively.

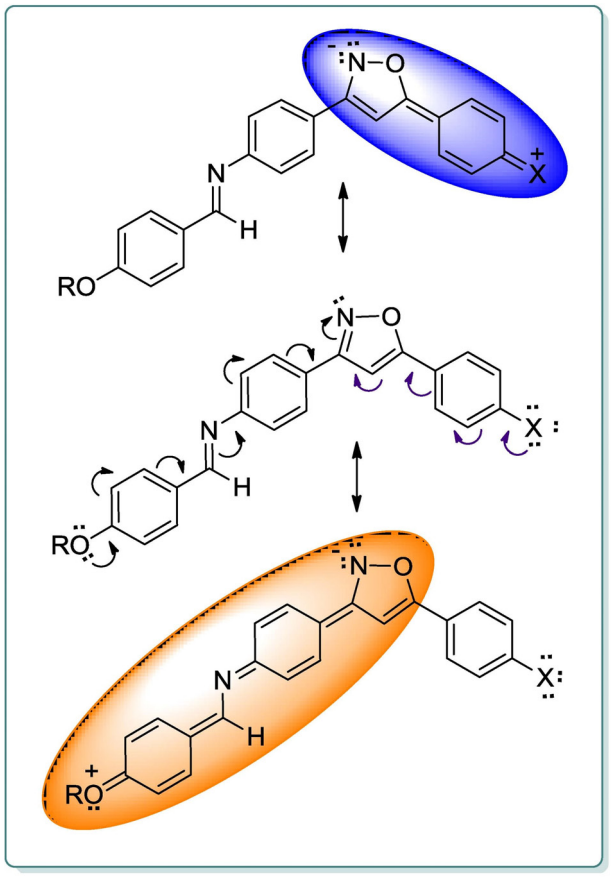

Figure 6. Delocalization of electrons over imine-isoxazole (orange colour) and phenyl-isoxazole (blue colour) of the Schiff base.

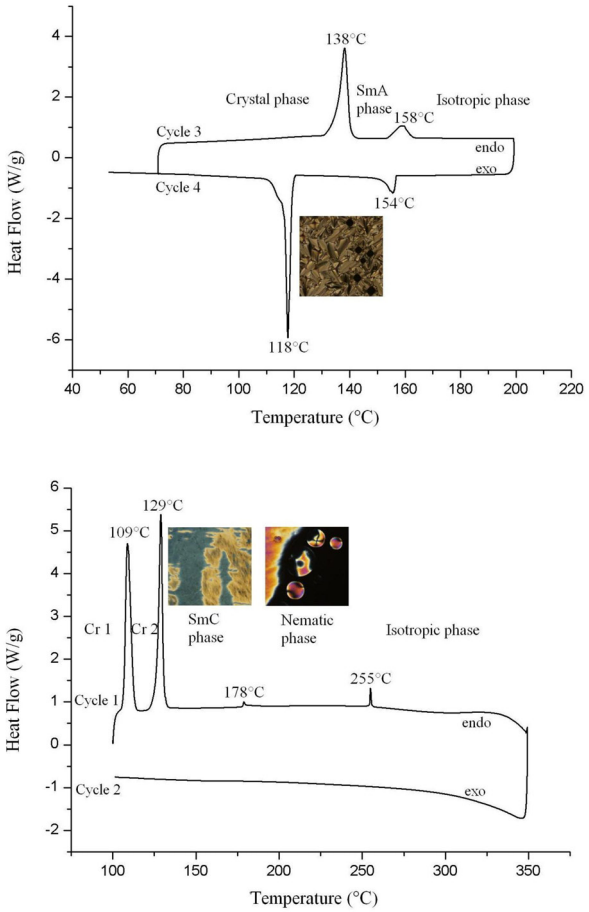

Figure 7. DSC traces for Schiff bases **9d** and **10d** with the corresponding mesophase texture. Transition temperature of the peak is showed. In Table 1, Tonset was considered.

However, samples experience thermal degradation after they enter the isotropic state. Upon cooling, samples should have the same thermal profile of the heating cycle. However, the baseline in Figure 7 (bottom) does not show any peaks related to the transitions between phases or mesophases. All the thermal data (temperatures, enthalpy and entropy) were lost, and the texture of the mesophase remains uncertain for samples belonging to series **10a–f.** The thermal degradation observed is a consequence of the high value of the clearing temperature of the SBs in series **10a–f.** To reach isotropic state, it is necessary to supply much more heat to the molecules belonging to the Schiff bases containing an isoxazole ring as a result of the better packing of this kind of molecules when compared with series of SBs containing an isoxazoline ring. Despite the thermal instability of SBs, it is worth highlighting the huge mesophase ranges for **10a–f**, which open up new opportunities and new challenges in how to heal or to fix this chemical defect presented by the Schiff bases here. This task should be done without disturbing or destroying the mesophase found in the primitive Schiff bases, as demonstrated by **10a–f.**

Conclusions

In summary, we have synthesized a collection of Schiff bases derived from isoxazolines **9a–f** and isoxazoles **10a–f.** All SBs displayed liquid-crystalline behaviour. Both series of LCs showed N, SmA and SmC mesophase. The mesophase temperature range, as well as the thermal stability, are dependent on the nature of 5-membered ring connected to the imine group. Isoxazoline SBs **9a–f** are more resistant to the thermal decomposition than isoxazoles SBs. However, isoxazoles SBs **10a–f** displayed a large mesophase range (**10e**, T = 164 °C) and high clearing temperature (> 250 °C).

Supporting information

Supporting information for this article is given via a link at the end of the document.

Acknowledgements

The authors gratefully acknowledge Fapergs (Edital PqG002/2014), CNPq, PPG-Química-UFRGS and Capes. The authors are also grateful to Sidnei Moura e Silva (Universidade de Caxias do Sul) for the HRMS analysis.

Keywords: Liquid Crystal · Schiff Base · Isoxazoline · Isoxazole · [3 + 2] 1,3-dipolar Cycloaddition

[1] H. Schiff, *Justus Liebigs Ann. Chem.* **1864**, *131*, 118–119.
[2] W. Qin, S. Long, M. Panunzio, S. Biondi, *Molecules* **2013**, *18*, 12264–12289.
[3] G. H. Heilmeier, L. A. Zanoni, L. A. Barton, *Proc. IEEE* **1968**, *56*, 1162–1171.
[4] a) R. B. Meyer, L. Liebert, L. Strzelecki, P. Keller, *J. Phys. Lett.* **1975**, *36*, 69–71; b) T. Geelhaar, K. Griesar, B. Reckmann, *Angew. Chem. Int. Ed.* **2013**, *52*, 2–14
[5] N. A. Clark, S. T. Lagerwall, *Appl. Phys. Lett.* **1980**, *36*, 899–901.
[6] A. A. Merlo, H. Gallardo, T. R. Taylor, *Quim. Nova* **2001**, *24*, 354–362.
[7] A. Reddy, C. Tschierske, *J. Mater. Chem.* **2006**, *16*, 907–961.
[8] H. Kim, Y. Yi, D. Chen, E. Korblova, D. M. Walba, N. A. Clark, K. D. Yoon, *Soft Matter* **2013**, *9*, 2793–2797.
[9] A. A. Merlo, H. Gallardo, T. R. Taylor, T. Kroin, *Mol. Cryst. Liq. Cryst.* **1994**, *250*, 31–39.
[10] R. Cristiano, A. A. Vieira, F. Ely, H. Gallardo, *Liq. Cryst.* **2006**, *33*, 381–390.
[11] a) K. J. K. Semmler, T. J. Dingemans, E. T. Samulski. *Liq. Cryst.* **1998**, *24*, 799–803; b) T. J. Dingemans, E. T. Samulski. *Liq. Cryst.* **2000**, *27*, 131–136.
[12] a) A. Tavares, O. M. S. Ritter, U. B. Vasconcelos, B. C. Arruda, A. Schrader, P. H. Schneider, A. A. Merlo, *Liq. Cryst.* **2010**, *37*, 159–169; b) A. Tavares, P. H. Schneider, A. A. Merlo, *Eur. J. Org. Chem.* **2009**, *2009*, 889–897.
[13] B. Roy, R. Narayan De, *Monatsh. Chem.* **2010**, *141*, 763–771.
[14] a) L. J. Kateley, W. B. Martin, D. C. Wiser, C. A. Brummond, *J. Chem. Edu.* **2002**, *79*, 225–227; b) O. M. S. Ritter, F. C. Giacomelli, J. A. Passo, N. P. da Silveira, A. A. Merlo, *Polymer Bulletin* **2006**, *56*, 549–561.
[15] F. D. Bellamy, K. Ou, *Tetrahedron Lett.* **1984**, *25*, 839–842.
[16] a) A. Barco, S. Benetti, P. Pollini, *Synthesis* **1977**, *12*, 837–837; b) A. J. Fatiadi, *Synthesis* **1976**, *3*, 133–167.
[17] V. Bezborodov, N. Kauhanka, V. Lapanik, *Mol. Cryst. Liq. Cryst.* **2004**, *411*, 103–110.
[18] a) C. Weygand, R. Gabler, *J. Prakt. Chem.* **1940**, *155*, 332–341; b) G. D. Vilela, R. R. Rosa, P. H. Schneider, I. H. Bechtold, J. Eccher, A. A. Merlo, *Tetrahedron Lett.* **2011**, *52*, 6569–6572; c) B. Zhang, J. Zhuo, Z. Gao, *Chinese Journal of Chemistry* **1990**, *2*, 169–174; d) R. Juárez, M. Ramos, J. L. Segura, J. Orduna, B. Villacampa, R. Alicante, *J. Org. Chem.* **2010**, *75*, 7542–7549.
[19] A. Carey, R. J. Sundberg, *Advanced Organic Chemistry, Part A. Structure and Mechanism*, Plenun Press, 4th ed. **2000**, New York.
[20] G. W. Gray, J. W. G. Goodby in *Smectic Liquid Crystals. Textures and Structures*; Leonard Hill, London, **1984**.
[21] L. Li, C. D. Jones, J. Magolan, R. P. Lemieux, *J. Mater. Chem.* **2007**, *17*, 2313–2318.
[22] a) T. K. Goncharov, V. V. Dubikhin, E. L. Ignat'eva, G. M. Nazin, Z. G. Aliev, S. M. Adoshin, *Russian J. General Chem.* **2013**, *83*, 717–721; b) E. S. Sales, *MSc Dissertation*, **2014** Chemistry Institute, UFRGS.
[23] A. Tavares, P. R. Livotto, P. F. B. Gonçalves, A. A. Merlo, *J. Braz. Chem. Soc.* **2009**, *20*, 1742–1752.
[24] J. M. F. M. Schneider, E. S. Sales, P. R. Livotto, P. H. Schneider, A. A. Merlo, *J. Braz. Chem. Soc.* **2014**, *25*, 1493–1503.
[25] a) I. Gaamoussi, I. Fichtali, A. B. Tama, E. M. E. Hadrami, D. Armentano, G. De Munno, M. Julve, S–E. Stiriba, *J. of Mol. Struct.* **2013**, *1048*, 130–137; b) A. A. Vieira, F. R. Bryk, G. Conte, A. J. Bortoluzzi, H. Gallardo, *Tetrahedron Lett.* **2009**, *50*, 905–908.
[26] L. Field, P. B. Hughmark, S. H. Shumaker, W. S. Marshall, *J. Am. Chem. Soc.* **1961**, *83,* 1983–1987.

Submitted: December 22, 2015
Accepted: January 4, 2016

Table of Contents

1. Experimental description
2. NMR spectrum – ^{1}H and ^{13}C NMR
3. DSC thermograms
4. Mesophase pictures

Experimental Section

Instruments and Techniques. 4-Nitrobenzaldehyde, 1-bromoalkanes, hydroxylamine hydrochloride, hypochlorite acid, K_2CO_3, sodium acetate, ethanol, chloroform, 4-X-styrenes, acetonitrile and toluene were used without further purification from Aldrich. All other commercial solvents and reagents were used without further purification. The melting points and mesophase transition temperatures and textures of the samples were measured on a Mettler Toledo FP82HT Hot Stage FP90 Central Processor and DSC 2910 TA Instruments. Nuclear magnetic resonance spectra were obtained on a Varian Inova 300, Varian VNMRs 300, Varian VNMRs 500 or Bruker Avance 400. Chemical shift are given in parts per million (δ) and are referenced from tetramethylsilane (TMS). Infrared spectra were recorded on a Perkin-Elmer Spectrum One FTIR Spectrometer Instruments using NaCl plates in case of solids and as thin film supported between NaCl plates in case of liquids and are reporter as wavenumber (cm^{-1}). CHN analyses were performed on a Perkin-Elmer 2400 CHN Elemental Analyzer. High resolution mass spectrometry (HRMS) spectra were obtained from a Fourier transform ion cyclotron resonance (FT-ICR) mass spectrometer equipped with an Infinity™ cell, a 7.0 Tesla superconducting magnet, an RF-only hexapole ion guide and an external electrospray ion source (off axis spray) and with ESI(+)-MS and tandem ESI(+)-MS/MS using a hybrid high-resolution and high accuracy MicroTOF-Q II mass spectrometer (Bruker Daltonics), or on a Micromass Q-TOFmicro instrument.

Synthesis of aldoxime. To 4-nitrobenzaldehyde (0.15 g, 1 mmol) and hydroxylamine hydrochloride (0.069 g, 1 mmol) were added 2 mL of ethanol. The reaction mixture was stirred for 1 minute and then sodium acetate (0.082 g, 1 mmol) in water (1 mL) was added. The mixture was heated at reflux during 1 hour. The reaction mixture was cooled and the white crystals were filtered off, washed with 50 mL of $EtOH/H_2O$ mixture (15:35 mL) and dried under a reduced pressure.

(*E*)-4-nitrobenzaldoxime (2): Yield: 0.15 g, 91%; Yellow solid; Mp 128-129 °C (lit. mp 132-133 °C[26]); ^1H NMR (300 MHz, $CDCl_3$) δ = 8.27 (d, *J* = 8.9 Hz, 2H); 8.23 (s, 1H); 7.98 (s, 1H); 7.77 (d, *J* = 8.8 Hz, 2H); ^{13}C NMR (75 MHz, $CDCl_3$) δ 148.48, 148.37, 138.16, 127.67, 124.07.

Cycloaddition reactions. 4-nitrobenzaldoxime (0.16 g, 1 mmol) and DCM (4 mL) were mixtured until complete dissolution. The dipolarophile **3a-c** (0,12 g**3a**, 0,18 g**3b**, 0,16 g**3c**, 1 mmol) was than added. Under vigorous stirring, the hypochlorite acid was added dropwise. The reaction was then stirred at room temperature for 30 min. The solution was washed with water (1x10 mL) and brine (2x10 mL) and dried over Na_2SO_4. The filtrate was evaporated under a reduced pressure and the residue was purified by recrystalization from ethanol.

3-(4-Nitrophenyl)-5-(4-methylphenyl)isoxazoline (4a): Yield: 0.24 g, 85%; Yellow solid; mp 116 °C; (lit[18b] mp 122 °C); ^1H NMR (300 MHz, $CDCl_3$): δ = 8.29 (d, *J* = 9.0 Hz, 2H); 7.88 (d, *J* = 9.0 Hz, 2H); 7.30 (d, *J* = 8.2 Hz, 2H); 7.23 (d, *J* = 7.9 Hz, 2H); 5.82 (dd, J_{cis} = 11.1 Hz, J_{trans} = 8.6 Hz, 1H); 3.81 (dd, J_{gem}= 16.7, J_{cis}= 11.1 Hz, 1H); 3.38 (dd, J_{gem}= 16.7 Hz, J_{trans} = 8.6 Hz, 1H); 2.39 (s, 2H). IR (ν_{max} in cm^{-1}) = 3111, 2939, 1512, 1350, 916, 850, 800, 750.

3-(4-Nitrophenyl)-5-(4-bromophenyl)isoxazoline (4b): Yield: 0.24 g, 67%; White solid; mp 132 °C (lit[18b] mp 132 °C); ^{1}H NMR (300 MHz, $CDCl_3$): δ = 8.30 (d, *J* = 9.0 Hz, 2H); 7.87 (d, *J* = 9.0 Hz, 2H); 7.55 (d, *J* = 8.5 Hz, 2H); 7.30 (d, *J* = 8.6 Hz, 2H); 5.82 (dd, J_{cis} = 11.2 Hz, J_{trans}= 8.3 Hz, 1H); 3.85 (dd, J_{gem} = 16.7 Hz, J_{cis}= 11.2 Hz, 1H); 3.35 (dd, J_{gem} = 16.7 Hz, J_{trans}= 8.3 Hz, 1H); ^{13}C NMR (75 MHz, $CDCl_3$) δ 154.63, 148.54, 139.21, 135.30, 132.06, 127.53, 127.49, 124.08, 122.54, 119.80, 82.89, 42.53. IR (ν_{max} in cm^{-1}) = 3088, 2927, 1579, 1510, 1340, 908, 846.

3-(4-Nitrophenyl)-5-(4-acetoxyphenyl)isoxazoline (4c): Yield: 0.32 g, 97%; White solid; mp 143-144 °C; ^{1}H NMR (300 MHz, $CDCl_3$): δ = 8.30 (d, *J* = 8.7 Hz, 2H); 7.88 (d, *J* = 8.6 Hz, 2H); 7.43 (d, *J* = 8.7 Hz, 2H); 7.15 (d, *J* = 8.5 Hz, 2H); 5.86 (dd, J_{cis} = 11.1 Hz, J_{trans}= 8.3 Hz, 1H); 3.84 (dd, J_{gem}= 16.7 Hz, J_{cis} = 11.2 Hz, 1H); 3.39 (dd, J_{gem}= 16.7 Hz, J_{trans}= 8.2 Hz, 1H); 2.33 (s, 3H); ^{13}C NMR (100 MHz, $CDCl_3$) δ 169.42, 154.71, 150.73, 148.51, 137.75, 135.45, 127.48, 127.02, 124.04, 122.11, 83.05, 42.48, 21.10. IR (ν_{max} in cm^{-1}) = 3076, 1749, 1577, 1510, 1350, 1219, 912, 846, 750; HRMS (ESI) *m/z* $[M + H]^+$ calcd. for $C_{17}H_{14}N_2O_5^+$: 327.0980; found: 327.0952.

General procedure for oxidation reaction. To a flask adapted with a Dean-Stark apparatus were added isoxazolines (0.34 g, **4a**; 0.42 g, **4b**; 0.39 g, **4c**; 1.2 mmol), toluene (25 mL) and γ-MnO_2 (2.5 g, 28.7 mmol). The mixture was heated under reflux for 10 hours. After cooled, the reaction mixture was filtered over celite and the solvent was removed. The crude product was recrystallized from ethanol to give the pure product as a solid.

3-(4-Nitrophenyl)-5-(4-methylphenyl)isoxazole (6a): Yield: 0.29 g 86%;Yellow solid; mp 180 °C (lit[18b,c] mp 182.5 °C); ^{1}H NMR (400 MHz, $CDCl_3$): δ = 8.36 (d, *J* = 8.8 Hz, 2H); 8.07 (d, *J* = 8.8 Hz, 2H); 7.76 (d, *J* = 8.2 Hz, 2H); 7.34 (d, *J* = 8.1 Hz, 2H); 6.86 (s, 1H); 2.45 (s, 3H); ^{13}C NMR (75 MHz, $CDCl_3$) δ 171.61, 161.07, 148.60, 141.10, 135.30, 129.81, 127.67, 127.61, 125.80, 124.18, 96.84, 21.53. IR (ν_{max} in cm^{-1}) = 1662, 1516, 1336, 852, 800.

3-(4-Nitrophenyl)-5-(4-bromophenyl)isoxazole (6b): Yield: 0.24 g, 58%; White solid; mp 223 °C (lit[18b] mp 224.8 °C); ^{1}H NMR (300 MHz, $CDCl_3$): δ = 8.39 (d, *J* = 9.0 Hz, 2H); 8.08 (d, *J* = 9.0 Hz, 2H); 7.76 (d, *J* = 8.8 Hz, 2H); 7.68 (d, *J* = 8.8 Hz, 2H); 6.94 (s, 1H). IR (ν_{max} in cm^{-1}) = 1579, 1510, 1338, 908, 846.

3-(4-Nitrophenyl)-5-(4-acetoxyphenyl)isoxazole (6c): Yield: 0.20 g, 52%; White solid; mp 181-183 °C; ^{1}H NMR (300 MHz, $CDCl_3$): δ = 8.35 (d, *J* = 8.8 Hz, 2H); 8.04 (d, *J* = 8.9 Hz, 2H); 7.87 (d, *J* = 8.7 Hz, 2H); 7.26 (d, *J* = 8.7 Hz, 2H); 6.87 (s, 1H); 2.34 (s, 3H); ^{13}C NMR (75 MHz, $CDCl_3$) δ 170.64, 169.12, 161.24, 152.36, 148.73, 135.11, 127.70, 127.24, 124.62, 124.27, 122.54, 97.53, 21.18. IR (ν_{max} in cm^{-1}) = 1747, 1514, 1342, 1222; HRMS (ESI) *m/z* $[M + H]^+$ calcd. for $C_{17}H_{13}N_2O_5^+$: 325.0824; found: 325.0784.

General procedure for deprotection reaction. To a flask were added **4c** (0.32 g, 1 mmol) or **6c** (0.32 g, 1 mmol), potassium hydroxide (0.067 g, 1.2 mmol) and the solvents ethanol/water 1:1 (10 mL). The mixture was stirred and heated under reflux for 1 hour. At the end, the mixture was poured in cooled water. The

reaction was acidified hydrochloric acid until pH 5 – 6. The precipitated was filtrated, washed with distillated water and evaporated under a reduced pressure.

3-(4-Nitrophenyl)-5-(4-hydroxiphenyl)isoxazoline: Yield: 0.27 g, 95%; Yellow solid; mp 194 °C; ^{1}H NMR (300 MHz, Acetone-d^6): δ = 8.35 (d, *J* = 8.8 Hz, 2H); 8.05 (d, *J* = 8.8 Hz, 2H); 7.33 (d, *J* = 8.7 Hz, 2H); 6.89 (d, *J* = 8.5 Hz, 2H); 5.80 (dd, J_{cis}= 11.0 Hz, J_{trans}= 9.3 Hz, 1H); 3.95 (dd, J_{gem}= 17.1 Hz, J_{cis}= 11.0 Hz, 1H); 3.51 (dd, J_{gem}= 17.1 Hz, J_{trans}= 9.3 Hz, 1H); IR (ν_{max} in cm^{-1}) = 3439, 3078, 2910, 1516, 1342, 908, 854; HRMS (ESI) *m/z* [M + H]$^+$ calcd. for $C_{15}H_{13}N_2O_4^+$: 285.0875; found: 285.0864.

3-(4-Nitrophenyl)-5-(4-hydroxiphenyl)isoxazole: Yield: 0.24 g, 83%: Yellow solid; mp 240-242 °C (lit[18b] mp 241 °C); ^{1}H NMR (300 MHz, Acetone-d^6): δ = 8.42 (d, *J* = 8.6 Hz, 2H); 8.25 (d,*J* = 8.6 H , 2Hz); 7.83 (d, *J* = 8.6 Hz, 2H); 7.35 (s, 1H); 7.06 (d, *J* = 8.6 Hz, 2H); 3.02 (sl, 1H); ^{13}C NMR (75 MHz,Acetone-d^6) δ = 171.59, 161.24, 160.01, 148.78, 135.58, 127.75, 127.56, 124.14, 118.64, 116.11, 96.23.

Alkylation reactions. The alkylation procedure was made according to the literature.[18] To 4 mL acetonitrile (CH_3CN) and 3-(4-nitrophenyl)-5-(4-hydroxiphenyl)isoxazoline (0.28 g, 1 mmol) or 3-(4-nitrophenyl)-5-(4-hydroxiphenyl)isoxazole (0.28 g, 1 mmol) was added potassium carbonate (0.16 g, 1.2 mmol). The solution was stirred at room temperature for 1h and then the bromobutane (0.26 g, 1.2 mmol) was added. The reaction mixture was refluxed for 8 h and the precipitate was filtered off. The filtrate was evaporated in vacuum and purified by recrystallization.

3-(4-Nitrophenyl)-5-(4-*n*-butoxyphenyl)isoxazoline: Yield: 0.31 g, 91%; White solid; ^{1}H NMR (300 MHz, $CDCl_3$): δ = 8.20 (d, *J* = 9.0 Hz, 2H); 7.79 (d, *J* = 9.0 Hz, 2H); 7.23 (d, *J* = 8.7 Hz, 2H); 6.84 (d, *J* = 8.8 Hz, 2H); 5.70 (dd, J_{cis} = 11.0 Hz, J_{trans} = 8.8 Hz, 1H); 3.89 (t, *J* = 6.5 Hz, 2H); 3.68 (dd, J_{gem}= 16.7, J_{cis}= 11.1 Hz, 1H); 3.28 (dd, J_{gem}= 16.7 Hz, J_{trans} = 8.8 Hz, 1H); 1.70 (m, 2H); 1.41 (m, 2H); 0.90 (t, *J* = 7.4 Hz, 3H). IR (ν_{max} in cm^{-1}) = 2954, 2926, 1608, 1512, 1346, 1247, 923, 850; HRMS (ESI) *m/z* [M + H]$^+$ calcd. for $C_{19}H_{21}N_2O_4^+$: 341.1501; found: 341.1464.

3-(4-Nitrophenyl)-5-(4-*n*-butoxyphenyl)isoxazole: Yield: 0.28 g, 83%; Brown solid; mp Cr 135 °C SmA 170 °C I; ^{1}H NMR (300 MHz, $CDCl_3$): δ = 8.37 (d,*J* = 9.0 H , 2Hz); 8.07 (d, *J* = 9.0 Hz, 2H); 7.80 (d, *J* = 9.0 Hz, 2H); 7.03 (d, *J* = 9.0 Hz, 2H); 6.79 (s, 1H); 4.06 (t, *J* = 6.5 Hz, 2H); 1.82 (m, 2H); 1.53 (m, 2H); 1.02 (t, *J* = 7.4 Hz, 3H); ^{13}C NMR (75 MHz, $CDCl_3$) δ 171.52, 161.09, 161.07, 148.61, 135.43, 127.60, 127.48, 124.17, 119.44, 115.01, 95.94, 67.93, 31.17, 19.20, 13.81. IR (ν_{max} in cm^{-1}) = 3107, 2941, 1616, 1521, 1452, 1348, 1263, 810; HRMS (ESI) *m/z* [M + H]$^+$ calcd. for $C_{19}H_{19}N_2O_4^+$: 339.1344; found: 339.1290.

Reduction reaction. Into a flask with nitrogen atmosphere, were added the isoxazolines (0.28 g, 1 mmol, **4a**; 0.34 g, 1 mmol, **4b**) or the isoxazoles (0.28 g, 1 mmol, **6a**; 0.34 g, 1 mmol, **6b**), tin(II) chloride dihydrated (5.0 mmol) and the solvent ethanol absolute (25 mL). The reaction was stirred under reflux for 2

hrs. After cooled, it was stirred at 0 °C during 1 h. The mixture was diluted with water and the pH was adjusted to 7 - 8 with a saturated solution of sodium bicarbonate. The product was extracted with ethyl acetate (6 x 10 mL). The organic fraction was washed with brine (2 x 5 mL), dried with Na_2SO_4, filtrated and the solvent was evaporated.

3-(4-Aminophenyl)-5-(4-methylphenyl)isoxazoline (5a): Yield: 0.23 g, 89%; Orange solid; ^{1}H NMR (300 MHz, $CDCl_3$): δ = 7.42 (d, *J* = 8.7 Hz, 2H); 7.21 (d, *J* = 8.2 Hz, 2H); 7.10 (d, *J* = 7.9 Hz, 2H); 6.60 (d, *J* = 8.7 Hz, 2H); 5.57 (dd, J_{cis} = 10.8 Hz, J_{trans} = 8.3 Hz, 1H); 3.63 (dd, J_{gem} = 16.5 Hz, J_{cis} = 10.8 Hz, 1H); 3.20 (dd, J_{gem} = 16.5 Hz, J_{trans} = 8.3 Hz, 1H); 2.27 (s, 3H); 1.68 (sl, 2H); ^{13}C NMR (100 MHz, $CDCl_3$) δ 156.15, 148.43, 138.22, 137.90, 129.38, 128.26, 125.98, 119.41, 114.73, 82.05, 43.44, 21.18. IR (ν_{max} in cm^{-1}) = 3462, 3317, 3215, 1631, 1606, 1519, 1354, 1305, 1180, 889, 812, 536; HRMS (ESI) *m/z* $[M + H]^+$ calcd. for $C_{16}H_{17}N_2O^+$: 253.1340; found: 253.1340.

3-(4-Aminophenyl)-5-(4-bromophenyl)isoxazoline (5b): Yield: 0.22 g, 70%; Yellow solid; ^{1}H NMR (300 MHz, $CDCl_3$): δ = 7.52 (d, *J* = 8.5 Hz, 2H); 7.51 (d, *J* = 8.7 Hz, 2H); 7.29 (d, *J* = 8.2 Hz, 2H + $CDCl_3$); 6.70 (d, *J* = 8.8 Hz, 2H); 5.66 (dd, J_{cis} = 10.9 Hz, J_{trans} = 7.9 Hz, 1H); 3.94 (s, 2H); 3.76 (dd, J_{gem} = 16.5 Hz, J_{cis} = 10.8 Hz, 1H); 3.26 (dd, J_{gem} = 16.5 Hz, J_{trans} = 7.8 Hz, 1H); ^{13}C NMR (100 MHz, $CDCl_3$) δ 156.01, 148.55, 140.40, 136.49, 131.81, 128.30, 127.63, 119.02, 114.72, 81.25, 43.54. IR (ν_{max} in cm^{-1}) = 3408, 3323, 3211, 1602, 1516, 1356, 889, 815, 542; HRMS (ESI) *m/z* $[M + H]^+$ calcd. for $C_{15}H_{14}BrN_2O^+$: 317.0289; found: 317.0256.

3-(4-Aminophenyl)-5-(4-*n*-butoxyphenyl)isoxazoline (5d): Yield: 0.28 g, 91%; Brown solid; mp 87-88 °C; ^{1}H NMR (300 MHz, $CDCl_3$): δ = 7.52 (d, *J* = 8.6 Hz, 2H); 7.33 (d, *J* = 8.8 Hz, 2H); 6.91 (d, *J* = 8.7 Hz, 2H); 6.70 (d, *J* = 8.6 Hz, 2H); 5.64 (dd, J_{cis} = 10.7 Hz, J_{trans} = 8.6 Hz, 1H); 3.98 (t, *J* = 6.5 Hz, 2H); 3.93 (s, 2H); 3.70 (dd, J_{gem} = 16.5 Hz, J_{cis} = 10.7 Hz, 1H); 3.30 (dd, J_{gem} = 16.5 Hz, J_{trans} = 8.5 Hz, 1H); 1.78 (m, 2H); 1.51 (m, 2H); 0.99 (t, *J* = 7.4 Hz, 3H); ^{13}C NMR (75 MHz, $CDCl_3$) δ 159.07, 156.19, 148.37, 132.84, 128.20, 127.38, 119.39, 114.69, 114.62, 81.97, 67.74, 43.24, 31.27, 19.23, 13.87. IR (ν_{max} in cm^{-1}) = 3450,3383, 3213, 2954, 1610, 1514, 1356, 1249, 887, 825, 545; HRMS (ESI) *m/z* $[M + H]^+$ calcd. for $C_{19}H_{23}N_2O_2^+$: 311.1759; found: 311.1743.

3-(4-Aminophenyl)-5-(4-methylphenyl)isoxazole (7a): Yield: 0.16 g, 64%; Brown solid; mp 147 °C; ^{1}H NMR (300 MHz, $CDCl_3$): δ = 7.74 (d, *J* = 8.2 Hz, 2H); 7.69 (d, *J* = 8.7 Hz, 2H); 7.30 (d, *J* = 8.0 Hz, 2H); 6.77 (d, *J* = 8.7 Hz, 2H); 6.72 (s, 1H); 3.92 (sl, 2H); 2.43 (s, 3H);^{13}C NMR (100 MHz, CDCl3) δ 170.04, 162.82, 148.09, 140.29, 129.63, 128.09, 125.75, 125.01, 119.30, 114.99, 96.53, 21.49; HRMS (ESI) *m/z* $[M + H]^+$ calcd. for $C_{16}H_{15}N_2O^+$: 251.1184; found: 251.1176.

3-(4-Aminophenyl)-5-(4-bromophenyl)isoxazole (7b): Yield: 0.28 g, 91%; White solid; mp 192 °C; ^{1}H NMR (300 MHz, $CDCl_3$): δ = 7.72 (d, *J* = 8.7 Hz, 2H); 7.68 (d, *J* = 8.7 Hz, 2H); 7.64 (d, *J* = 8.8 Hz, 2H); 6.78 (d, *J* = 8.7 Hz, 2H); 6.77 (s, 1H); 3.93 (s, 2H); HRMS (ESI) *m/z* $[M + H]^+$ calcd. for $C_{15}H_{12}BrN_2O^+$: 315.0133; found: 315.0122.

3-(4-Aminophenyl)-5-(4-*n*-butoxyphenyl)isoxazole (7d): Yield: 0.11g, 35%; Brown solid; mp 170 ℃; ^{1}H NMR (300 MHz, $CDCl_3$): δ = 7.77 (d, *J* = 8.9 Hz, 2H); 7.69 (d, *J* = 8.7 Hz, 2H); 7.00 (d, *J* = 9.0 Hz, 2H); 6.77 (d, *J* = 8.7 Hz, 2H); 6.64 (s, 1H); 4.04 (t, *J* = 6.5 Hz, 2H); 3.90 (broad, 2H); 1.82 (m, 2H); 1.54 (m, 2H); 1.02 (t, *J* = 7.4 Hz, 3H); ^{13}C NMR (100 MHz, $CDCl_3$) δ 169.92, 162.82, 160.62, 148.08, 128.07, 127.35, 120.29, 119.34, 114.99, 114.86, 95.69, 67.87, 31.22, 19.23, 13.84.

Preparation of the aldehydes. Alkylation was performed as described above for the alkylation procedure for **5d** and **7d**, respectively.[18a,b,d] The purification was made with silica column and dichloromethane as a solvent.

4-Hexyloxybenzaldehyde (8a): Yield: 1.8 g, 87%; Colorless liquid; ^{1}H NMR (400 MHz, $CDCl_3$): δ = 9.87 (s, 1H); 7.82 (d, *J* = 8.6 Hz, 2H); 6.98 (d, *J* = 8.8 Hz, 2H); 4.03 (t, *J* = 6.6 Hz, 2H); 1.81 (qt, 2H); 1.47 (qt, 2H); 1.34 (m, 4H); 0.91 (t, *J* = 7.1 Hz, 3H).

4-Octyloxybenzaldehyde (8b): Yield: 1.2 g, 50%; Colorless liquid; ^{1}H NMR (300 MHz, $CDCl_3$): δ = 9.89 (s, 1H); 7.84 (d, *J* = 8.9 Hz, 2H); 7.01 (d, *J* = 8.7 Hz, 2H); 4.05 (t, *J* = 6.6 Hz, 2H), 1.83 (qt, 2H); 1.38 (m, 10H); 0.91 (t, *J* = 6.8 Hz, 3H).

4-Decyloxybenzaldehyde (8c): Yield: 2.0 g, 77%; Colorless liquid; ^{1}H NMR (300 MHz, $CDCl_3$): δ = 9.89 (s, 1H); 7.84 (d, *J* = 8.9 Hz, 2H); 7.01 (d, *J* = 8.7 Hz, 2H); 4.06 (t, *J* = 6.6 Hz, 2H), 1.83 (m, 2H); 1.44 (m, 14H); 0.90 (t, *J* = 6.7 Hz, 3H).

4-Dodecyloxybenzaldehyde (8d): Yield: 1.8 g, 64%; Colorless liquid; ^{1}H NMR (400 MHz, $CDCl_3$): δ = 9.89 (s, 1H); 7.84 (d, *J* = 8.8 Hz, 2H); 7.00 (d, *J* = 8.7 Hz, 2H); 4.05 (t, *J* = 6.6 Hz, 2H), 1.82 (qt, 2H); 1.48 (qt, 2H); 1.34 (m, 16H); 0.90 (t, *J* = 6.9 Hz, 3H).

Synthesis of the Schiff bases. General procedure. Amine (1 mmol) and aldehyde (1 mmol) were dissolved in ethanol (50 mL). One drop of glacial acetic acid was added and the mixture was refluxed for 2 hours. After cooling, the solid product was filtrated and recrystalized in ethanol. To remove dusts, paper fibers, etc, the solid was added to dichloromethane and solution was filtered using Millipore filters. The solvent was evaporated and the solid was washed with cold ethanol, filtered and store under vacuum for 4 hours.

(*E*)-*N*-[4-(hexyloxy)benzylidene]-4-[5-(*p*-tolyl)isoxazoline-3-yl]aniline (9a): Yield: 0.26 g, 59%; White solid; mp Cr (135℃) SmA 144℃ N 159℃ I; ^{1}H NMR (400 MHz, $CDCl_3$): δ = 8.40 (s, 1H); 7.87 (d, *J* = 8.8 Hz, 2H); 7.73 (d, *J* = 8.5 Hz, 2H); 7.33 (d, *J* = 8.1 Hz, 2H); 7.24 (d, *J* = 8.5 Hz, 2H); 7.21 (d, *J* = 8.0 Hz, 2H); 7.01 (d, *J* = 8.8 Hz, 2H); 5.72 (dd, J_{cis} = 10.8 Hz, J_{trans} = 8.5 Hz, 1H); 4.05 (t, *J* = 6.6 Hz, 2H); 3.77 (dd, J_{gem} = 16.6 Hz, J_{cis} = 10.9 Hz, 1H); 3.36 (dd, J_{gem} = 16.6 Hz, J_{trans} = 8.5 Hz, 1H); 3.13 (s, 3H); 1.84 (m, 2H); 1.51 (m, 2H); 1.39 (m, 4H); 0.95 (t, *J* = 7.0 Hz, 3H); ^{13}C NMR (100 MHz, $CDCl_3$) δ 162.20, 160.30, 155.89, 153.90, 138.04, 137.94, 130.75, 129.43, 128.78, 127.74, 126.72, 125.96, 121.32, 114.78, 82.58, 68.27, 43.17, 31.59, 29.15, 25.71, 22.62, 21.18, 14.07;

Elem. anal. calcd for $C_{29}H_{32}N_2O_2$: C, 79.11; H, 7.34; N, 6.36; found: C, 79.05; H, 6.92; N, 6.57.

(*E*)-*N*-[4-(octyloxy)benzylidene]-4-[5-(*p*-tolyl)isoxazoline-3-yl]aniline (9b): Yield: 0.34 g, 73%; White solid; mp Cr_1 135 °C Cr_2 140 °C SmA 149 °C N 155 °C I; ^{1}H NMR (400 MHz, $CDCl_3$): δ = 8.40 (s, 1H); 7.87 (d, *J* = 8.7 Hz, 2H); 7.73 (d, *J* = 8.5 Hz, 2H); 7.33 (d, *J* = 8.1 Hz, 2H); 7.24 (d, *J* = 8.6 Hz, 2H); 7.21 (d, *J* = 8.1 Hz, 2H); 7.01 (d, *J* = 8.8 Hz, 2H); 5.72 (dd, J_{cis} = 10.8 Hz, J_{trans} = 8.5 H, 1Hz); 4.05 (t, *J* = 6.6 Hz, 2H); 3.77 (dd, J_{gem} = 16.6 Hz, J_{cis} = 10.9 Hz, 1H); 3.36 (dd, J_{gem} = 16.6 Hz, J_{trans} = 8.5 Hz, 1H); 2.38 (s, 3H); 1.84 (qt, 2H); 1.51 (m, 2H); 1.37 (m, 8H); 0.94 (t, *J* = 6.9 Hz, 3H); ^{13}C NMR (100 MHz, $CDCl_3$) δ 162.20, 160.28, 155.89, 153.89, 138.03, 137.94, 130.76, 129.44, 128.79, 127.74, 126.72, 125.97, 121.33, 114.78, 82.59, 68.27, 43.17, 31.84, 29.38, 29.26, 29.20, 26.05, 22.69, 21.19, 14.15; Elem. anal. calcd for $C_{31}H_{36}N_2O_2$: C, 79.51; H, 7.76; N, 5.98; found: C, 79.86; H, 7.76; N, 6.08.

(*E*)-*N*-[4-(decyloxy)benzylidene]-4-[5-(*p*-tolyl)isoxazoline-3-yl]aniline (9c): Yield: 0.40 g, 79%; White solid; mp Cr_1 131 °C Cr_2 138 °C SmA 155 °C I; ^{1}H NMR (400 MHz, $CDCl_3$): δ = 8.41 (s, 1H); 7.87 (d, *J* = 8.8 Hz, 2H); 7.73 (d, *J* = 8.6 Hz, 2H); 7.33 (d, *J* = 8.1 Hz, 2H); 7.24 (d, *J* = 8.6 Hz, 2H); 7.22 (d, *J* = 8.0 Hz, 2H); 7.01 (d, *J* = 8.8 Hz, 2H); 5.72 (dd, J_{cis} = 10.8 Hz, J_{trans} = 8.5 Hz, 1H); 4.05 (t, *J* = 6.6 Hz, 2H); 3.76 (dd, J_{gem} = 16.6 Hz, J_{cis} = 10.9 Hz, 1H); 3.35 (dd, J_{gem} = 16.6 Hz, J_{trans} = 8.5 Hz, 1H); 2.38 (s, 3H); 1.84 (qt, 2H); 1.51 (m, 2H); 1.37 (m, 12H); 0.93 (t, *J* = 6.9 Hz, 3H); ^{13}C NMR (75 MHz, $CDCl_3$) δ 162.18, 160.32, 155.89, 153.87, 138.04, 137.93, 130.75, 129.43, 128.74, 127.74, 126.70, 125.96, 121.33, 114.77, 82.58, 68.26, 43.19, 31.94, 29.61, 29.60, 29.43, 29.37, 29.20, 26.05, 22.73, 21.21, 14.19; Elem. anal. calcd for $C_{33}H_{40}N_2O_2$: C, 79.86; H, 8.14; N, 5.64; found: C, 79.79; H, 7.99; N, 5.77.

(*E*)-*N*-[4-(dodecyloxy)benzylidene]-4-[5-(*p*-tolyl)isoxazoline-3-yl]aniline (9d): Yield: 0.41 g, 78%; White solid; mp Cr 135 °C SmA 154 °C I; ^{1}H NMR (400 MHz, $CDCl_3$): δ = 8.40 (s, 1H); 7.87 (d, *J* = 8.5 Hz, 2H); 7.73 (d, *J* = 8.2 Hz, 2H); 7.32 (d, *J* = 7.9 Hz, 2H); 7.24 (d, *J* = 8.9 Hz, 2H); 7.22 (d, *J* = 9.3 Hz, 2H); 7.00 (d, *J* = 8.5 Hz, 2H); 5.73 (dd, J_{cis} = 10.5 Hz, J_{trans} = 8.7 Hz, 1H); 4.05 (t, *J* = 6.5 Hz, 2H); 3.78 (dd, J_{gem} = 16.6 Hz, J_{cis} = 10.9 Hz, 1H); 3.36 (dd, J_{gem} = 16.6 Hz, J_{trans} = 8.4 Hz, 1H); 2.38 (s, 3H); 1.83 (qt, 2H); 1.50 (m, 2H); 1.35 (m, 16H); 0.92 (t, *J* = 6.7 Hz, 3H); ^{13}C NMR (100 MHz, $CDCl_3$) δ 162.20, 160.30, 155.88, 153.90, 138.04, 137.94, 130.74, 129.43, 128.77, 127.73, 126.71, 125.95, 121.31, 114.78, 82.58, 68.27, 43.18, 31.94, 29.68, 29.66, 29.62, 29.59, 29.40, 29.37, 29.18, 26.03, 22.71, 21.18, 14.15; Elem. anal. calcd for $C_{35}H_{44}N_2O_2$: C, 80.17; H, 8.46; N, 5.34; found: C, 79.90; H, 8.46; N, 5.43.

(*E*)-*N*-[4-(octyloxy)benzylidene]-4-[5-(4-bromophenyl)isoxazoline-3-yl]aniline (9e): Yield: 0.17 g, 33%; White solid; mp Cr 161 °C SmA 186 °C I; ^{1}H NMR (400 MHz, $CDCl_3$): δ = 8.40 (s, 1H); 7.86 (d, *J* = 8.8 Hz, 2H); 7.72 (d, *J* = 8.5 Hz, 2H); 7.53 (d, *J* = 8.5 Hz, 2H); 7.31 (d, *J* = 8.5 Hz, 2H); 7.24 (d, *J* = 8.5 Hz, 2H); 7.00 (d, *J* = 8.8 Hz, 2H); 5.72 (dd, J_{cis} = 10.9 Hz, J_{trans} = 8.0 Hz, 1H); 4.05 (t, *J* = 6.6 Hz, 2H); 3.82 (dd, J_{gem} = 16.6 Hz, J_{cis} = 11.0 Hz, 1H); 3.32 (dd, J_{gem} = 16.6 Hz, J_{trans} = 8.0 Hz, 1H); 1.84 (qt, 2H); 1.50 (m, 2H); 1.36 (m, 8H); 0.92 (t, *J* = 6.9 Hz, 3H); ^{13}C NMR (100 MHz, $CDCl_3$) δ 162.23, 160.41, 155.79, 154.11, 140.10, 131.90, 130.75, 128.71, 127.77, 127.60, 126.30, 122.14,

121.36, 114.78, 81.77, 68.27, 43.32, 31.81, 29.35, 29.23, 29.17, 26.02, 22.67, 14.11; Elem. anal. calcd for $C_{30}H_{33}BrN_2O_2$: C, 67.54; H, 6,23; N, 5.25; found: C, 66.98; H, 5.14; N, 5.28. **9e** decomposed on attempted HRMS measurement, and repeated elemental analysis on a freshly recrystallized sample did not improve the agreement of the carbon found value with the calculated value.

(*E*)-*N*-[4-(octyloxy)benzylidene]-4-[5-(4-*n*-butoxyphenyl)isoxazoline-3-yl]aniline (9f): Yield:0.41 g, 78%; White solid; mp Cr 138 °C SmC 159 °C I; ^{1}H NMR (400 MHz, $CDCl_3$): δ = 8.41 (s, 1H); 7.86 (d, *J* = 8.8 Hz, 2H); 7.74 (d, *J* = 8.6 Hz, 2H); 7.34 (d, *J* = 8.6 Hz, 2H); 7.24 (d, *J* = 8.6 Hz, 2H); 7.00 (d, *J* = 8.8 Hz, 2H); 6.92 (d, *J* = 8.7 Hz, 2H); 5.71 (dd, J_{cis} = 10.8 Hz, J_{trans} = 8.7 Hz, 1H); 4.05 (t, *J* = 6.6 Hz, 2H); 3.99 (t, *J* = 6.5 Hz, 2H); 3.76 (dd, J_{gem} = 16.6 Hz, J_{cis} = 10.8 Hz, 1H); 3.37 (dd, J_{gem} = 16.6 Hz, J_{trans} = 8.6 Hz, 1H); 1.81 (m, 4H); 1.50 (m, 4H); 1.35 (m, 8H); 1.00 (t, *J* = 7.4 Hz, 3H); 0.92 (t, *J* = 6.9 Hz, 3H); ^{13}C NMR (75 MHz, $CDCl_3$) δ 162.14, 160.29, 159.17, 155.92, 153.84, 132.54, 130.70, 128.70, 127.68, 127.36, 126.71, 121.28, 114.73, 114.67, 82.52, 68.23, 67.74, 42.99, 31.80, 31.27, 29.34, 29.22, 29.15, 26.00, 22.66, 19.22, 14.11, 13.85. Elem. anal. calcd for $C_{34}H_{42}N_2O_3$: C, 77.58; H, 8.06; N, 5.32; found: C, 78.07; H, 8.07; N, 5.45. **9f** decomposed on attempted HRMS measurement, and repeated elemental analysis on a freshly recrystallized sample did not improve the agreement of the carbon found value with the calculated value.

(*E*)-*N*-[4-(hexyloxy)benzylidene]-4-[5-(*p*-tolyl)isoxazole-3-yl]aniline (10a): Yield: 0.18 g, 42%; White solid; mp Cr 143 °C N 287 °C I; ^{1}H NMR (500 MHz, $CDCl_3$): δ = 8.43 (s, 1H); 7.90 (d, *J* = 8.3 Hz, 2H); 7.87 (d, *J* = 8.7 Hz, 2H); 7.75 (d, *J* = 8.1 Hz, 2H); 7.31 (d, *J* = 7.4 Hz, 2H); 7.30 (d, *J* = 8.2 Hz, 2H); 7.00 (d, *J* = 8.7 Hz, 2H); 6.80 (s, 1H); 4.04 (t, *J* = 6.6 Hz, 2H); 2.43 (s, 3H); 1.83 (qt, 2H); 1.50 (m, 2H); 1.38 (m, 4H); 0.93 (t, *J* = 6.9 Hz, 3H); ^{13}C NMR (75 MHz, $CDCl_3$) δ 170.51, 162.60, 162.13, 160.33, 153.84, 140.51, 130.72, 129.70, 128.79, 127.72, 126.32, 125.79, 124.81, 121.47, 114.75, 96.83, 68.25, 31.60, 29.15, 25.71, 22.63, 21.54, 14.08. Elem. anal. calcd for $C_{29}H_{30}N_2O_2$: C, 79.47; H, 6.91; N, 6.39; found: C, 79.46; H, 6.90; N, 6.43.

(*E*)-*N*-[4-(octyloxy)benzylidene]-4-[5-(*p*-tolyl)isoxazole-3-yl]aniline (10b): Yield: 0.29 g, 62%; White solid; mp Cr_1 121 °C Cr_2 141 °C N 278 °C I; ^{1}H NMR (500 MHz, $CDCl_3$): δ = 8.43 (s, 1H); 7.90 (d, *J* = 8.4 Hz, 2H); 7.87 (d, *J* = 8.7 Hz, 2H); 7.75 (d, *J* = 8.1 Hz, 2H); 7.31 (d, *J* = 7.6 Hz, 2H); 7.30 (d, *J* = 8.3 Hz, 2H); 7.00 (d, *J* = 8.7 Hz, 2H); 6.80 (s, 1H); 4.04 (t, *J* = 6.6 Hz, 2H); 2.43 (s, 3H); 1.83 (qt, 2H); 1.49 (m, 2H); 1.35 (m, 8H); 0.91 (t, *J* = 6.9 Hz, 3H); ^{13}C NMR (75 MHz, $CDCl_3$) δ 170.50, 162.59, 162.13, 160.32, 153.84, 140.50, 130.71, 129.70, 128.79, 127.71, 126.32, 125.78, 124.80, 121.46, 114.75, 96.83, 68.25, 31.84, 29.38, 29.26, 29.19, 26.03, 22.69, 21.54, 14.15. Elem. anal. calcd for $C_{31}H_{34}N_2O_2$: C, 79.85; H, 7.36; N, 6.01; found: C, 78.81; H, 7.20; N, 6.09.

(*E*)-*N*-[4-(decyloxy)benzylidene]-4-[5-(*p*-tolyl)isoxazole-3-yl]aniline (10c) Yield: 0.35 g, 70%; White solid; mp Cr 125 °C (140 °C SmC) N 253 °C I; ^{1}H NMR (300 MHz, $CDCl_3$): δ = 8.43 (s, 1H); 7.91 (d, *J* = 8.7 Hz, 2H); 7.88 (d, *J* = 9.0 Hz, 2H); 7.76 (d, *J* = 8.2 Hz, 2H); 7.31 (d, *J* = 7.0 Hz, 2H); 7.31 (d, *J* = 8.5 Hz, 2H); 7.00 (d, *J* = 8.8 Hz, 2H); 6.80 (s, 1H); 4.04 (t, *J* = 6.6 Hz, 2H); 2.44 (s, 3H); 1.84 (qt, 2H); 1.47 (m, 2H); 1.31 (m, 12H); 0.92 (t, *J* = 6.7 Hz,3H); ^{13}C NMR (75 MHz, $CDCl_3$) δ 170.50, 162.59, 162.13, 160.30, 153.82, 140.49,

130.72, 129.70, 128.79, 127.71, 126.32, 125.78, 124.80, 121.48, 114.74, 96.83, 68.25, 31.94, 29.61, 29.60, 29.43, 29.37, 29.20, 26.04, 22.73, 21.54, 14.18; Elem. anal. calcd for $C_{33}H_{38}N_2O_2$: C, 80.12; H, 7.74; N, 5.66; found: C, 79.50; H, 7.62; N, 5.68. **10c** decomposed on attempted HRMS measurement, and repeated elemental analysis on a freshly recrystallized sample did not improve the agreement of the carbon found value with the calculated value.

(*E*)-*N*-[4-(dodecyloxy)benzylidene]-4-[5-(*p*-tolyl)isoxazole-3-yl]aniline (10d): Yield: 0.35 g, 66%; White solid; mp Cr_1 106 °C Cr_2 126 °C SmC 178 °C N 255 °C I; ^{1}H NMR (300 MHz, $CDCl_3$): δ = 8.45 (s, 1H); 7.91 (d, *J* = 8.8 Hz, 2H); 7.88 (d, *J* = 9.3 Hz, 2H); 7.77 (d, *J* = 8.2 Hz, 2H); 7.32 (d, *J* = 8.6 Hz, 2H); 7.31 (d, *J* = 8.6 Hz, 2H); 7.01 (d, *J* = 8.8 Hz, 2H); 6.82 (s, 1H); 4.05 (t, *J* = 6.6 Hz, 2H); 2.45 (s, 3H); 1.84 (qt, 2H); 1.48 (m, 2H); 1.33 (m, 16H); 0.91 (t, 3H); ^{13}C NMR (75 MHz, $CDCl_3$) δ 170.51, 162.60, 162.13, 160.32, 153.85, 140.50, 130.71, 129.70, 128.79, 127.72, 126.32, 125.79, 124.81, 121.47, 114.75, 96.83, 68.25, 31.95, 29.70, 29.67, 29.63, 29.60, 29.42, 29.39, 29.19, 26.03, 22.73, 21.55, 14.17; Elem. anal. calcd for $C_{35}H_{42}N_2O_2$: C, 80.48; H, 8.12; N, 5.36; found: C, 80.62; H, 8.19; N, 5.49.

(*E*)-*N*-[4-(octyloxy)benzylidene]-4-[5-(4-bromophenyl)isoxazole-3-yl]aniline (10e): Yield: 0.25 g, 47%; White solid; mp Cr 137 °C SmA 301 °C I; ^{1}H NMR (300 MHz, $CDCl_3$): δ = 8.41 (s, 1H); 7.87 (t, *J* = 8.4 Hz, 4H); 7.85 (t, *J* = 8.6 Hz, 4H); 7.71 (d, *J* = 8.6 Hz, 2H); 7.63 (d, *J* = 8.6 Hz, 2H); 7.28 (d, *J* = 8.5 Hz, 2H); 6.98 (d, *J* = 8.7 Hz, 2H); 6.84 (s, 1H); 4.03 (t, *J* = 6.6 Hz, 2H); 1.82 (qt, 2H); 1.46 (m, 2H); 1.32 (m, 8H); 0.89 (t, *J* = 6.7 Hz, 3H); ^{13}C NMR (75 MHz, $CDCl_3$) δ 169.20, 162.74, 162.15, 160.36, 154.02, 132.27, 130.70, 128.74, 127.70, 127.26, 126.36, 125.92, 124.54, 121.48, 114.75, 97.79, 68.24, 31.79, 29.32, 29.21, 29.15, 25.99, 22.64, 14.08; Elem. anal. calcd for $C_{30}H_{31}BrN_2O_2$: C, 67.96; H, 5.91; N, 5.28; found: C, 68.24; H, 5.69; N, 5.42.

(*E*)-*N*-[4-(octyloxy)benzylidene]-4-[5-(4-*n*-butoxyphenyl)isoxazole-3-yl]aniline (10f): Yield: 0.26 g, 49%; White solid; mp $Cr_1$84°C $Cr_2$122°C SmC 248°C I; ^{1}H NMR (300 MHz, $CDCl_3$): δ = 8.42 (s, 1H); 7.89 (d, *J* = 7.3 Hz, 2H); 7.87 (d, *J* = 7.4 Hz, 2H); 7.29 (d, *J* = 8.1 Hz, 2H); 7.00 (d, *J* = 8.3 Hz, 4H); 6.71 (s, 1H); 4.03 (t, *J* = 6.1 Hz, 4H); 1.80 (m, 4H); 1.53 (m, 4H); 1.33 (m, 8H); 1.01 (t, *J* = 7.3 Hz, 3H); 0.91 (t, 3H); ^{13}C NMR (75 MHz, $CDCl_3$) δ 170.38, 162.57, 162.12, 160.72, 160.29, 153.77, 130.71, 128.79, 127.69, 127.39, 126.40, 121.45, 120.07, 114.89, 114.74, 95.95, 68.24, 67.87, 31.83, 31.22, 29.37, 29.26, 29.19, 26.03, 22.68, 19.24, 14.14, 13.87; Elem. anal. calcd for $C_{34}H_{40}N_2O_3$: C, 77.82; H, 7.68; N, 5.33; found: C, 76.91; H, 7.35; N, 5.87. **10f** decomposed on attempted HRMS measurement, and repeated elemental analysis on a freshly recrystallized sample did not improve the agreement of the carbon found value with the calculated value.

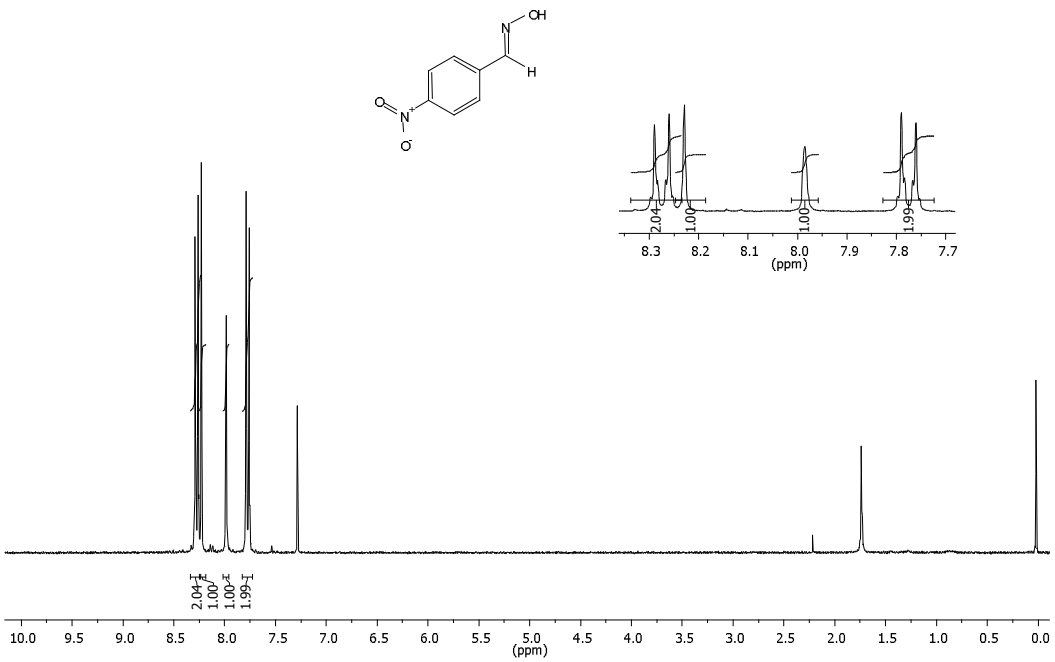

S 1. ^{1}H NMR spectrum of compound **2** ($CDCl_3$, 300 MHz).

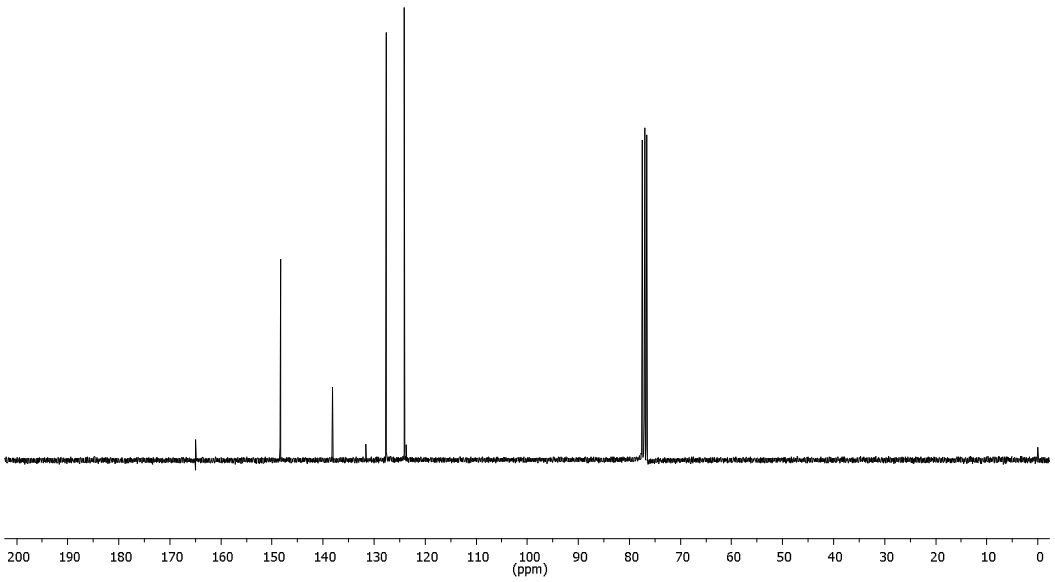

S 2. ^{13}C NMR spectrum of compound **2** ($CDCl_3$, 75 MHz).

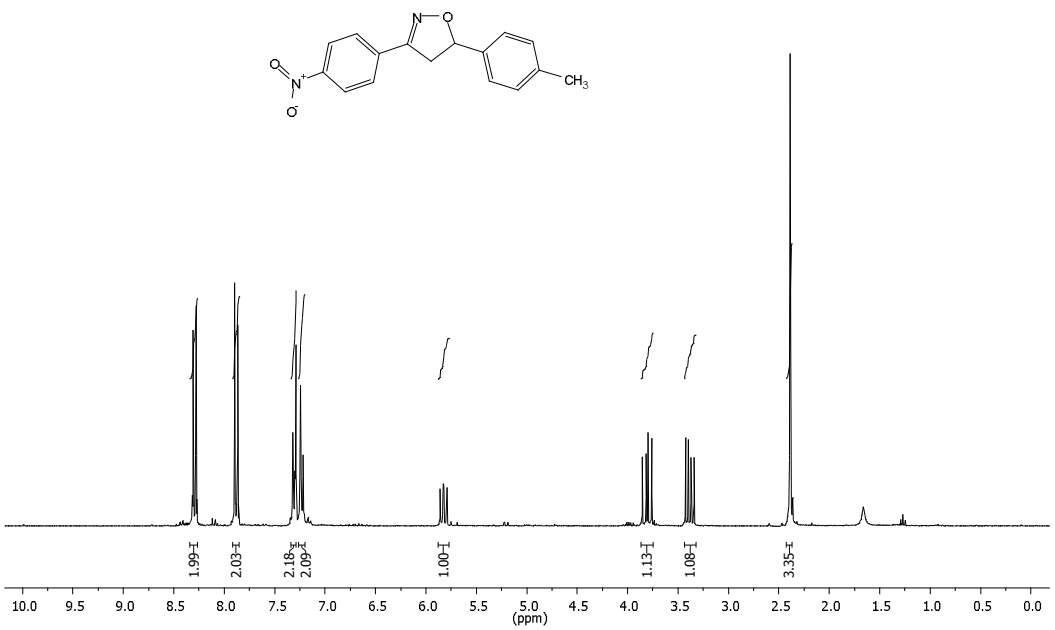

S 3. ^{1}H NMR spectrum of compound **4a** ($CDCl_3$, 300 MHz).

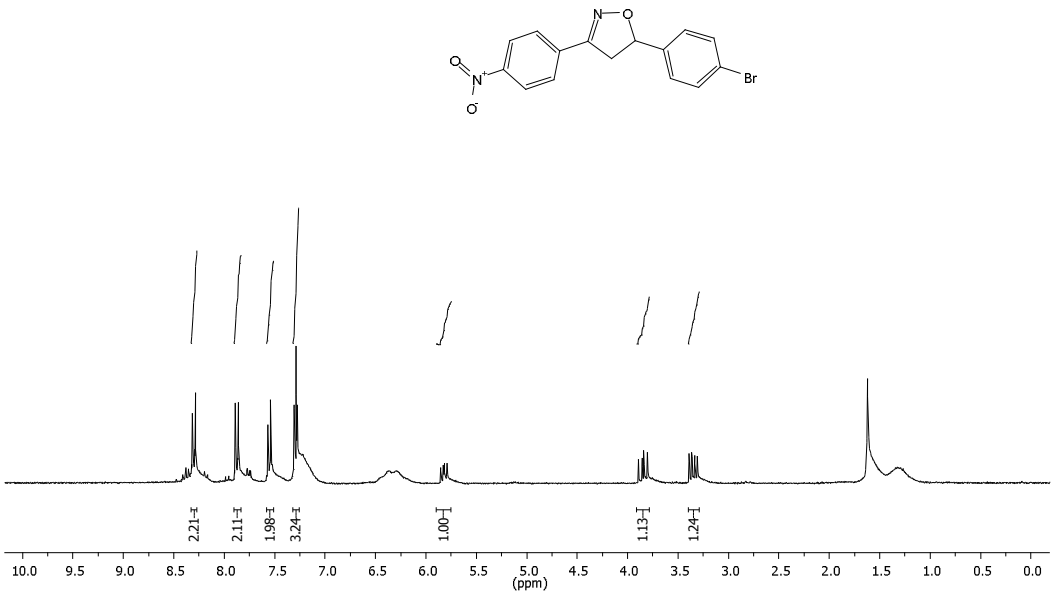

S 4. ^{1}H NMR spectrum of compound **4b** ($CDCl_3$, 300 MHz).

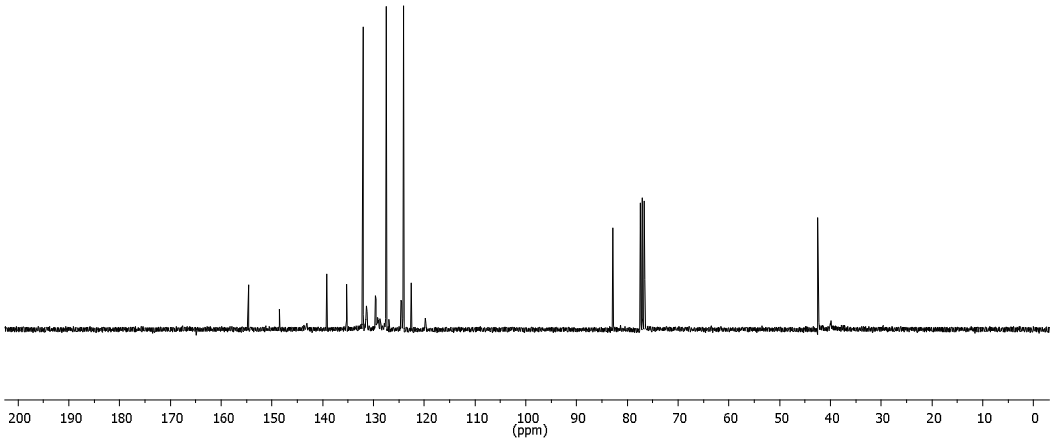

S 5. ^{13}C NMR spectrum of compound **4b** ($CDCl_3$, 75 MHz).

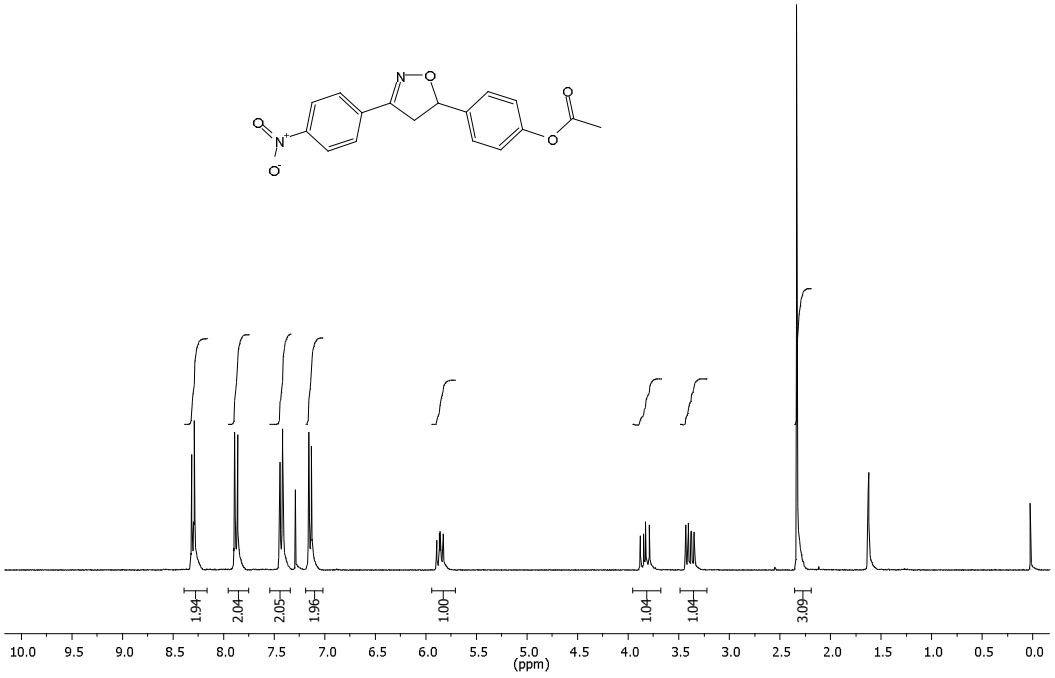

S 6. ^{1}H NMR spectrum of compound **4c** ($CDCl_3$, 300 MHz).

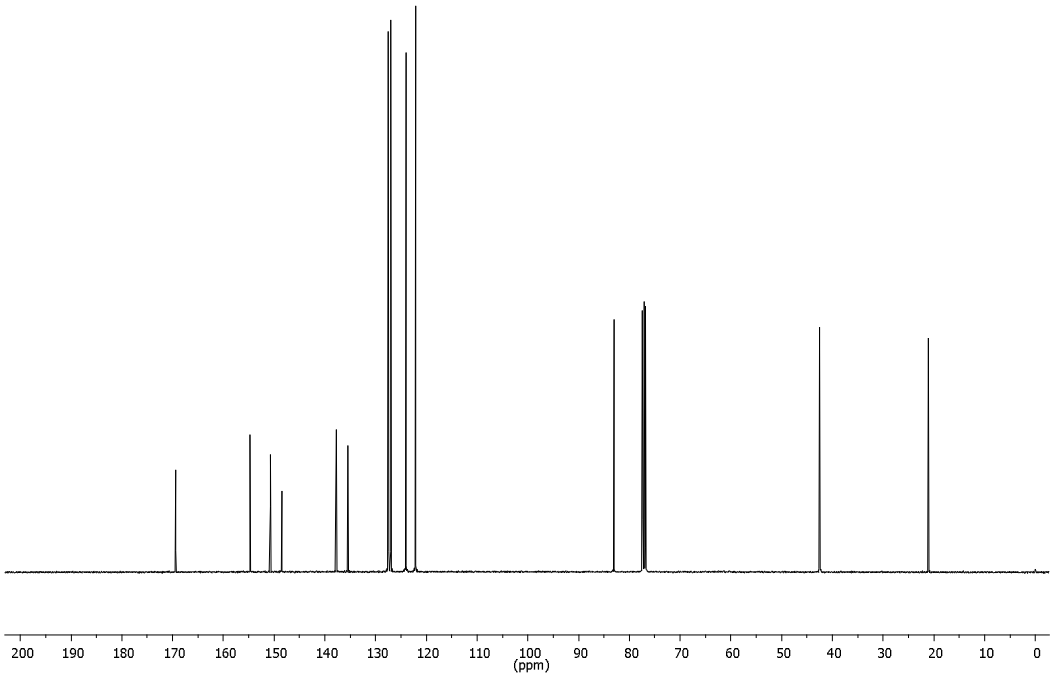

S 7. ^{13}C NMR spectrum of compound **4c** ($CDCl_3$, 100 MHz).

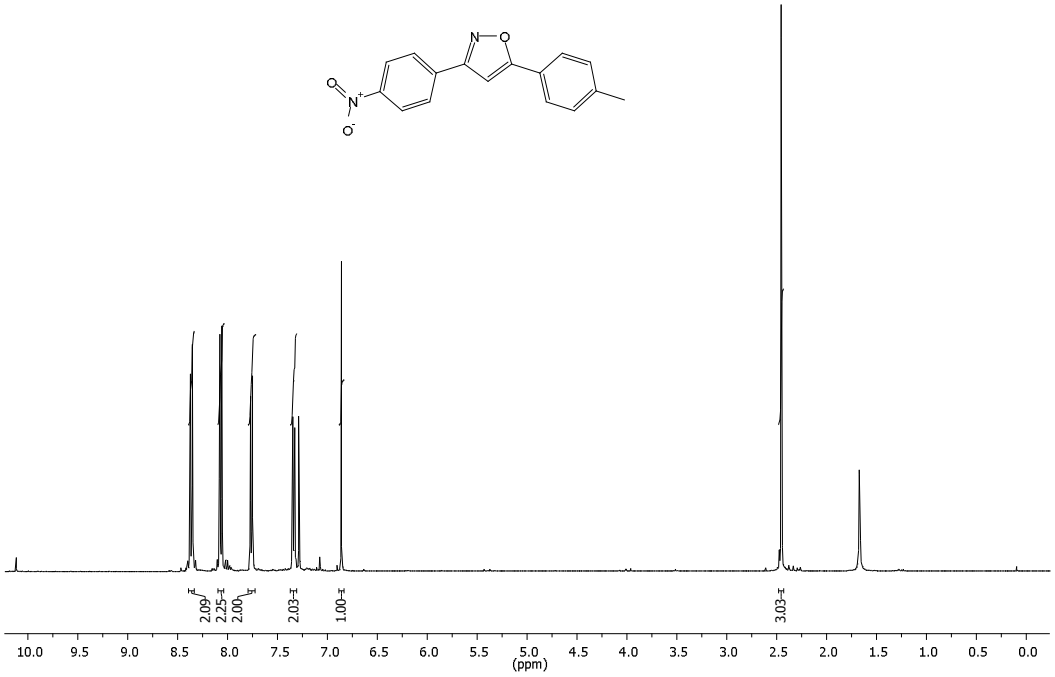

S 8. ^{1}H NMR spectrum of compound **6a** ($CDCl_3$, 400 MHz).

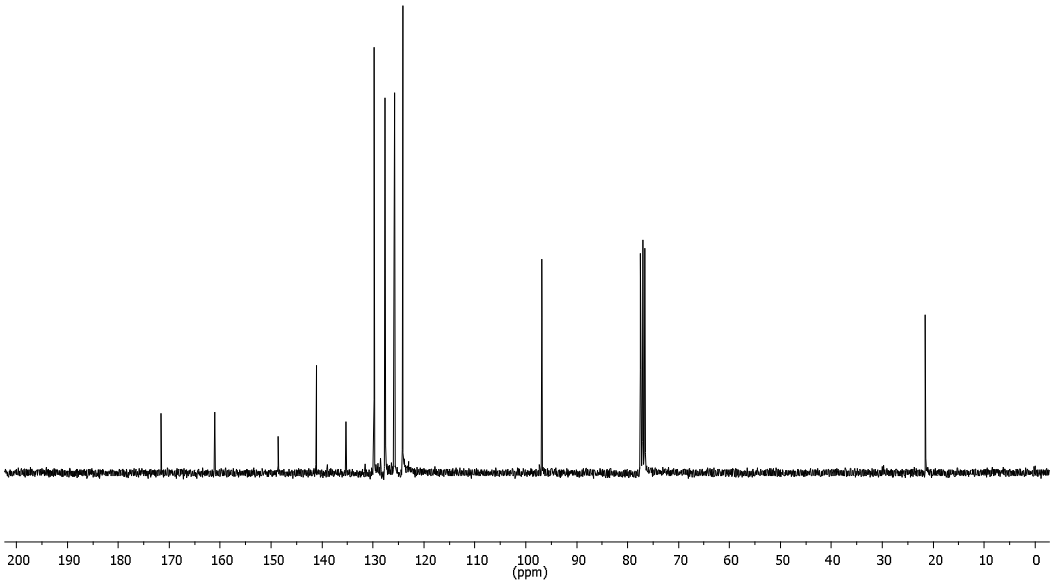

S 9. ^{13}C NMR spectrum of compound **6a** ($CDCl_3$, 75 MHz).

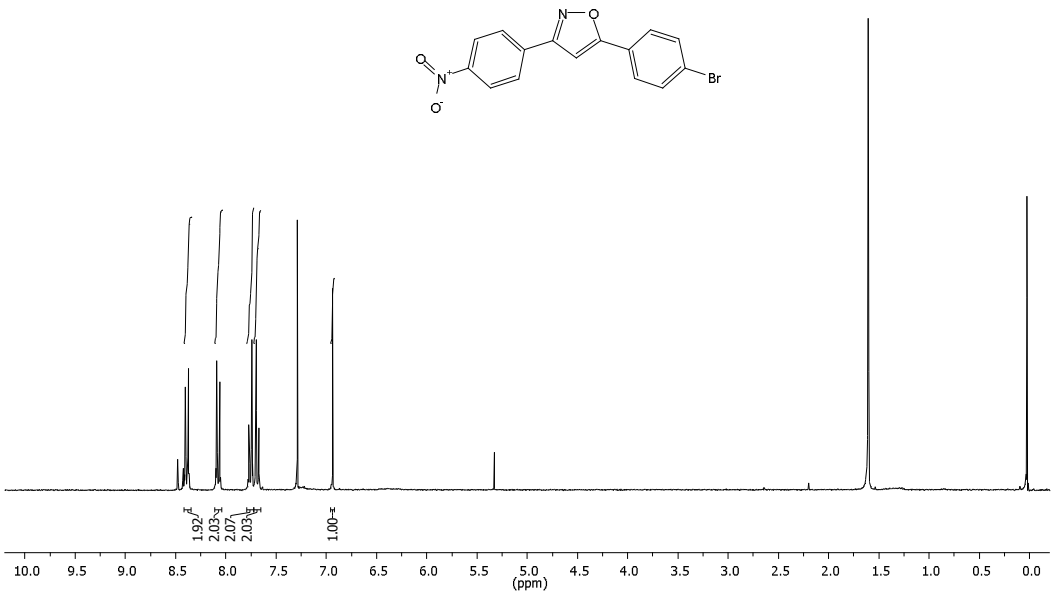

S 10. ^{1}H NMR spectrum of compound **6b** ($CDCl_3$, 300 MHz).

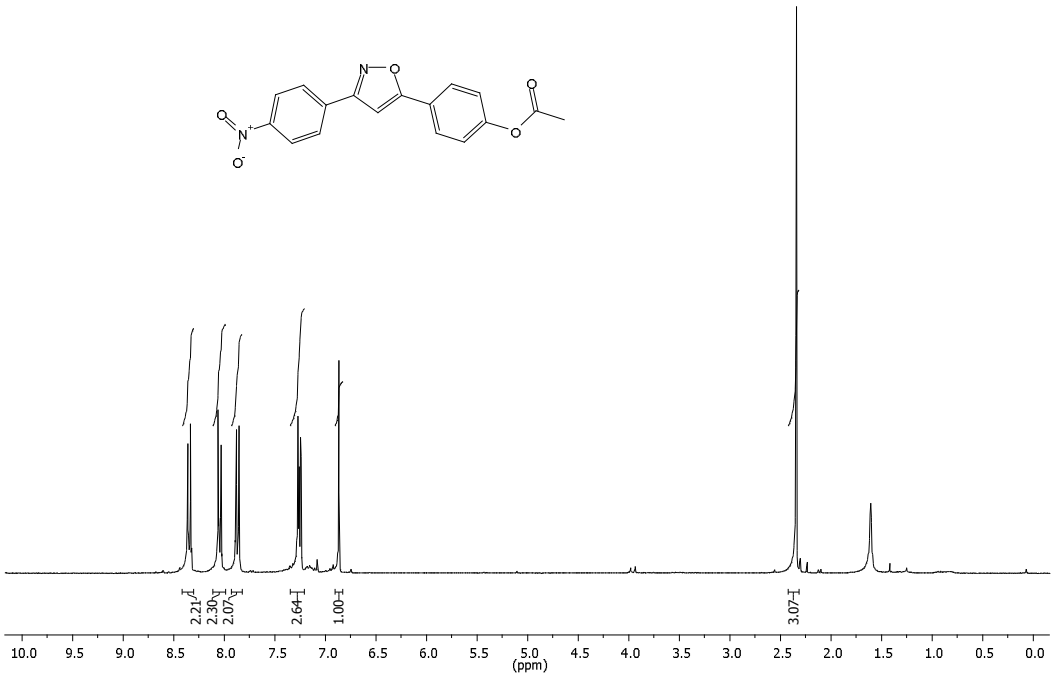

S 11. ^{1}H NMR spectrum of compound **6c** ($CDCl_3$, 300 MHz).

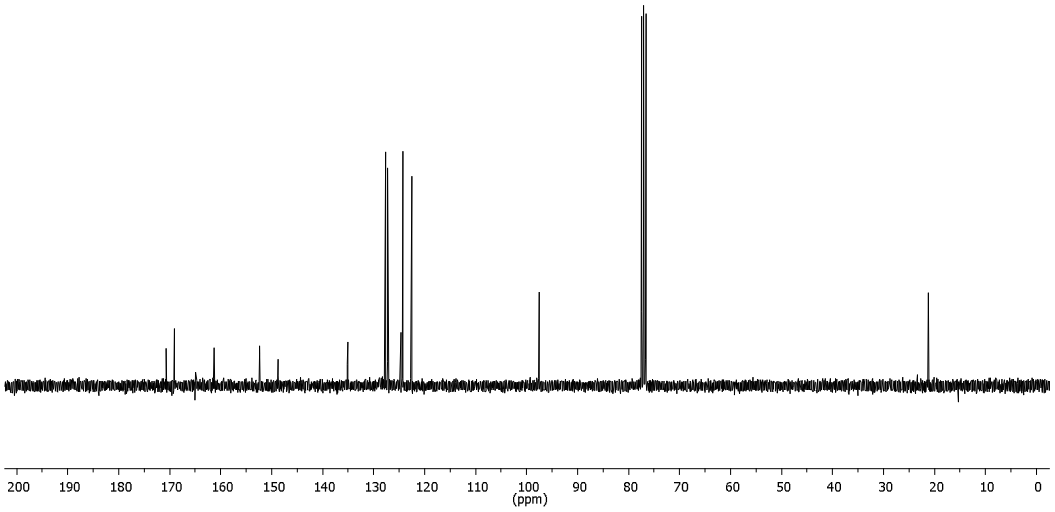

S 12. ^{13}C NMR spectrum of compound **6c** ($CDCl_3$, 75 MHz).

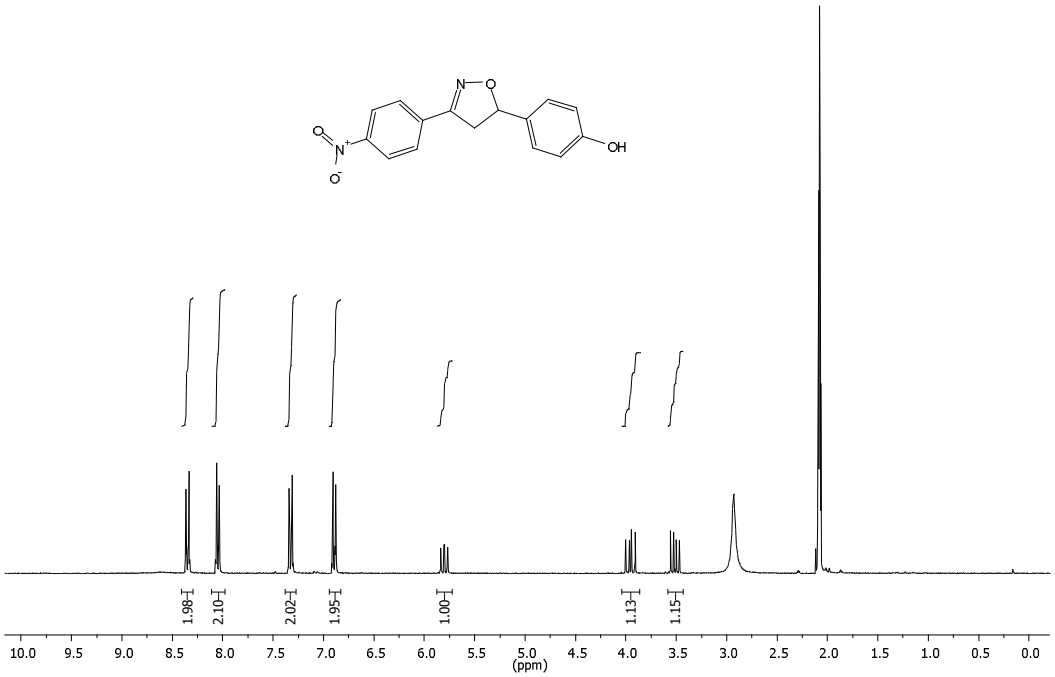

S 13. ^{1}H NMR spectrum of compound 3-(4-nitrophenyl)-5-(4-hydroxiphenyl)isoxazoline (Acetone-d^{6}, 300 MHz).

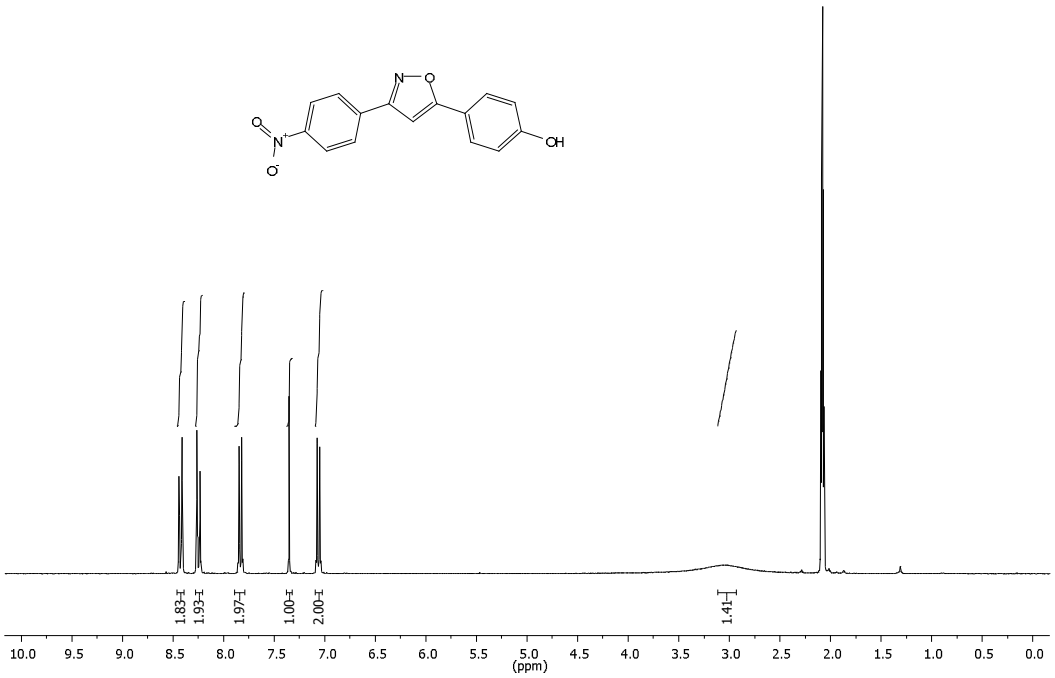

S 14. ^{1}H NMR spectrum of compound 3-(4-nitrophenyl)-5-(4-hydroxiphenyl)isoxazole (Acetone-d^{6}, 300 MHz).

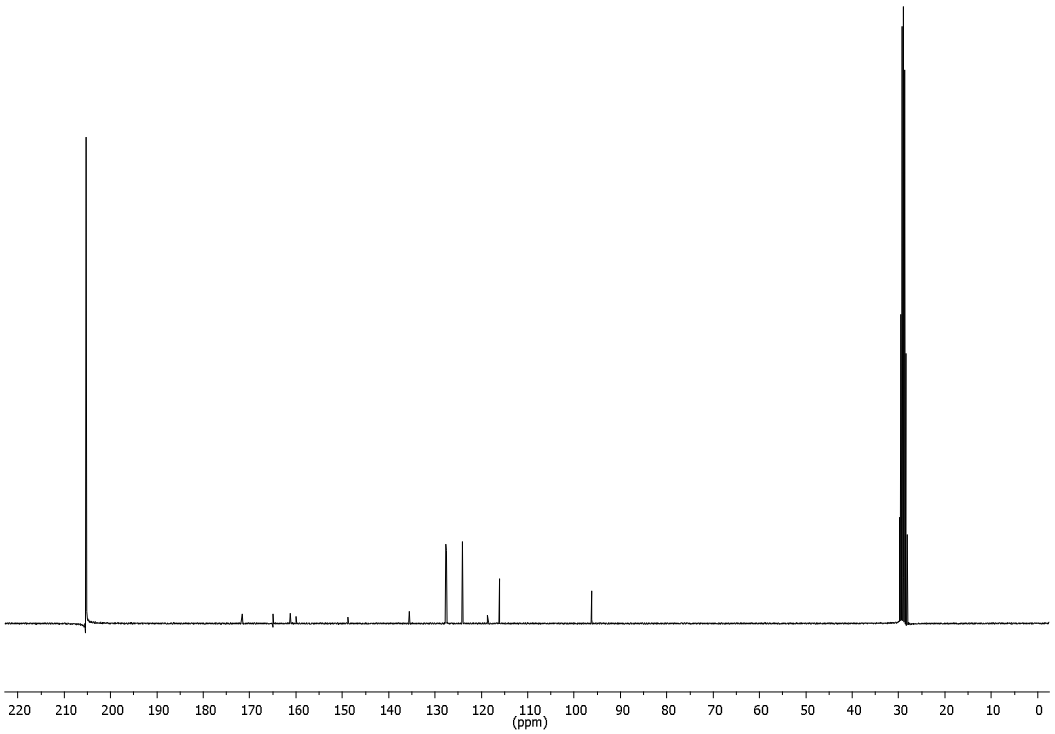

S 15. ^{13}C NMR spectrum of compound 3-(4-nitrophenyl)-5-(4-hydroxiphenyl)isoxazole (Acetone-d^6, 75 MHz).

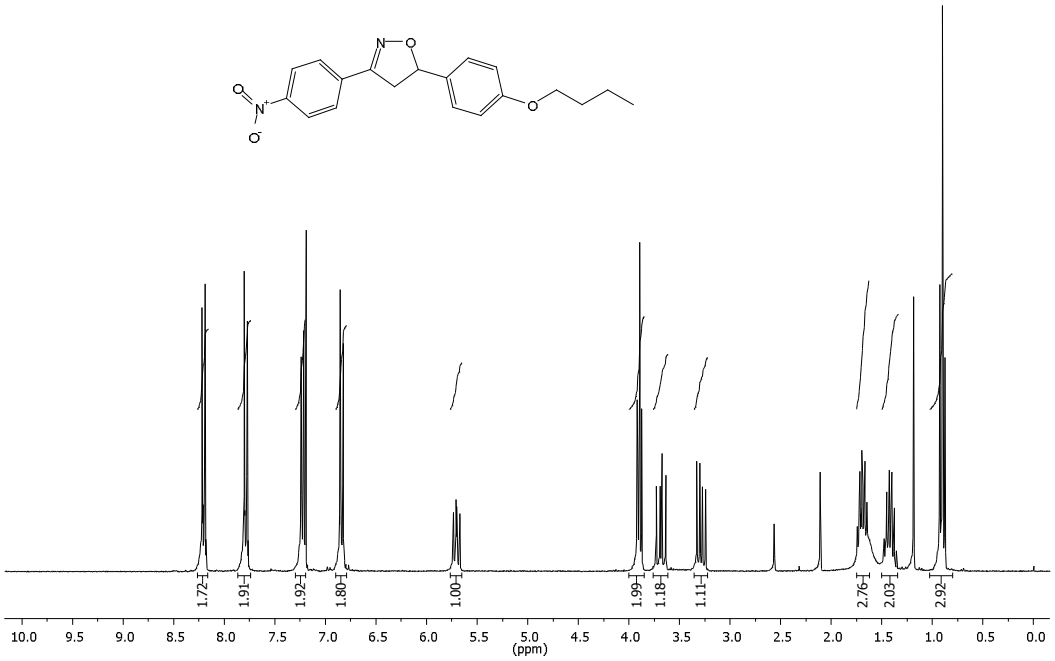

S 16. ^{1}H NMR spectrum of compound 3-(4-nitrophenyl)-5-(4-*n*-butoxyphenyl)isoxazoline ($CDCl_3$, 300 MHz).

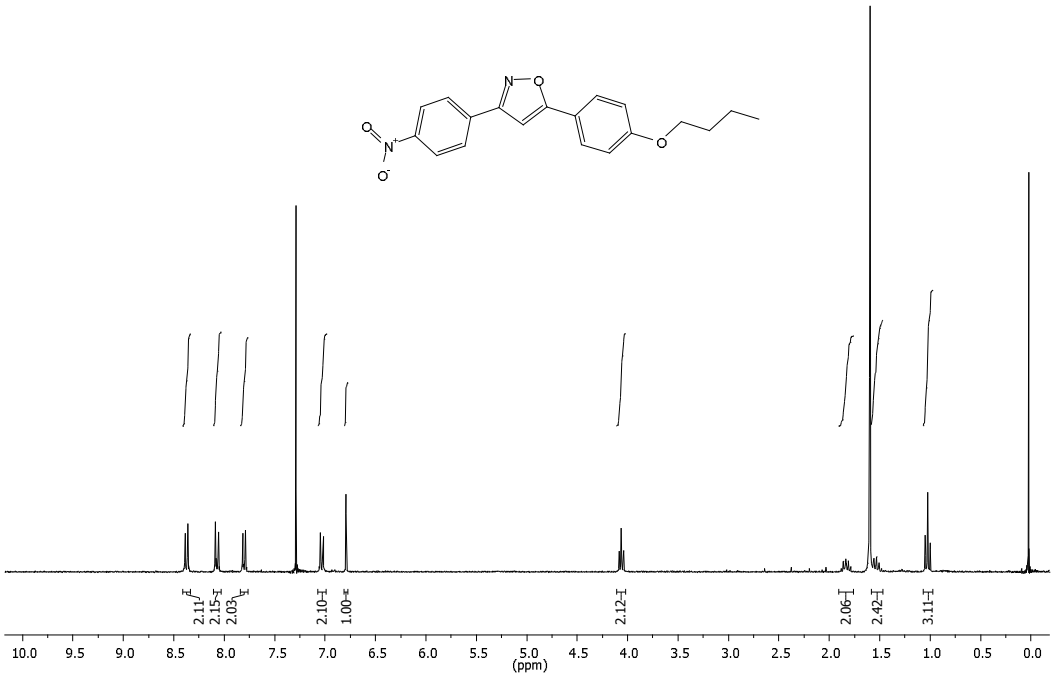

S 17. ^{1}H NMR spectrum of compound 3-(4-nitrophenyl)-5-(4-*n*-butoxyphenyl)isoxazole ($CDCl_3$, 300 MHz).

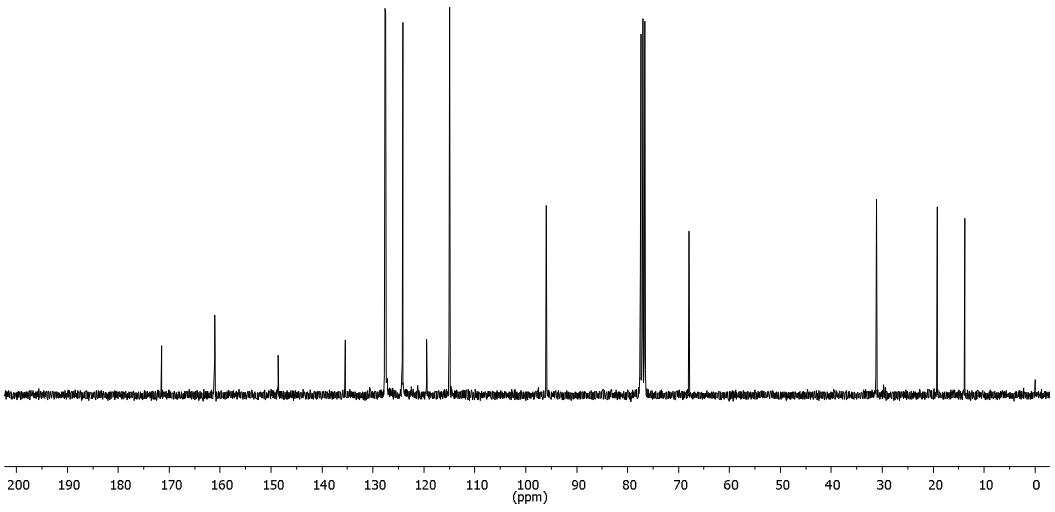

S 18. ^{13}C NMR spectrum of compound 3-(4-nitrophenyl)-5-(4-*n*-butoxyphenyl)isoxazole ($CDCl_3$, 75 MHz).

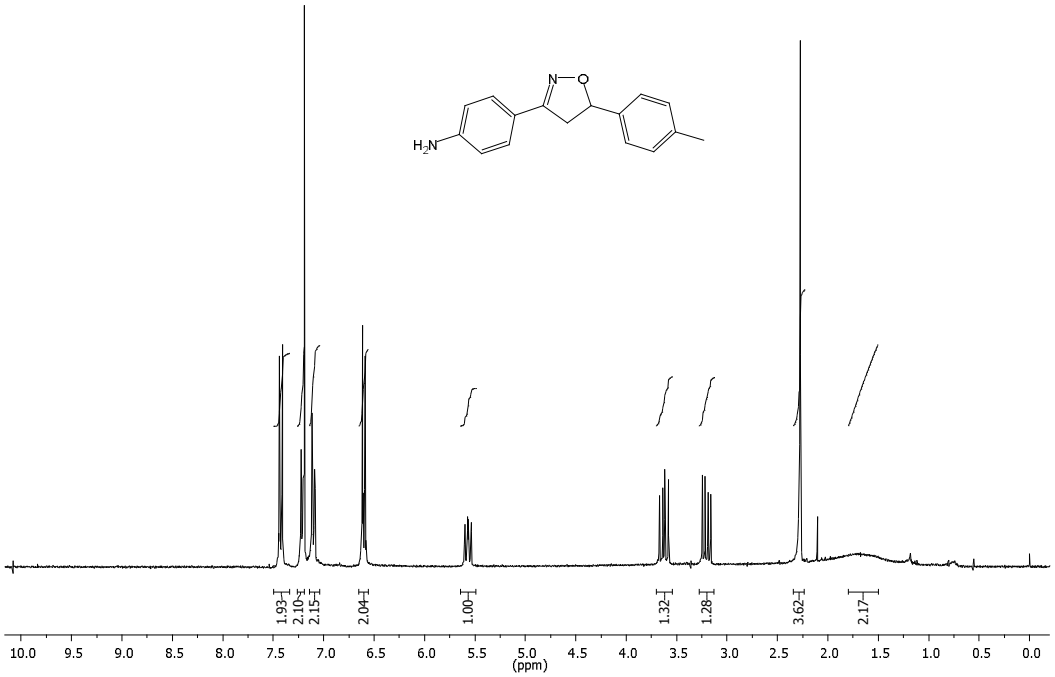

S 19. ^{1}H NMR spectrum of compound **5a** ($CDCl_3$, 300 MHz).

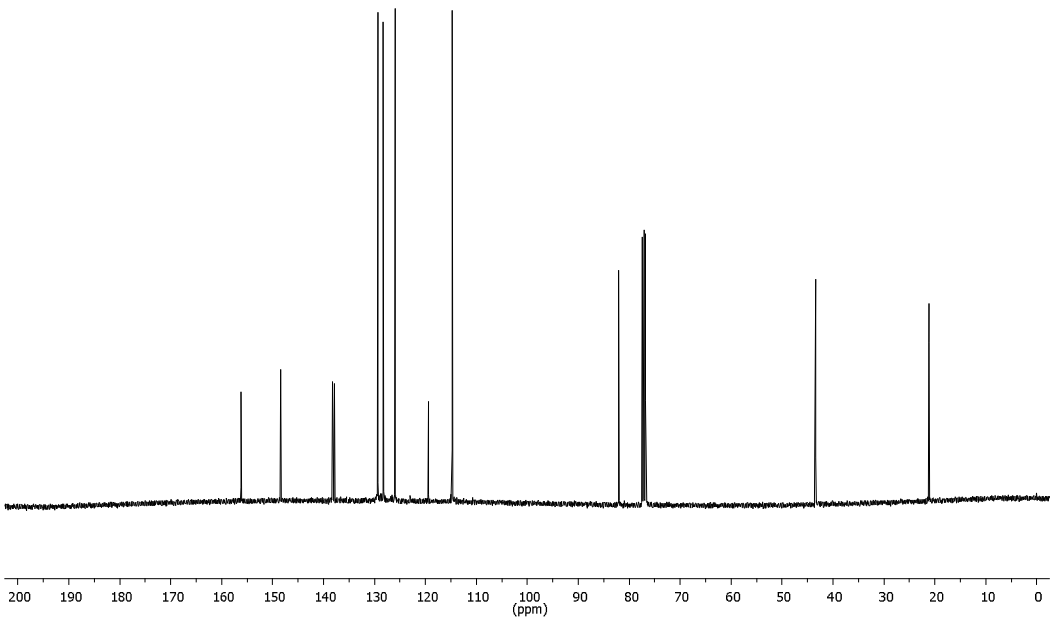

S 20. ^{13}C NMR spectrum of compound **5a** ($CDCl_3$, 100 MHz).

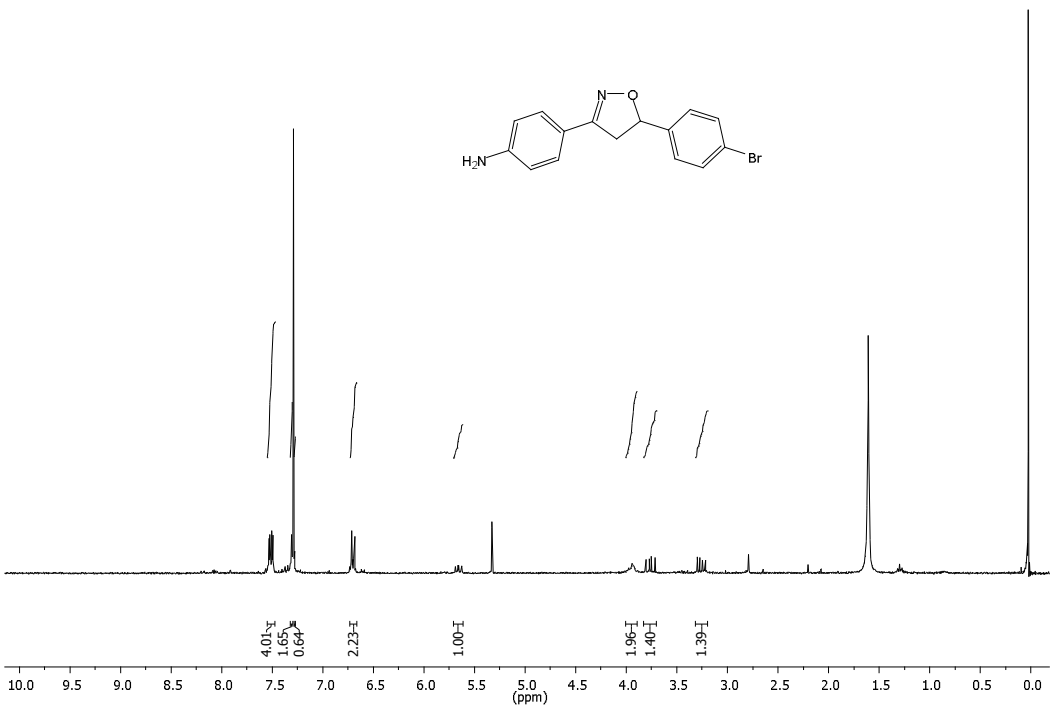

S 21. ^{1}H NMR spectrum of compound **5b** ($CDCl_3$, 300 MHz).

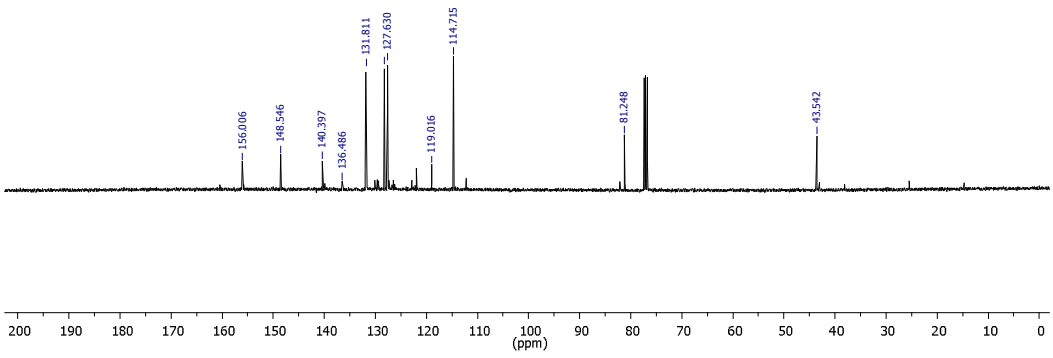

S 22. ^{13}C NMR spectrum of compound **5b** ($CDCl_3$, 100 MHz).

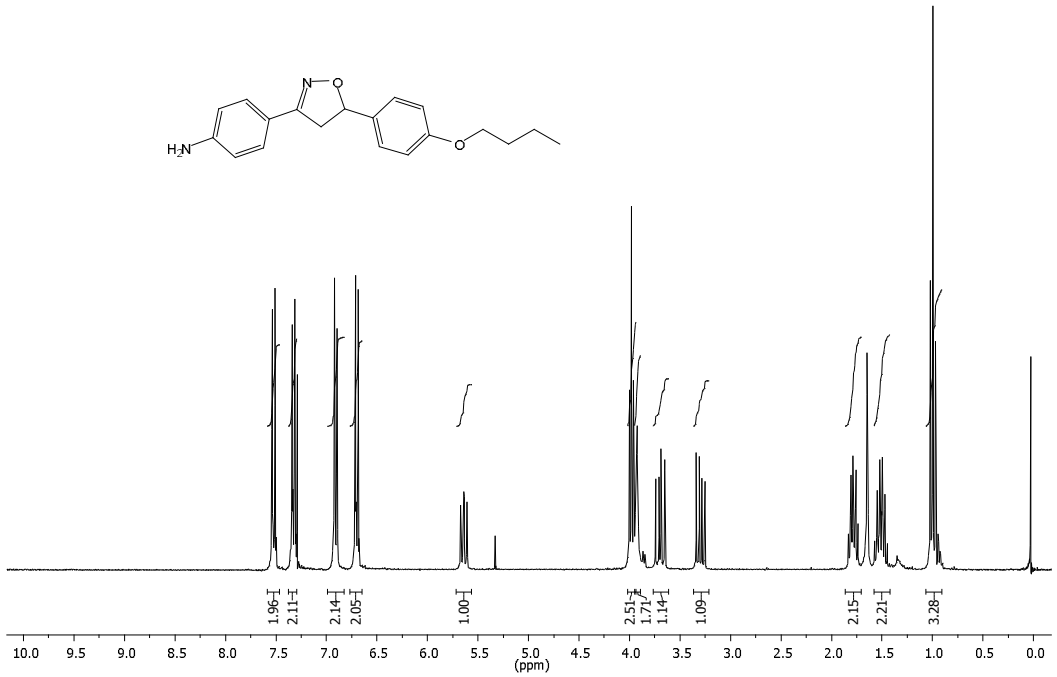

S 23. ^{1}H NMR spectrum of compound **5d** ($CDCl_3$, 300 MHz).

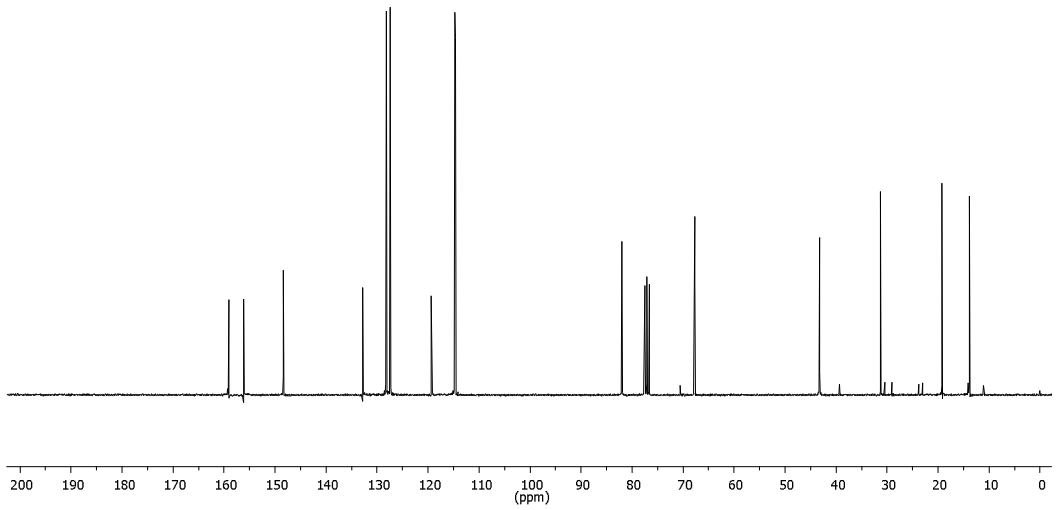

S 24. ^{13}C NMR spectrum of compound **5d** ($CDCl_3$, 75 MHz).

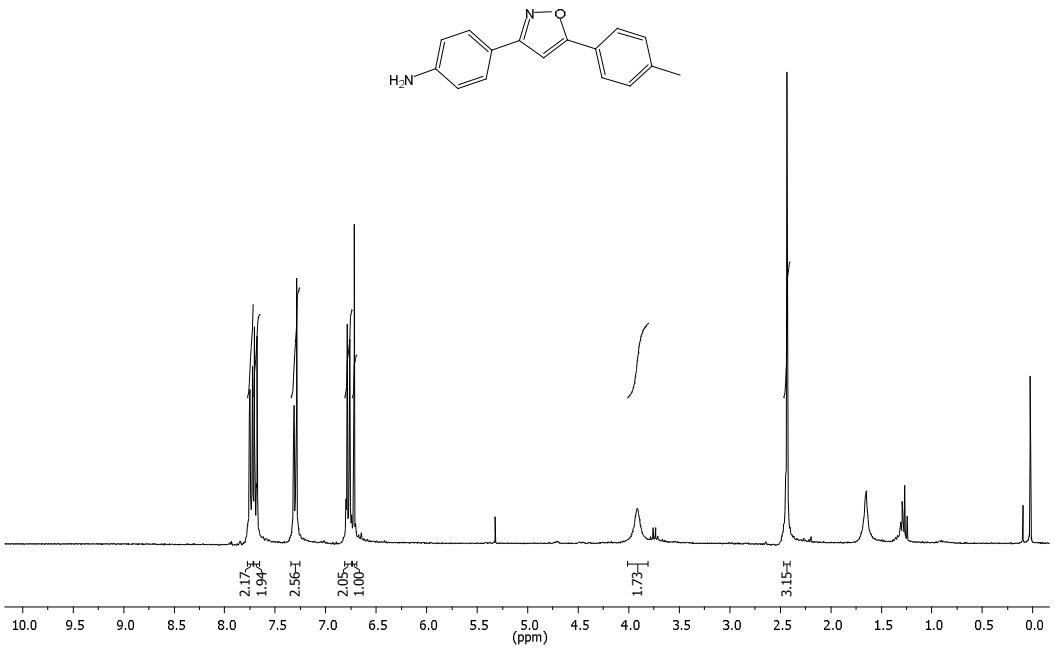

S 25. ^{1}H NMR spectrum of compound **7a** ($CDCl_3$, 300 MHz).

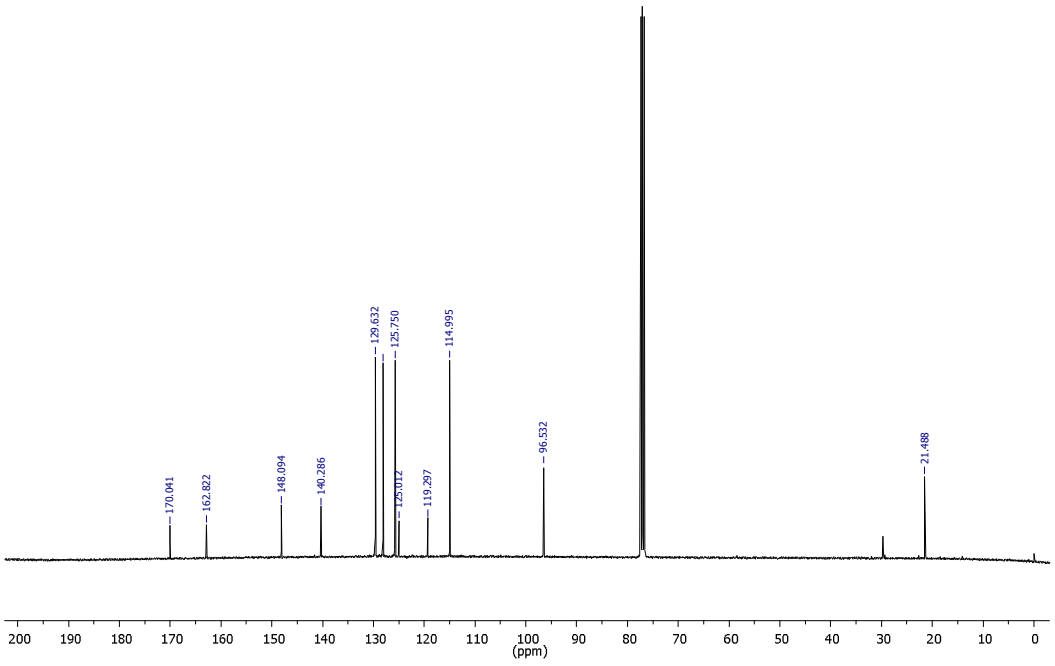

S 26. ^{13}C NMR spectrum of compound **7a** ($CDCl_3$, 100 MHz).

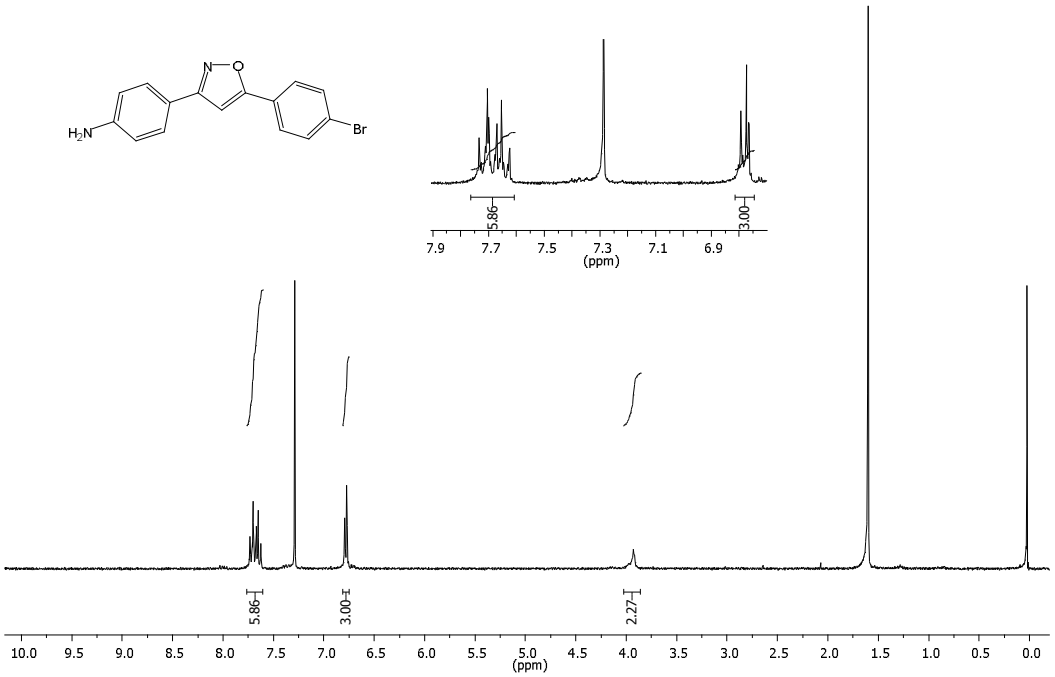

S 27. ^{1}H NMR spectrum of compound **7b** ($CDCl_3$, 300 MHz).

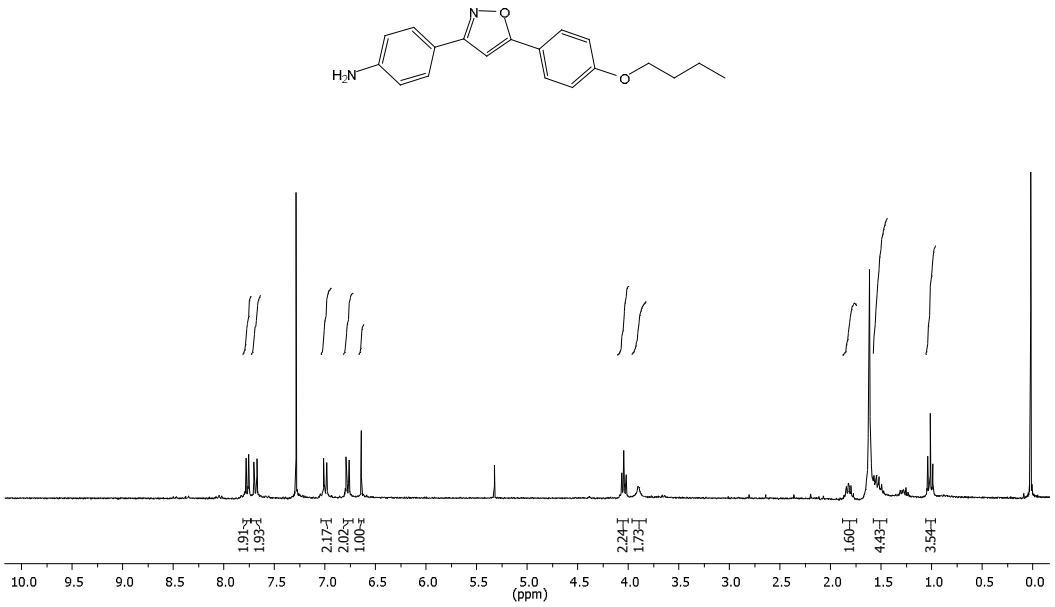

S 28. ^{1}H NMR spectrum of compound **7d** ($CDCl_3$, 300 MHz).

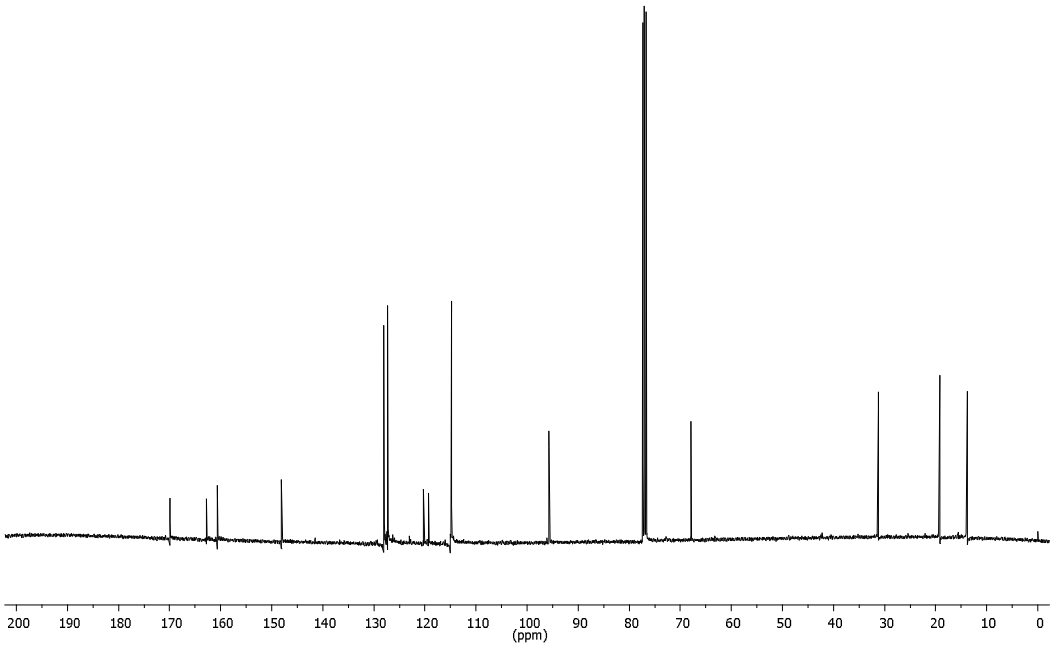

S 29. ^{13}C NMR spectrum of compound **7d** ($CDCl_3$, 300 MHz).

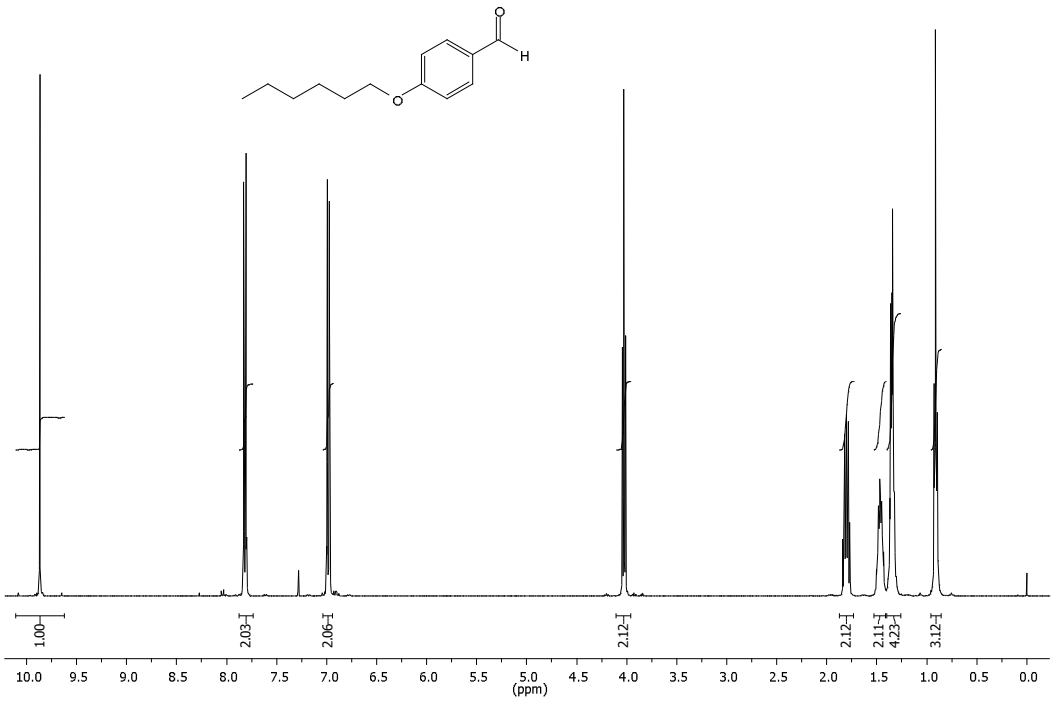

S 30. ^{1}H NMR spectrum of compound **8a** ($CDCl_3$, 400 MHz).

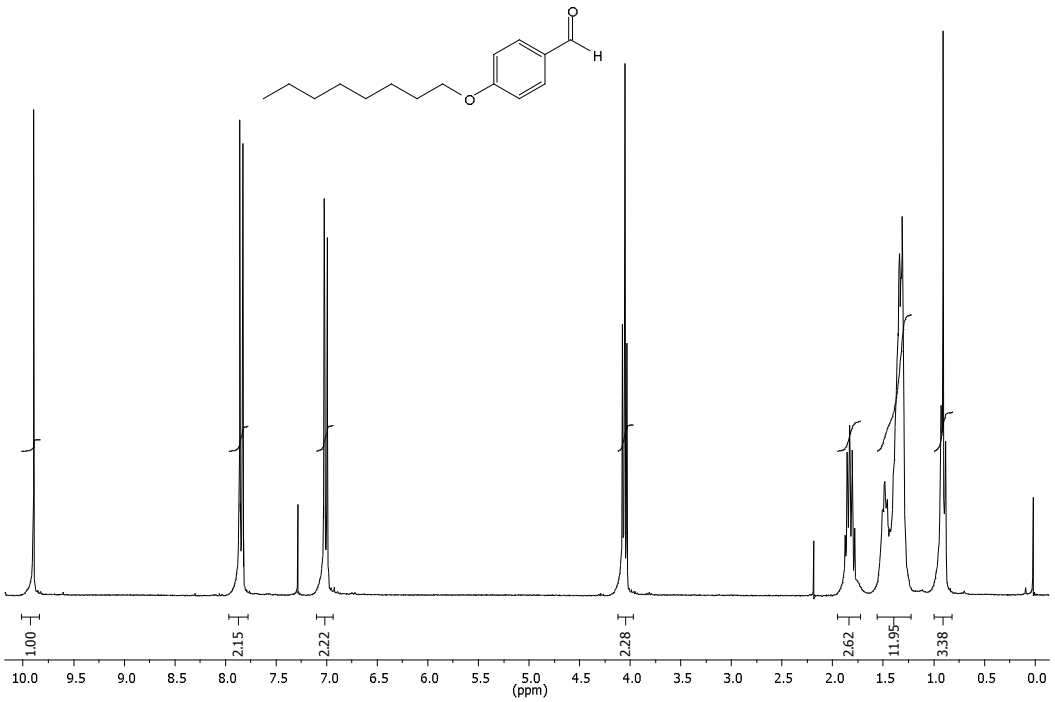

S 31. ^{1}H NMR spectrum of compound **8b** ($CDCl_3$, 300 MHz).

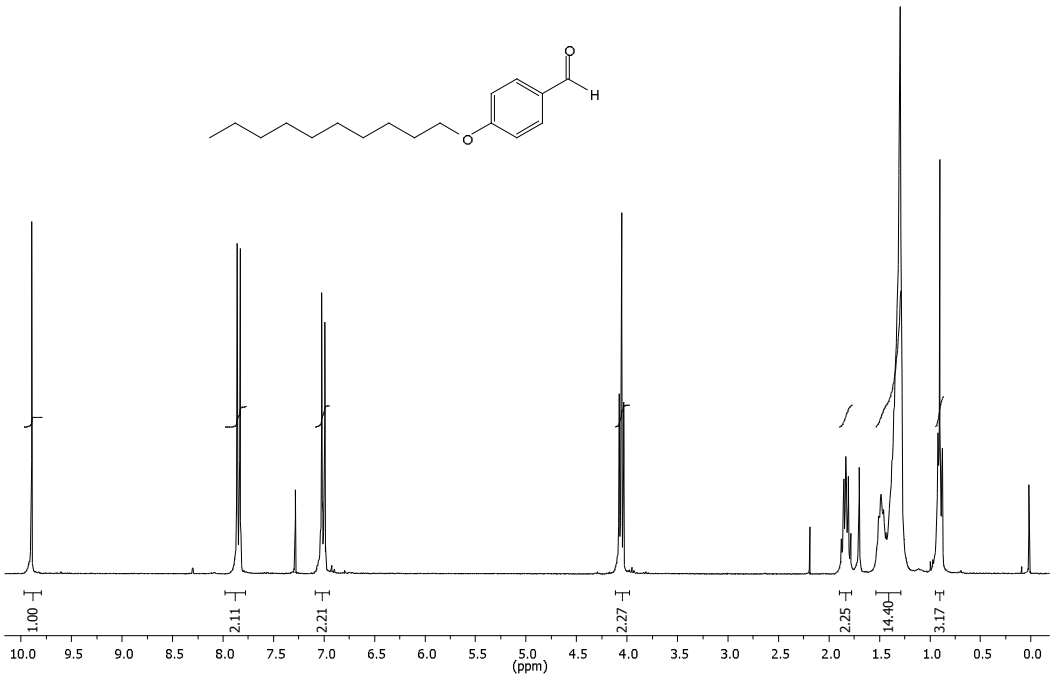

S 32. ^{1}H NMR spectrum of compound **8c** ($CDCl_3$, 300 MHz).

S 33. ^{1}H NMR spectrum of compound **8d** ($CDCl_3$, 400 MHz).

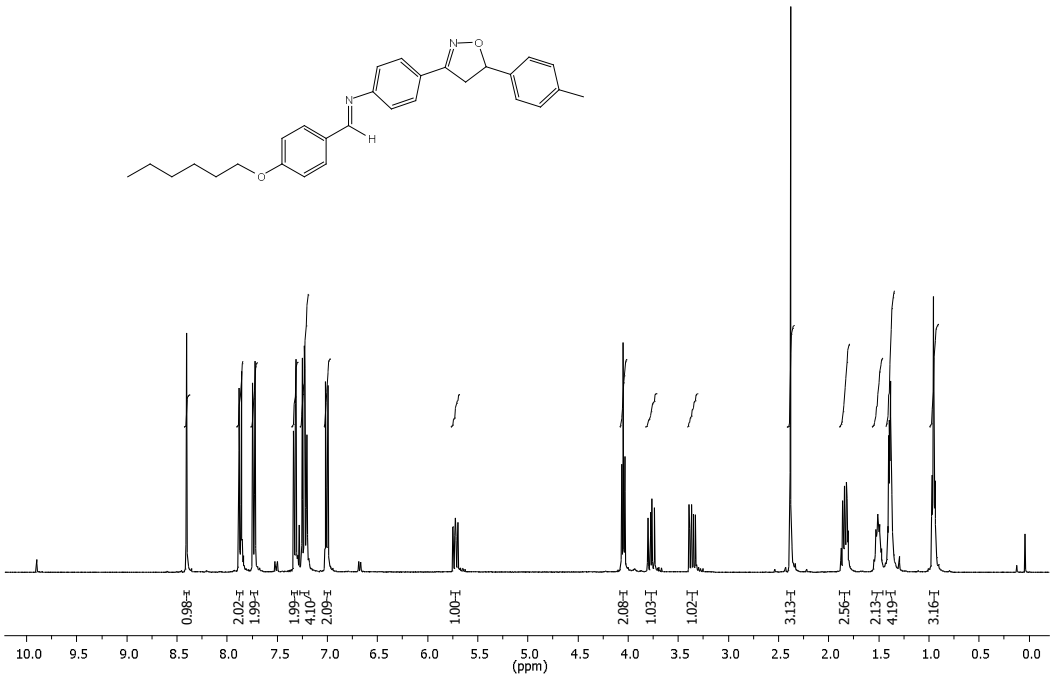

S 34. ^{1}H NMR spectrum of compound **9a** ($CDCl_3$, 400 MHz).

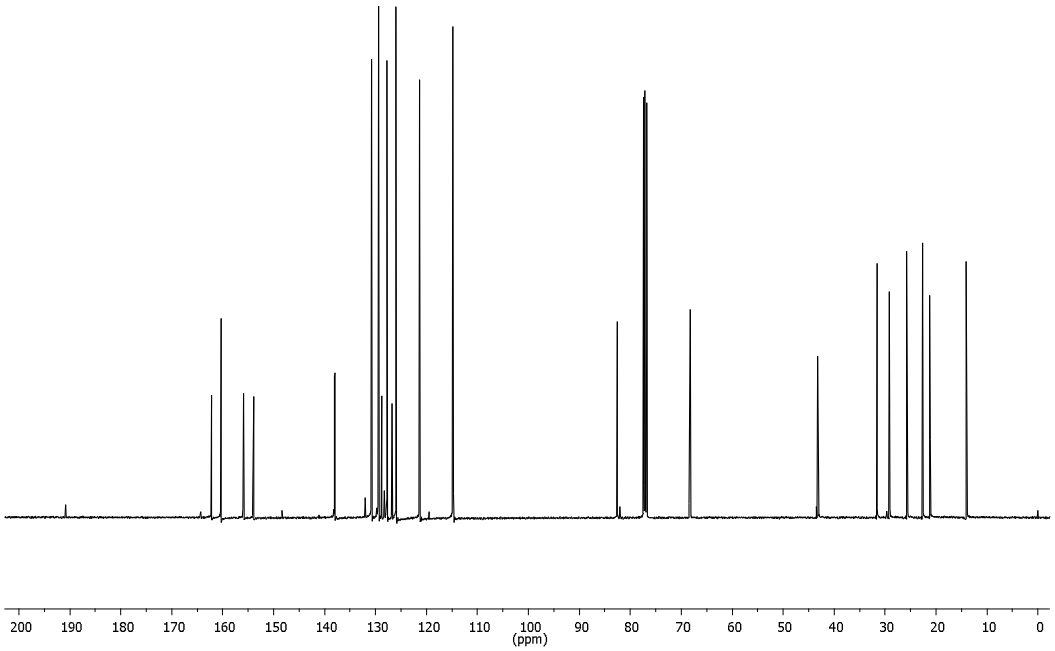

S 35. ^{13}C NMR spectrum of compound **9a** ($CDCl_3$, 100 MHz).

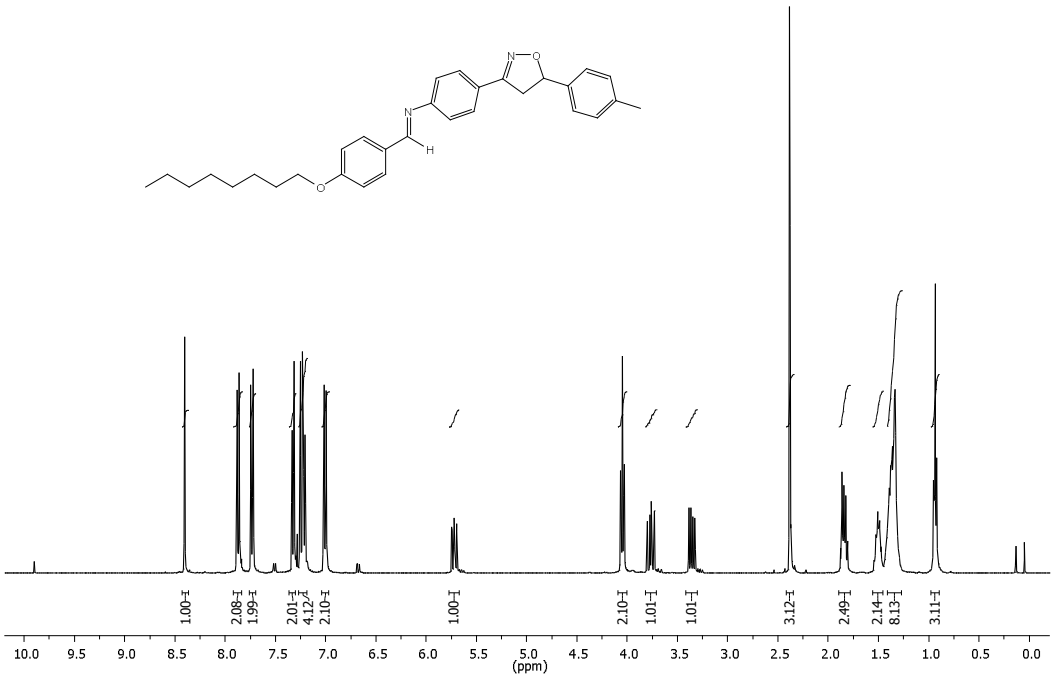

S 36. ^{1}H NMR spectrum of compound **9b** ($CDCl_3$, 400 MHz).

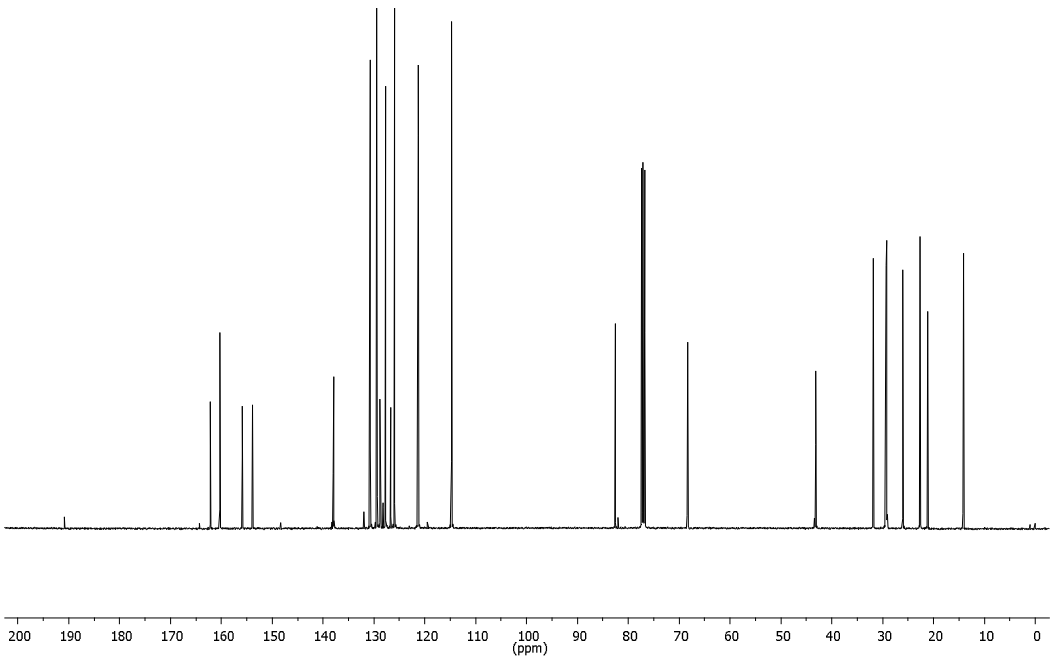

S 37. ^{13}C NMR spectrum of compound **9b** ($CDCl_3$, 100 MHz).

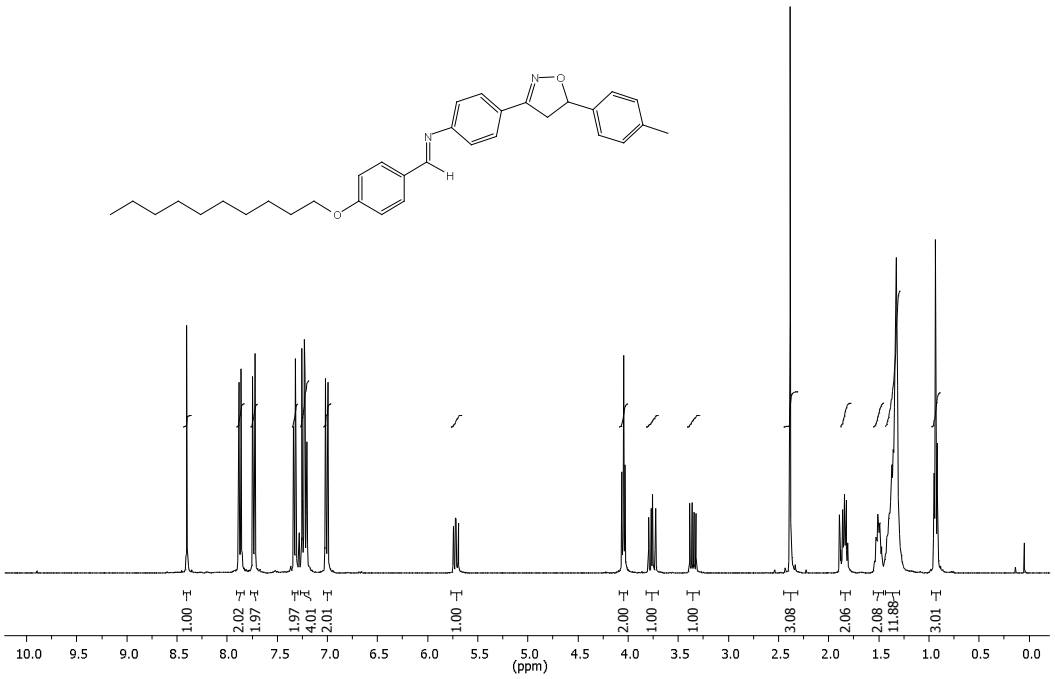

S 38. ^{1}H NMR spectrum of compound **9c** ($CDCl_3$, 400 MHz).

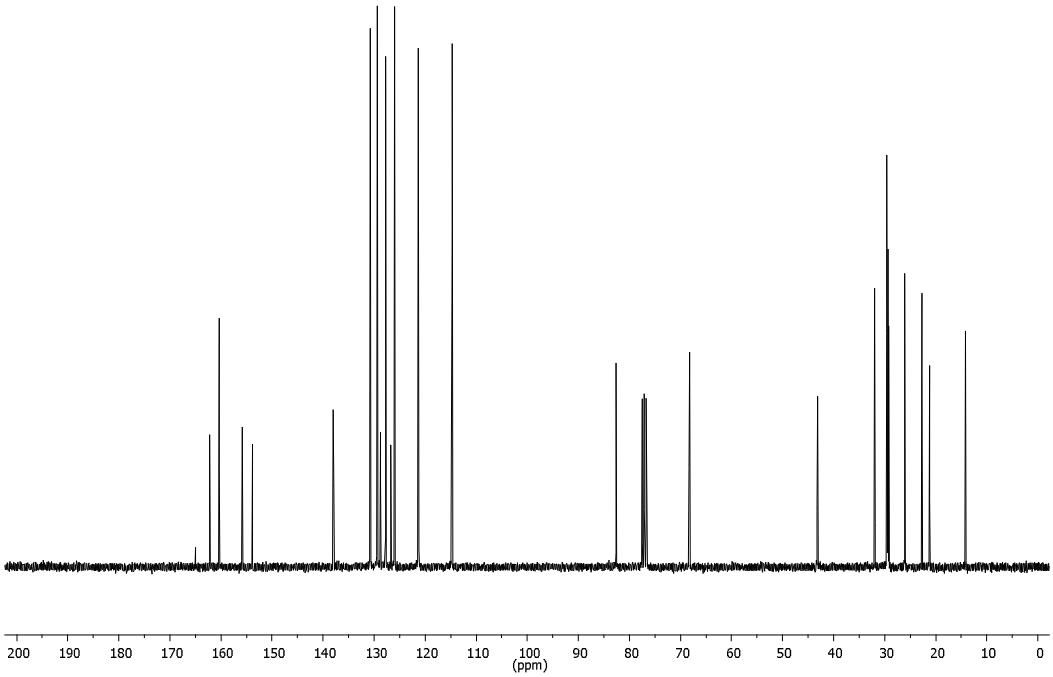

S 39. ^{13}C NMR spectrum of compound **9c** ($CDCl_3$, 75 MHz).

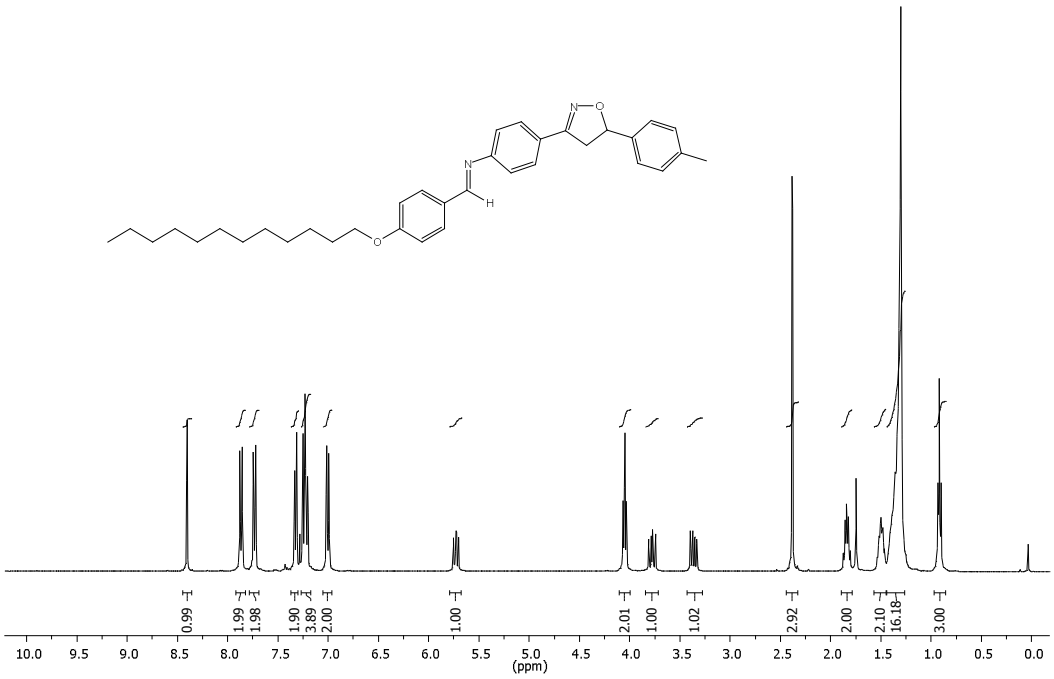

S 40. ^{1}H NMR spectrum of compound **9d** ($CDCl_3$, 400 MHz).

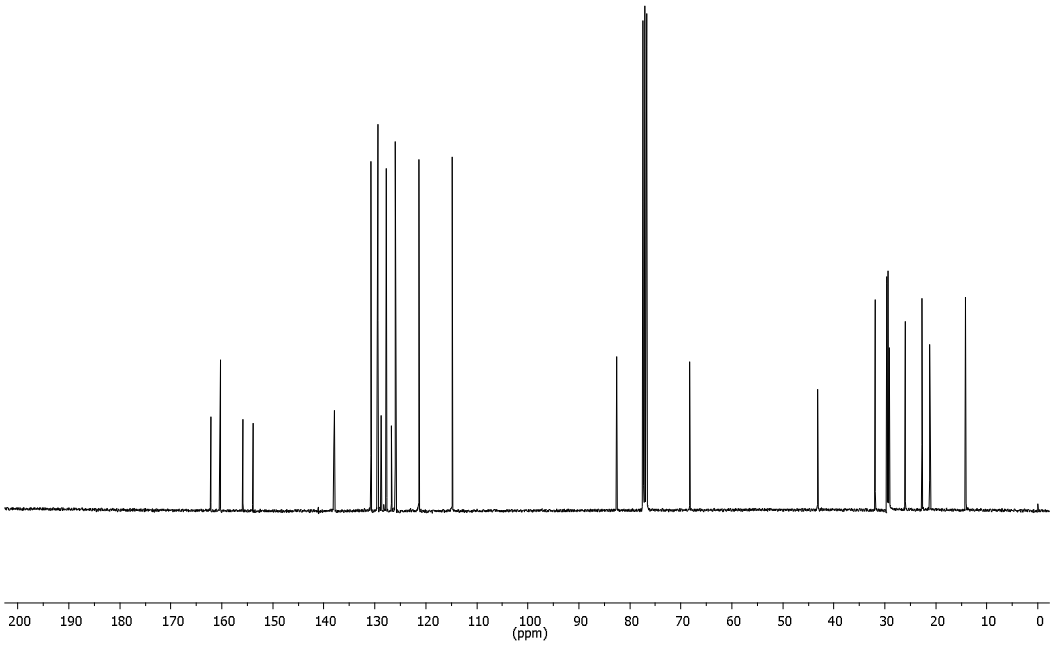

S 41. ^{13}C NMR spectrum of compound **9d** ($CDCl_3$, 100 MHz).

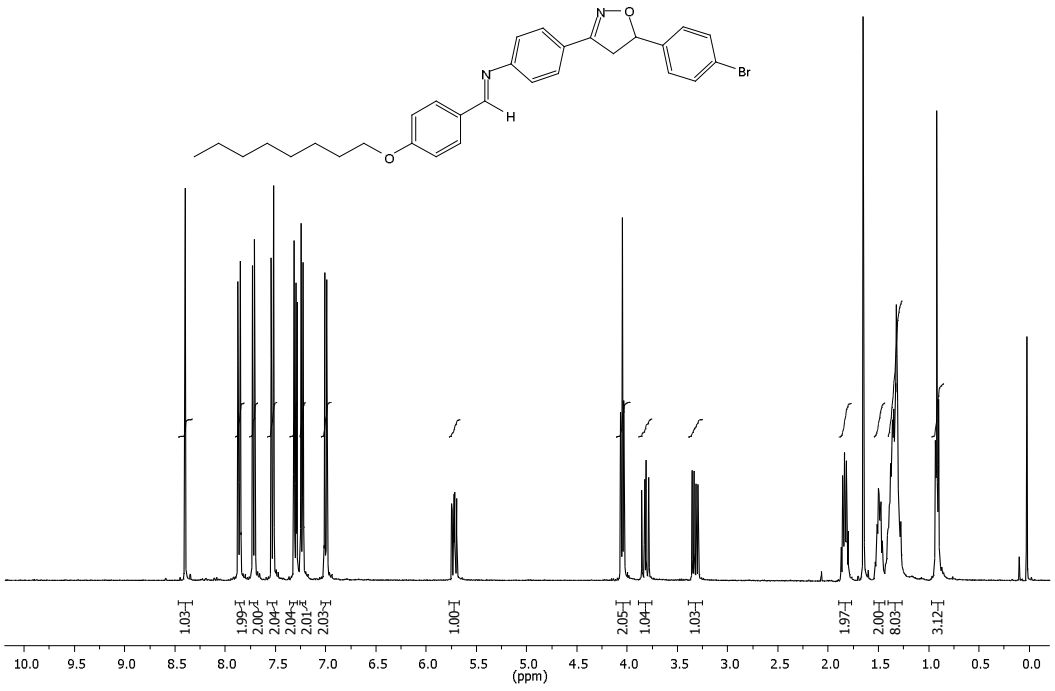

S 42. ^{1}H NMR spectrum of compound **9e** ($CDCl_3$, 400 MHz).

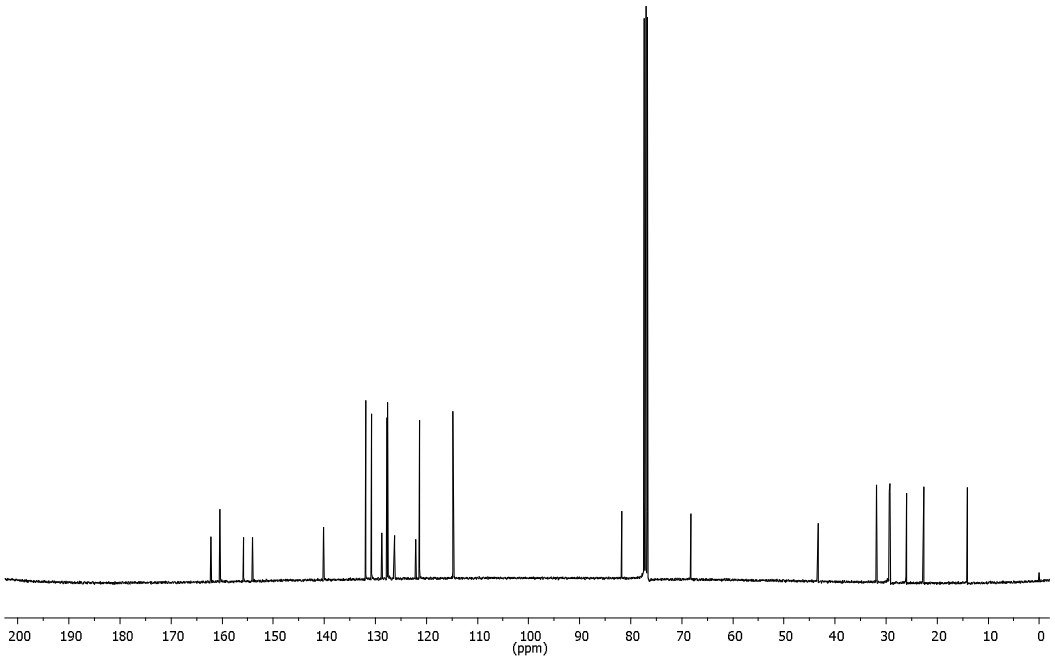

S 43. ^{13}C NMR spectrum of compound **9e** ($CDCl_3$, 100 MHz).

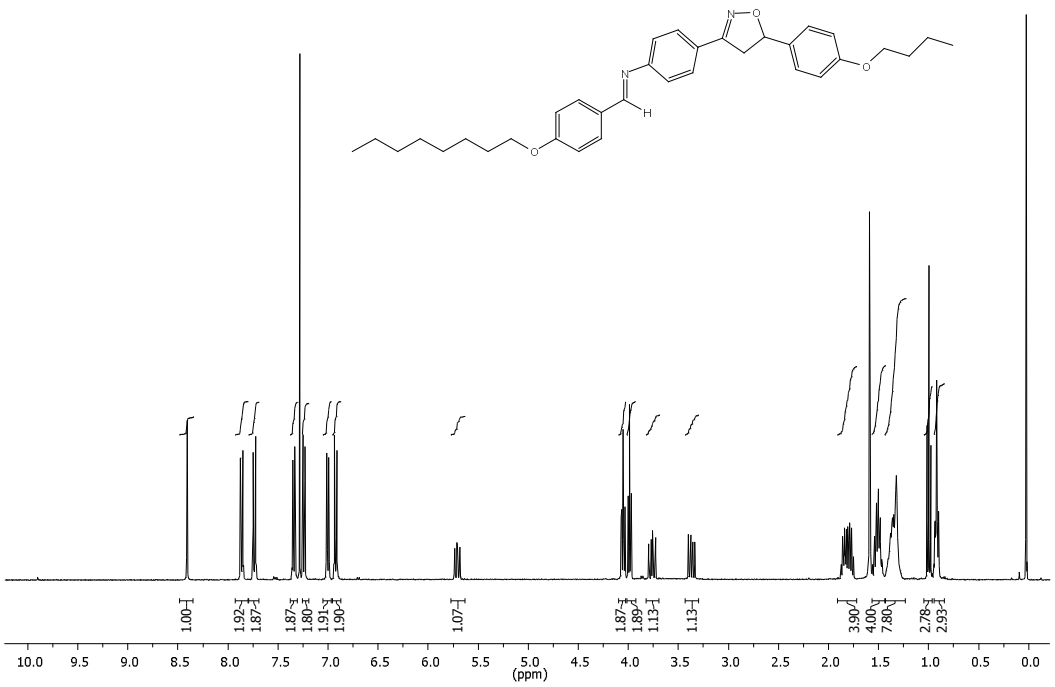

S 44. ^{1}H NMR spectrum of compound **9f** ($CDCl_3$, 400 MHz).

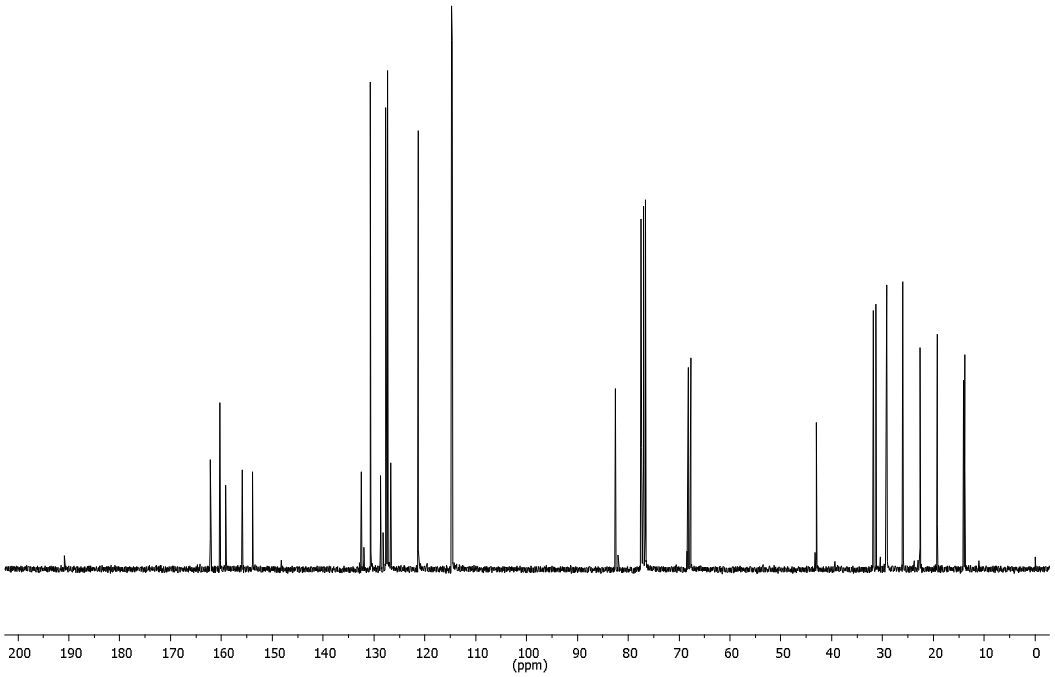

S 45. ^{13}C NMR spectrum of compound **9f** ($CDCl_3$, 75 MHz).

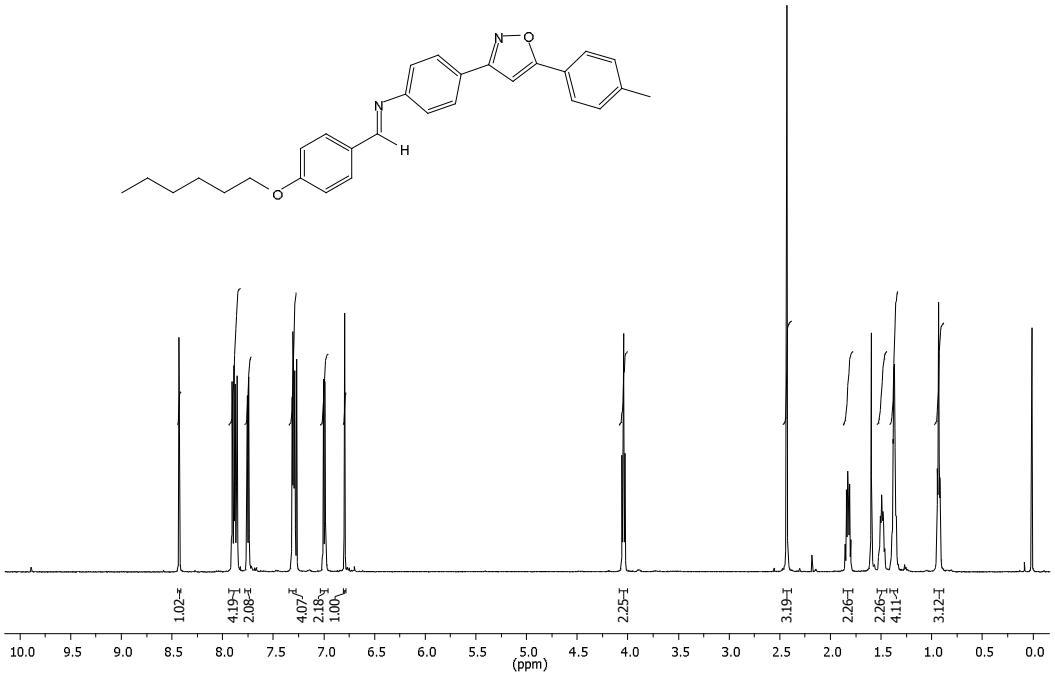

S 46. ^{1}H NMR spectrum of compound **10a** ($CDCl_3$, 500 MHz).

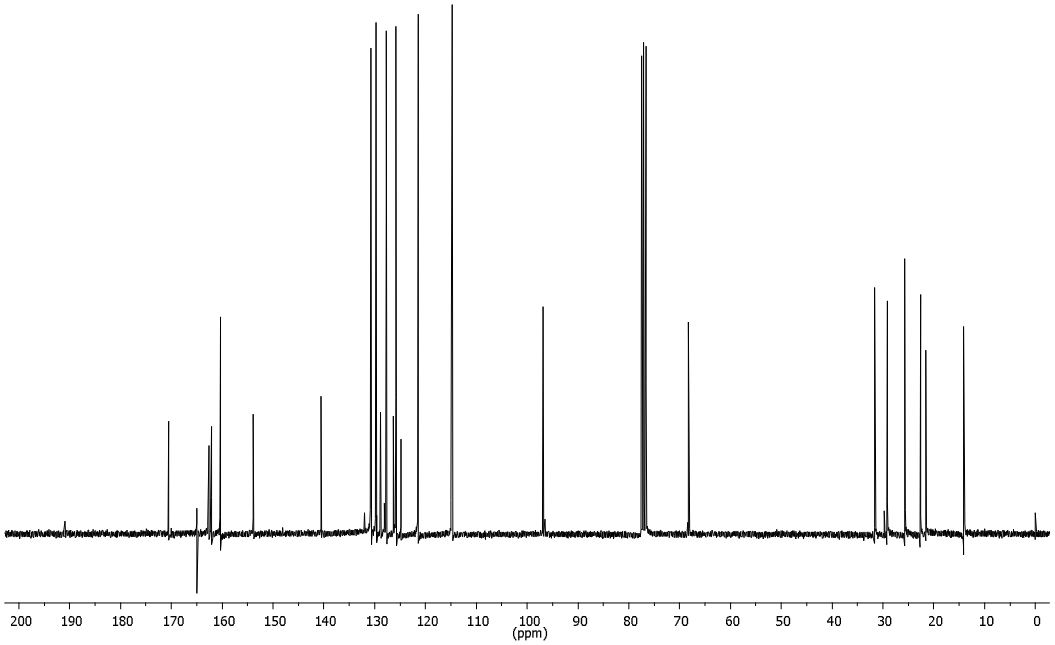

S 47. ^{13}C NMR spectrum of compound **10a** ($CDCl_3$, 75 MHz).

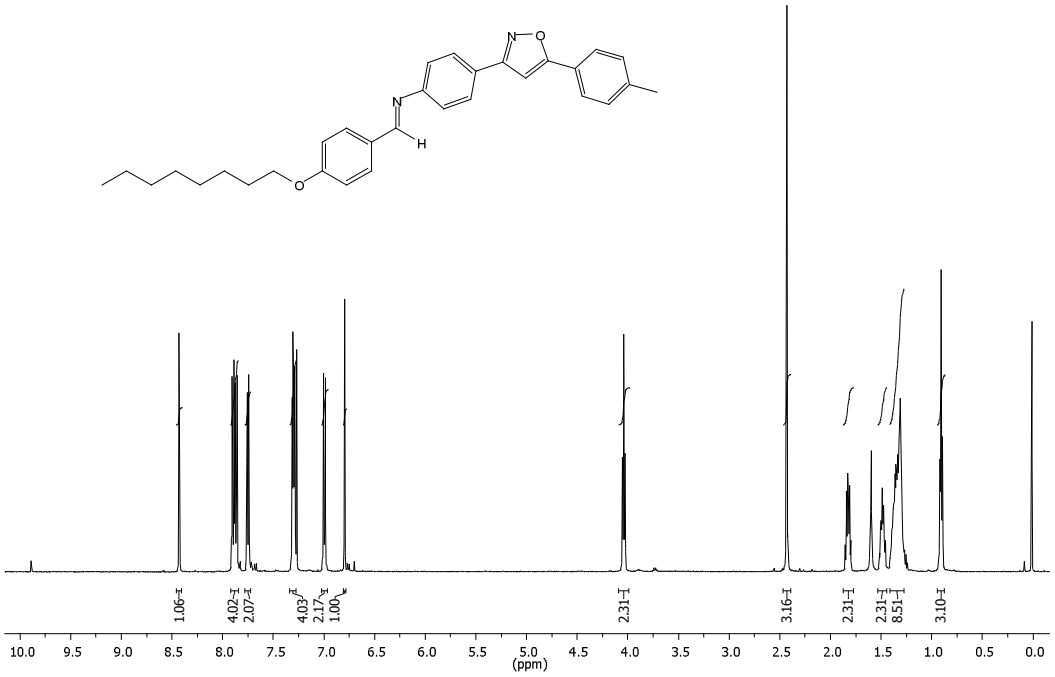

S 48. ^{1}H NMR spectrum of compound **10b** ($CDCl_3$, 500 MHz).

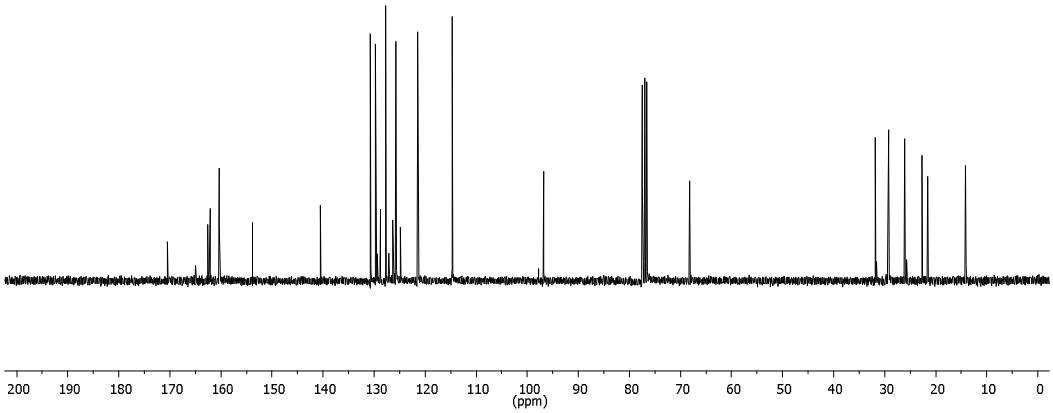

S 49. ^{13}C NMR spectrum of compound **10b** ($CDCl_3$, 75 MHz).

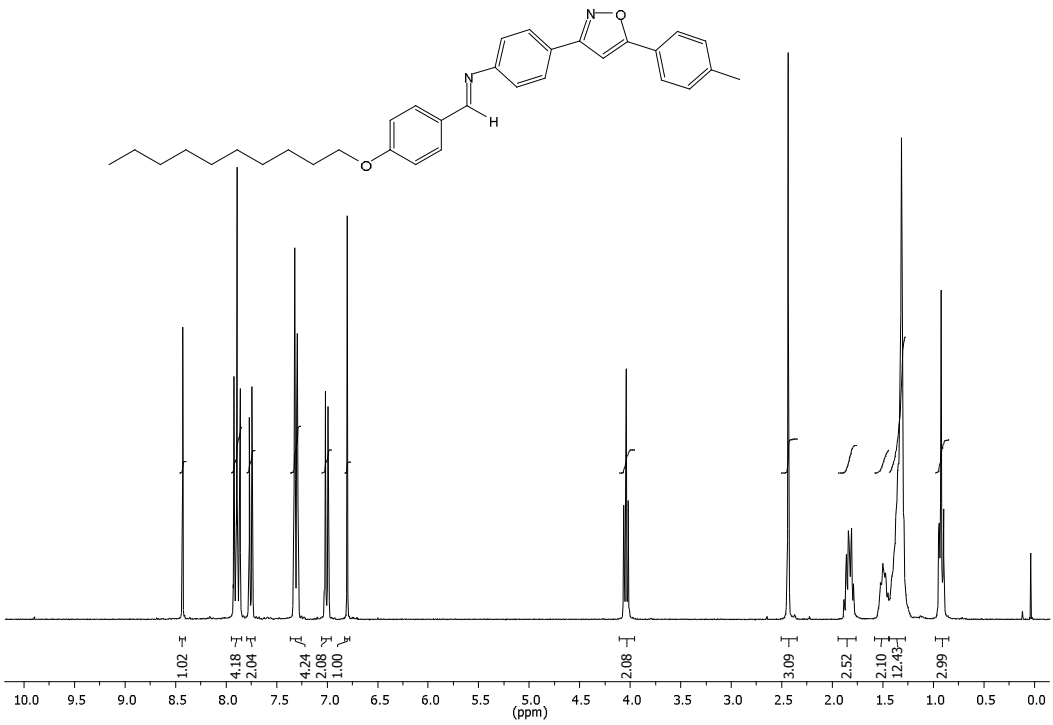

S 50. ^{1}H NMR spectrum of compound **10c** ($CDCl_3$, 300 MHz).

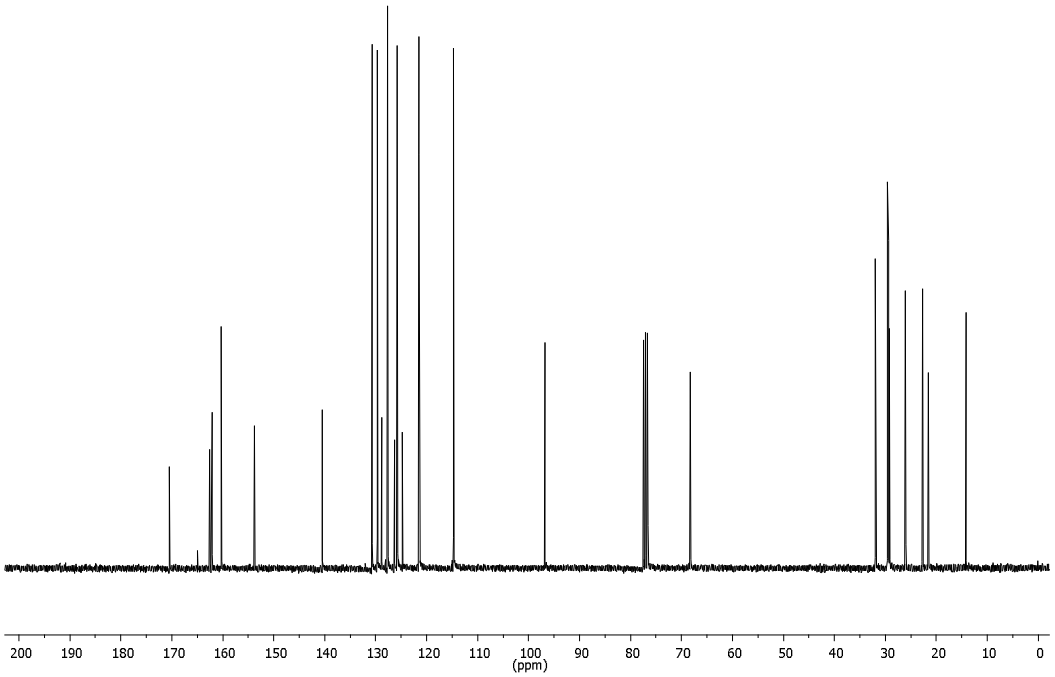

S 51. ^{13}C NMR spectrum of compound **10c** ($CDCl_3$, 75 MHz).

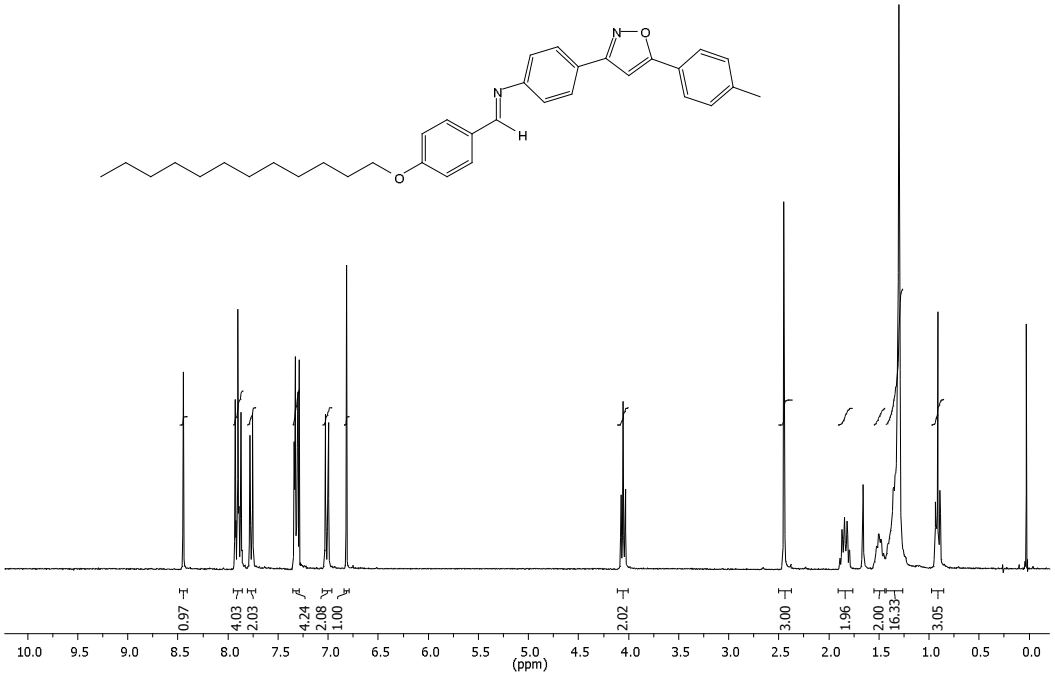

S 52. ^{1}H NMR spectrum of compound **10d** ($CDCl_3$, 300 MHz).

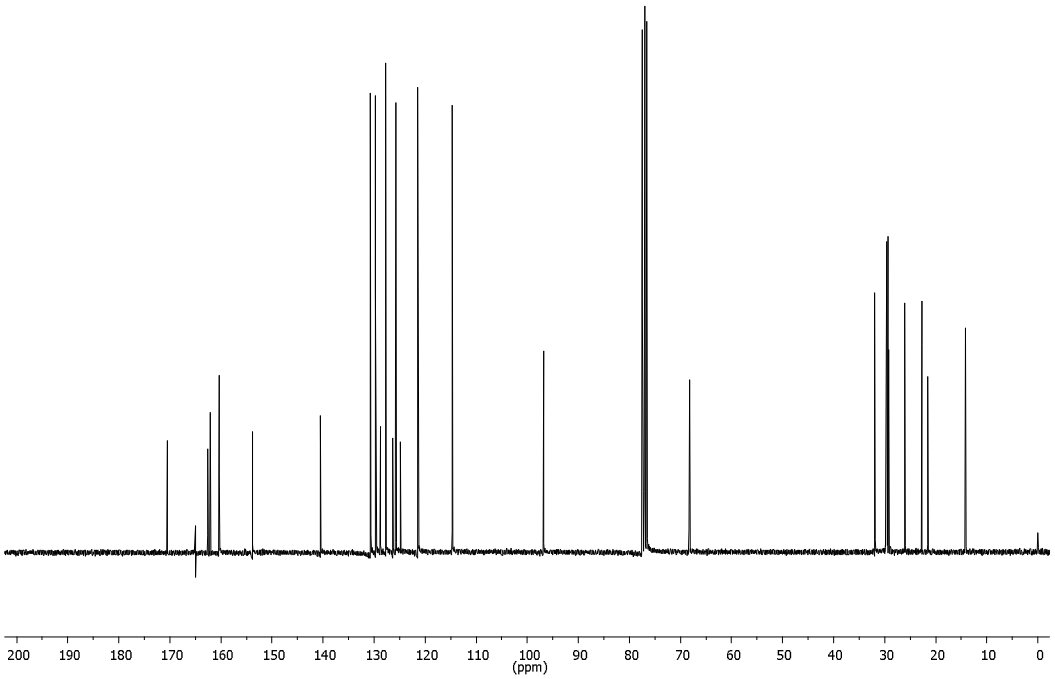

S 53. ^{13}C NMR spectrum of compound **10d** ($CDCl_3$, 75 MHz).

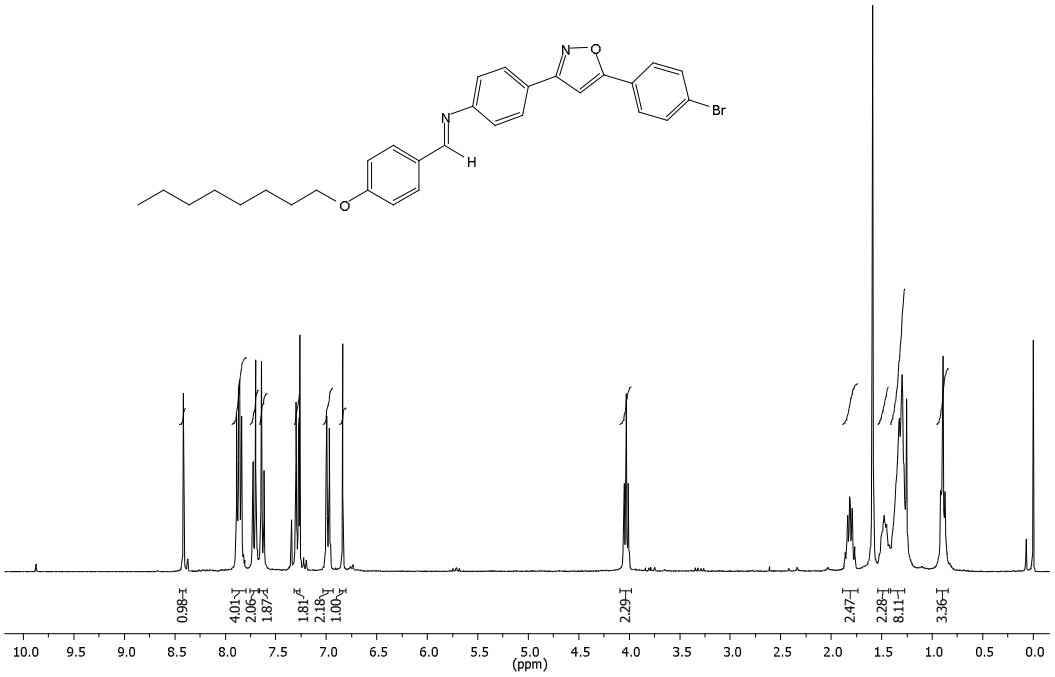

S 54. ^{1}H NMR spectrum of compound **10e** ($CDCl_3$, 300 MHz).

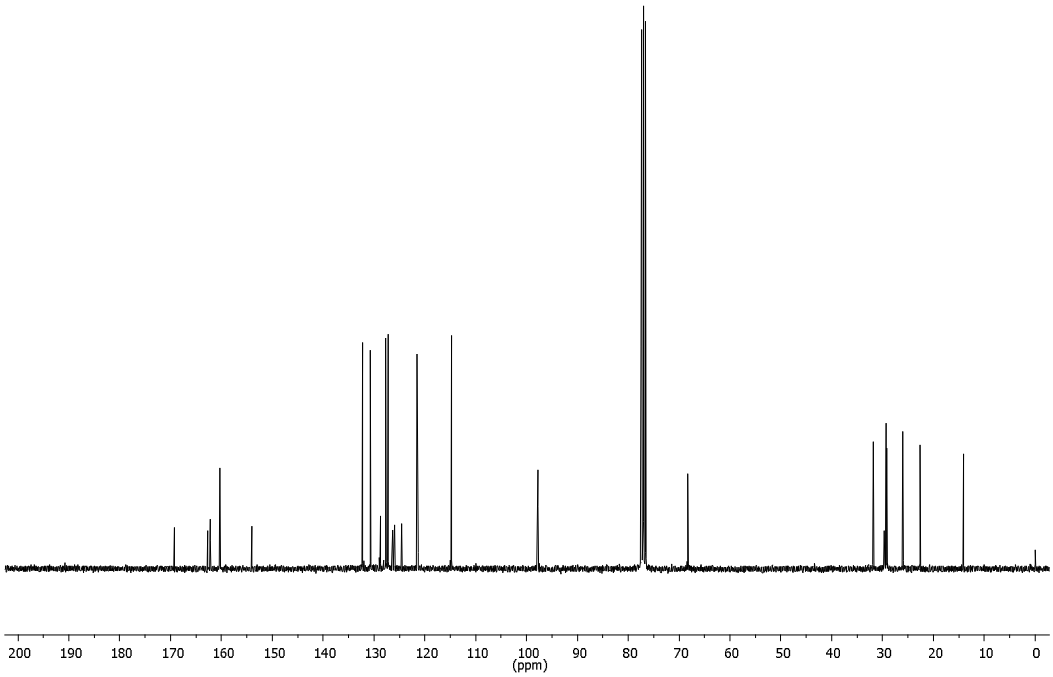

S 55. ^{13}C NMR spectrum of compound **10e** ($CDCl_3$, 75 MHz).

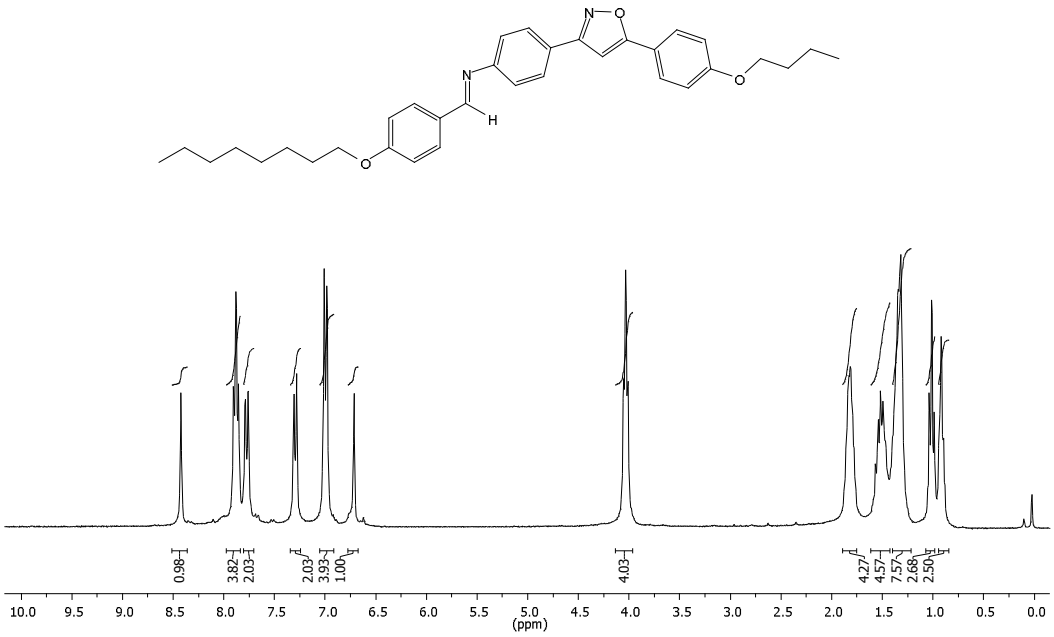

S 56. ^{1}H NMR spectrum of compound **10f** ($CDCl_3$, 300 MHz).

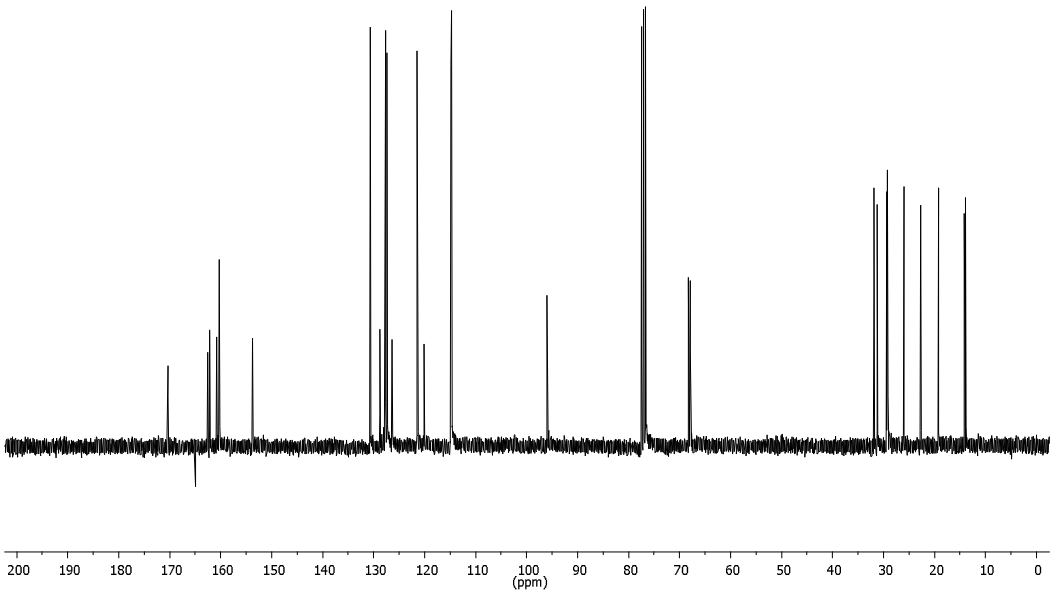

S 57. ^{13}C NMR spectrum of compound **10f** ($CDCl_3$, 75 MHz).

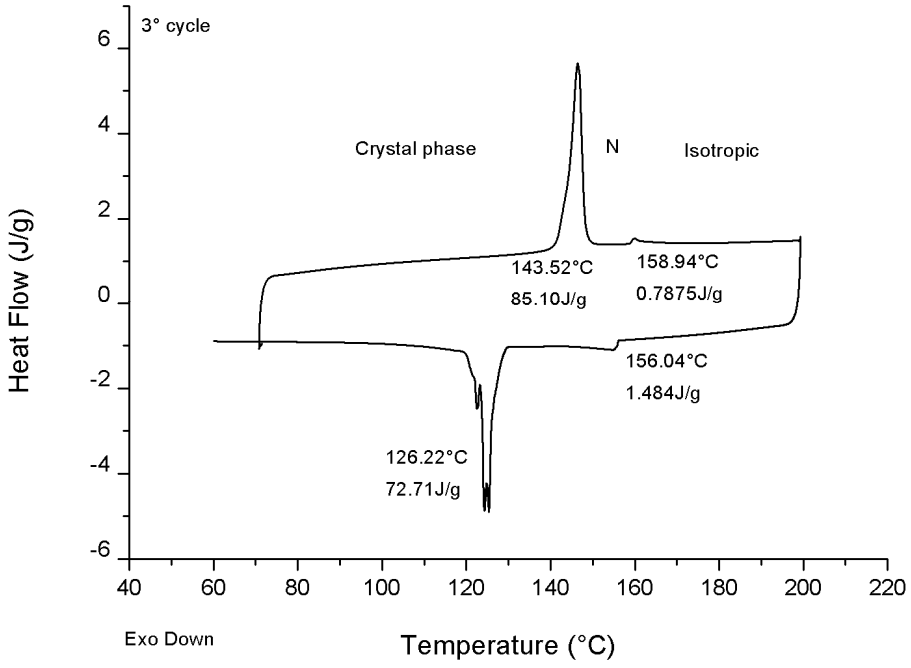

S 58. DSC thermogram for compound **9a**.

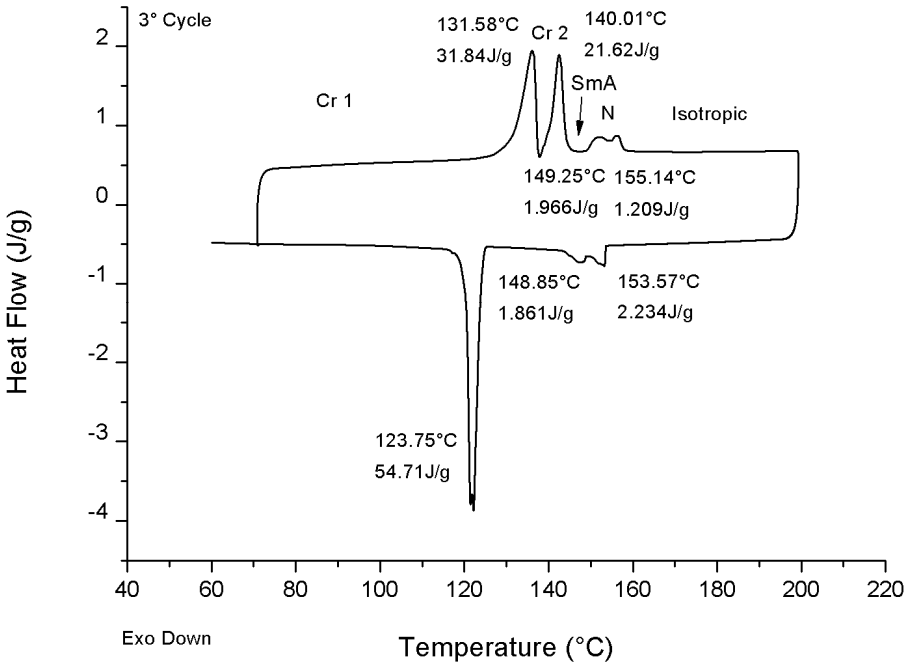

S 59. DSC thermogram for compound **9b**.

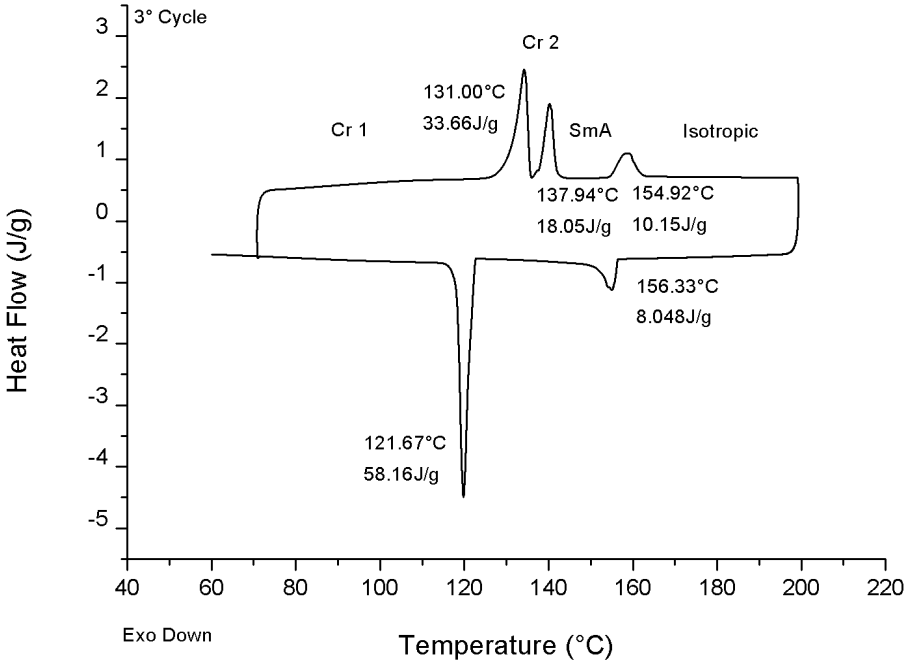

S 60. DSC thermogram for compound **9c**.

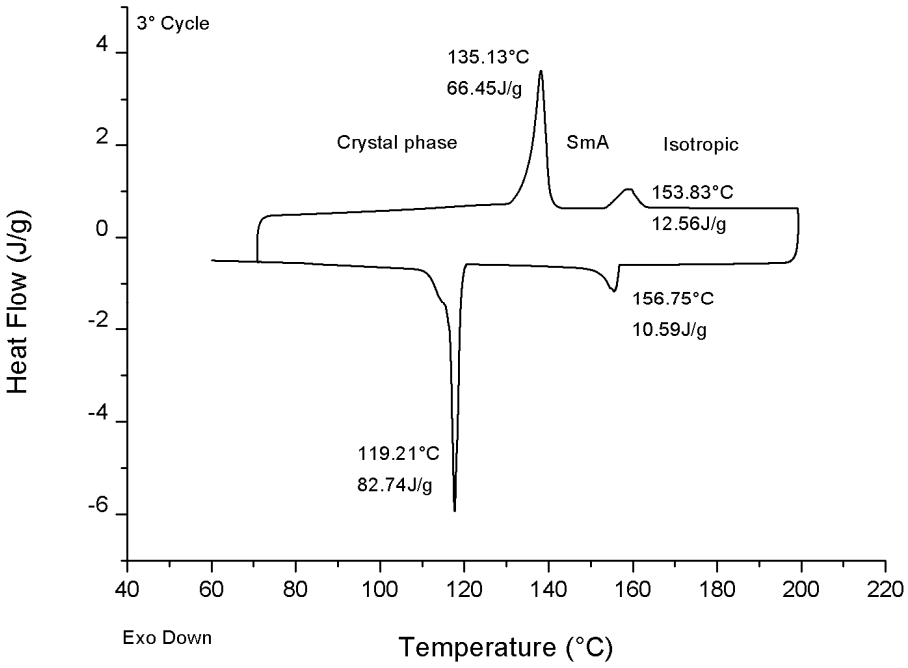

S 61. DSC thermogram for compound **9d**.

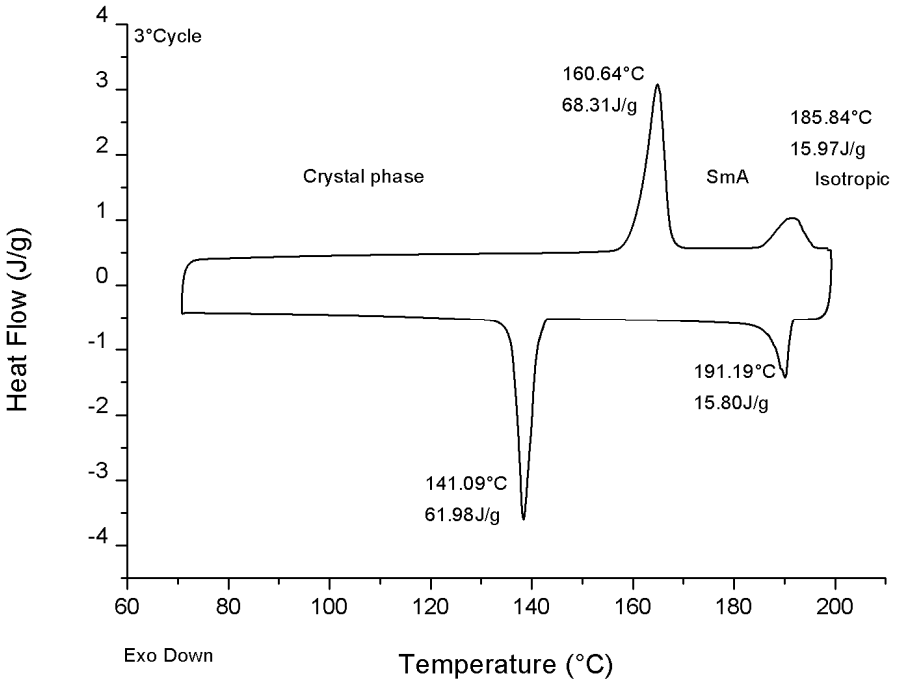

S 62. DSC thermogram for compound **9e**.

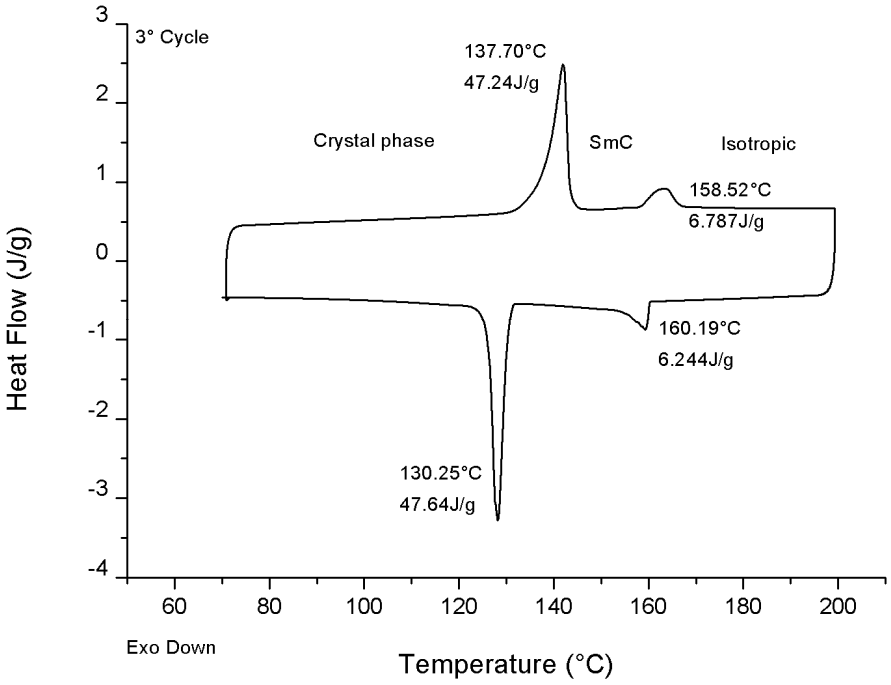

S 63. DSC thermogram for compound **9f**.

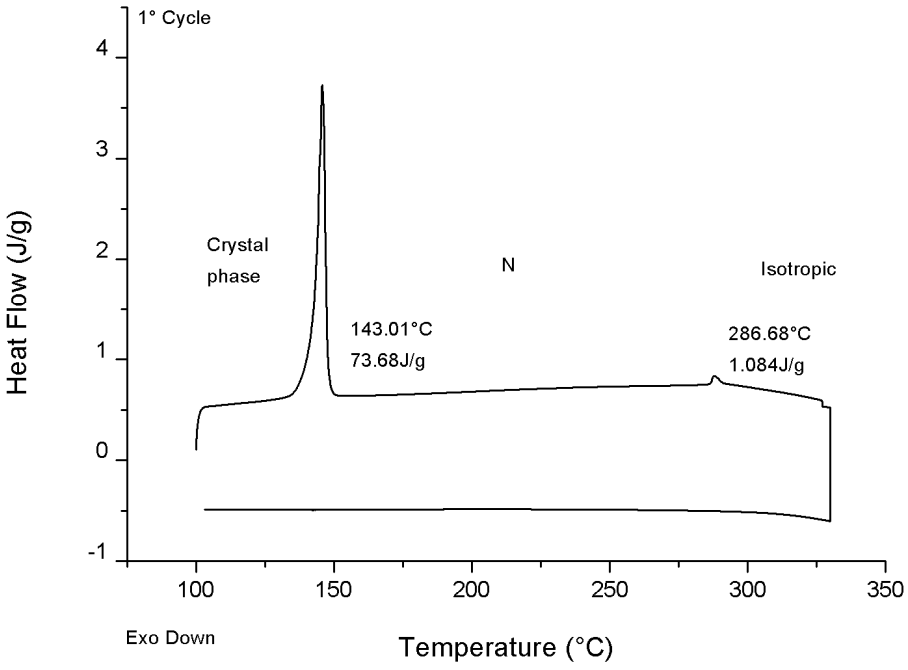

S 64. DSC thermogram for compound **10a**.

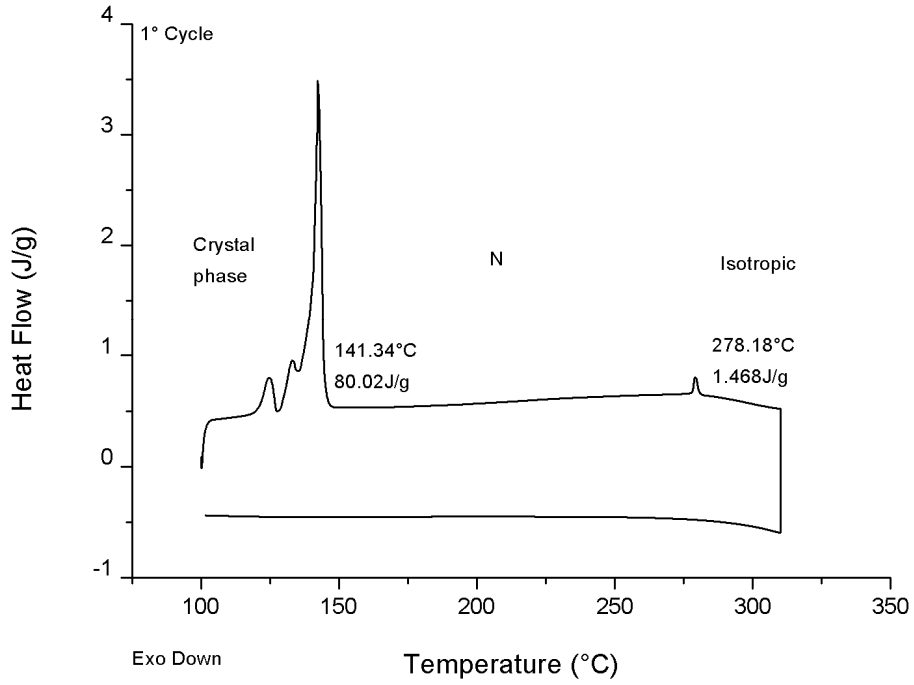

S 65. DSC thermogram for compound **10b**.

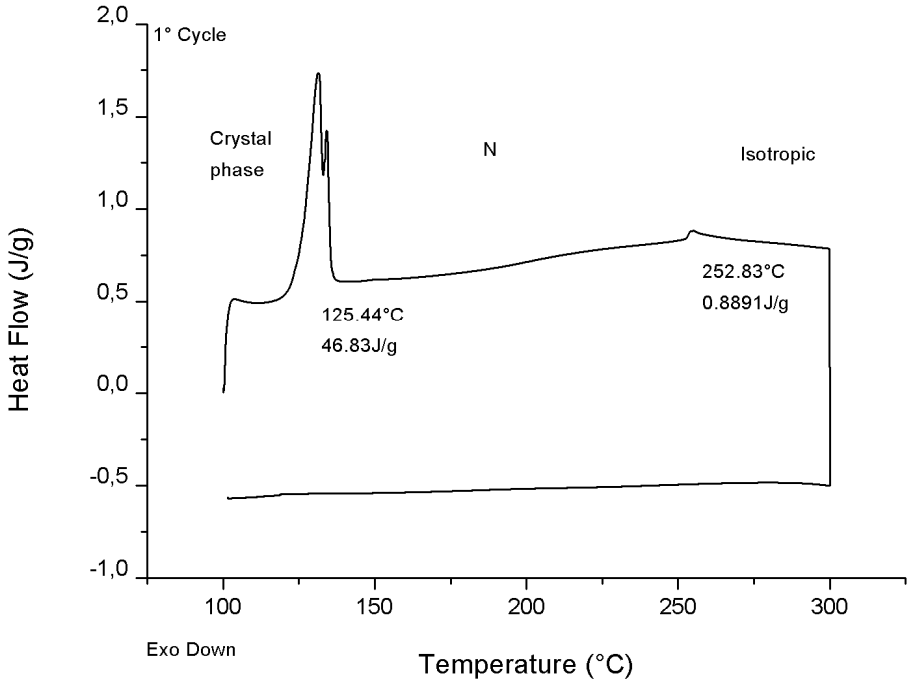

S 66. DSC thermogram for compound **10c**.

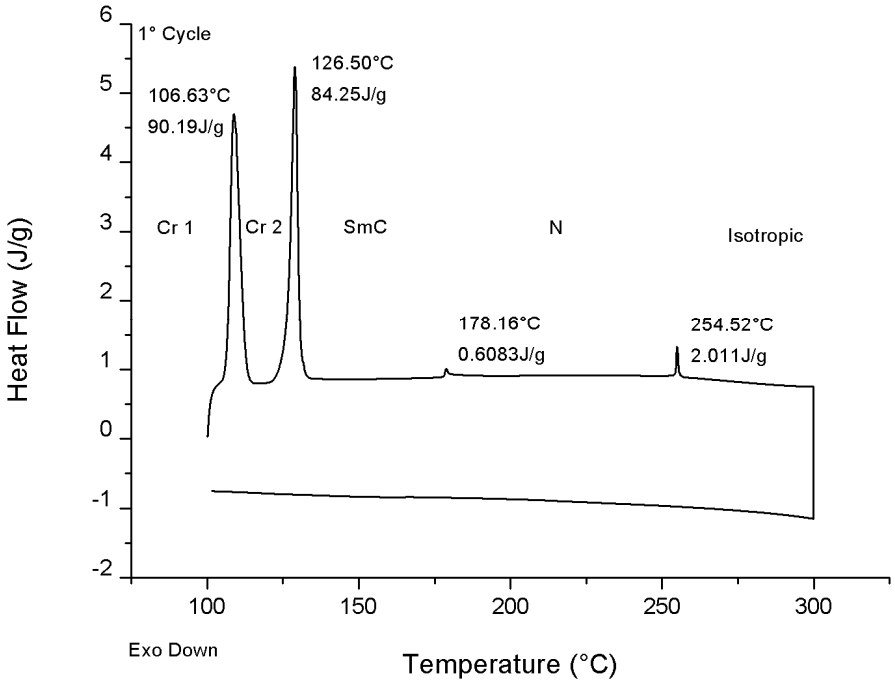

S 67. DSC thermogram for compound **10d**.

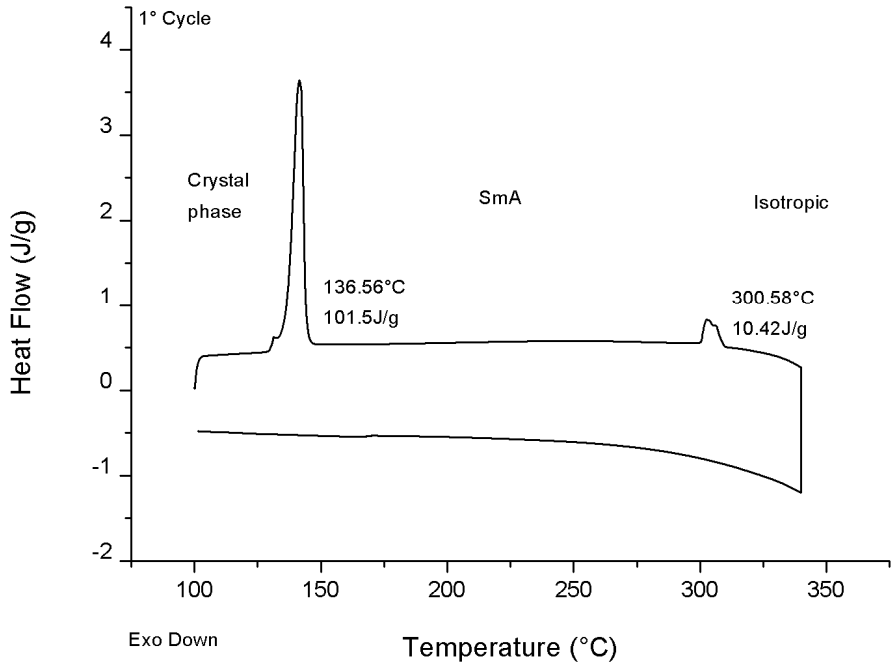

S 68. DSC thermogram for compound **10e**.

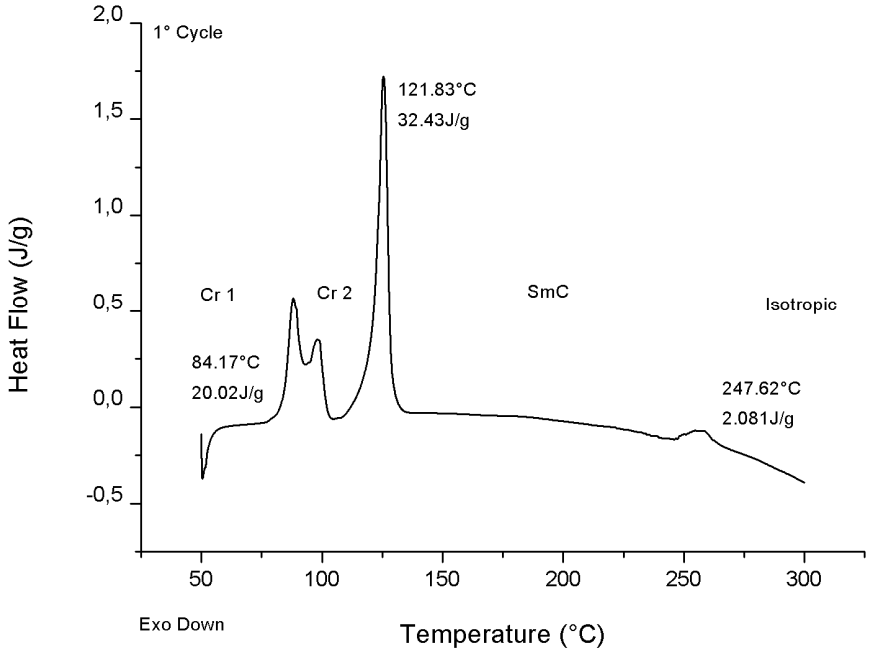

S 69. DSC thermogram for compound **10f**.

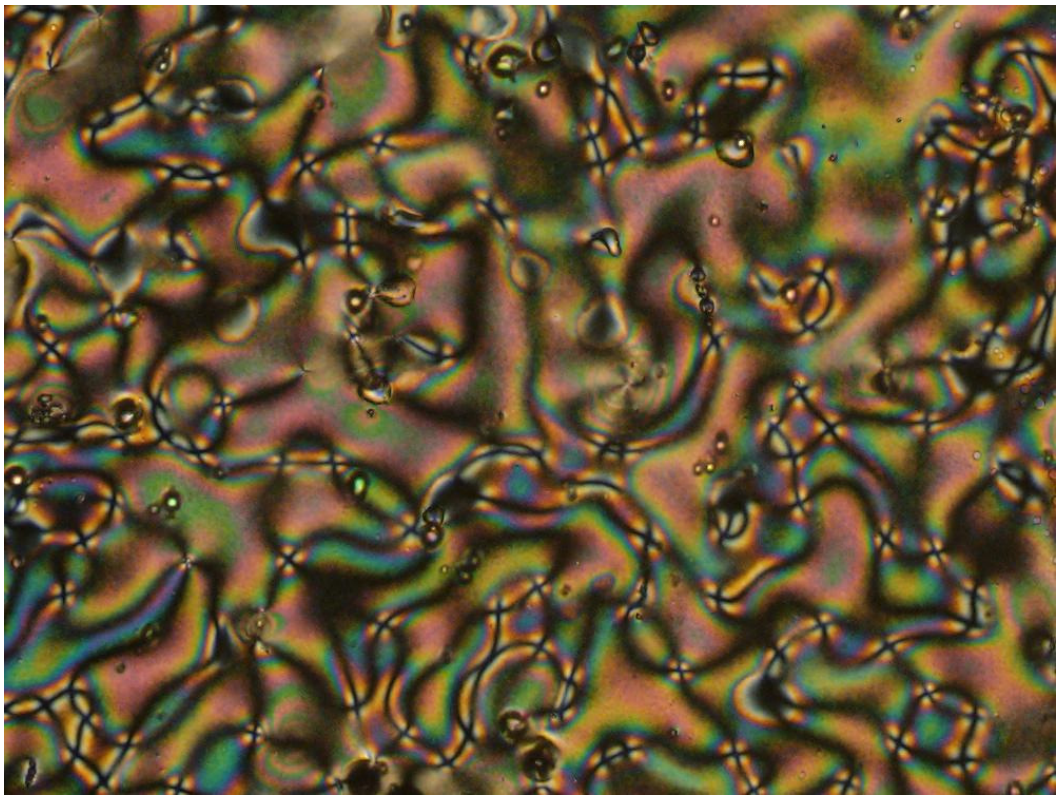

S70. Schlieren texture (4-point singularity) for nematic mesophase by POM upon cooling of **9b** at 154◦C.

S71. SmA mesophase (Homeotropic texture) by POM upon cooling of **9b** at 123 ◦C.

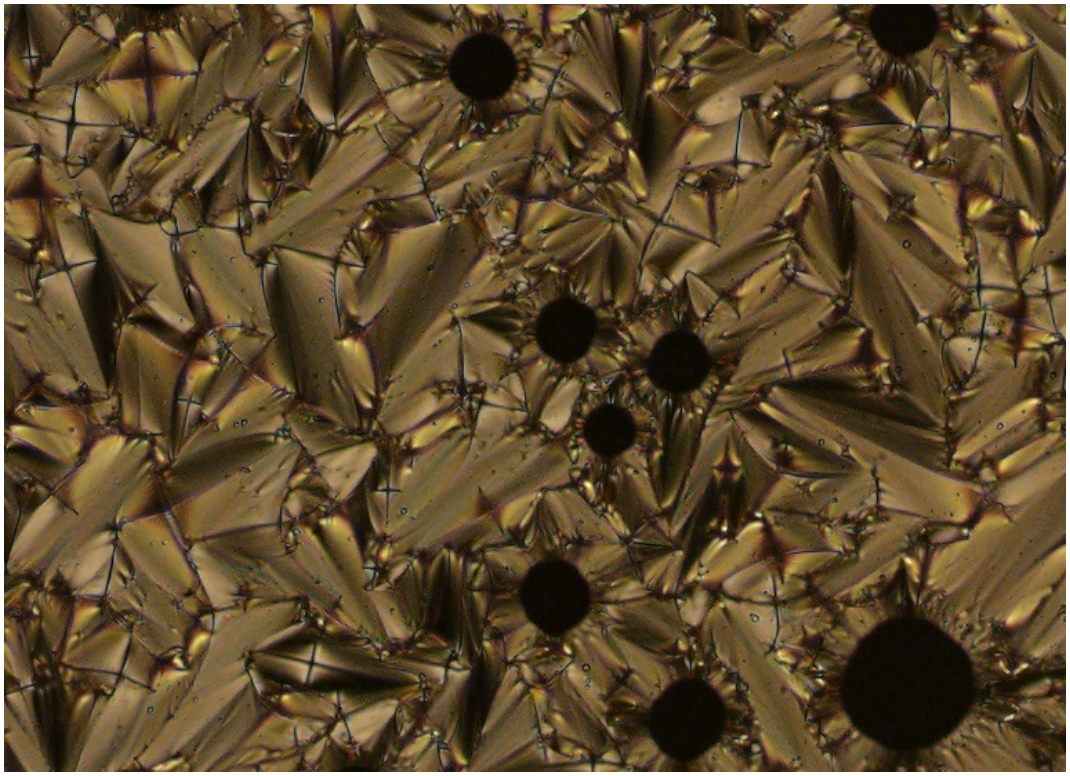

S72. SmA mesophase (focal conic fan-shaped texture) by POM upon cooling of **9d** at 123 ◦C.

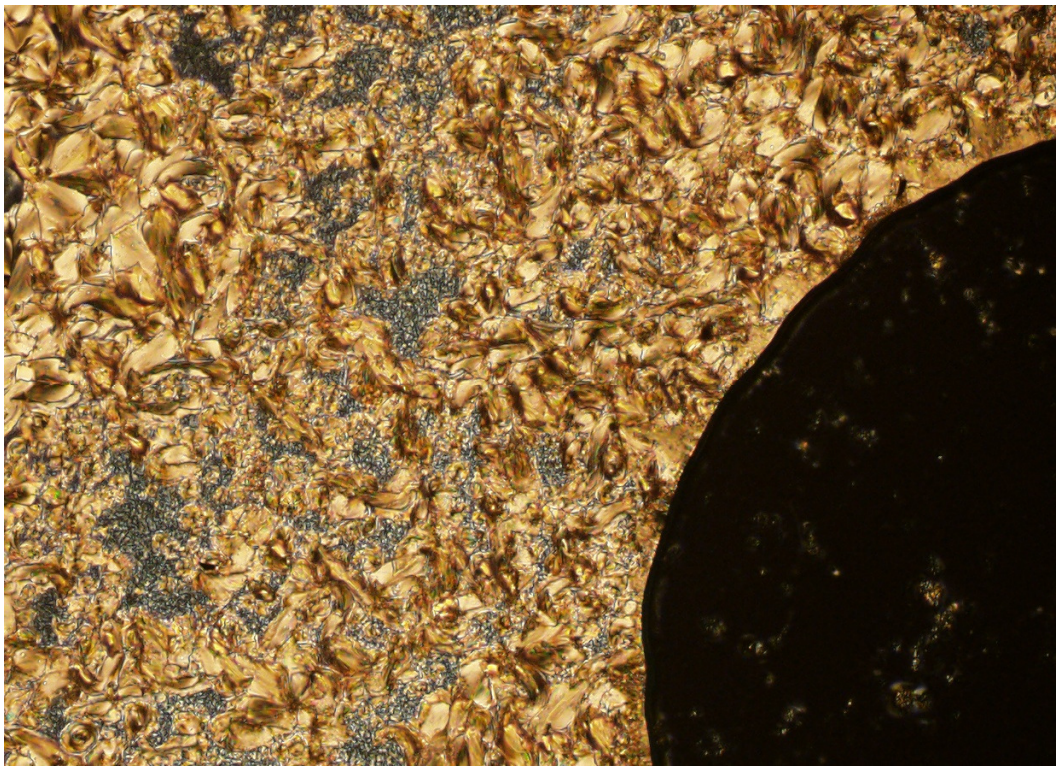

S73. SmC mesophase (broken focal conic texture+Schlieren texture-gray color) by POM upon cooling of **9f** at 157 ◦C.

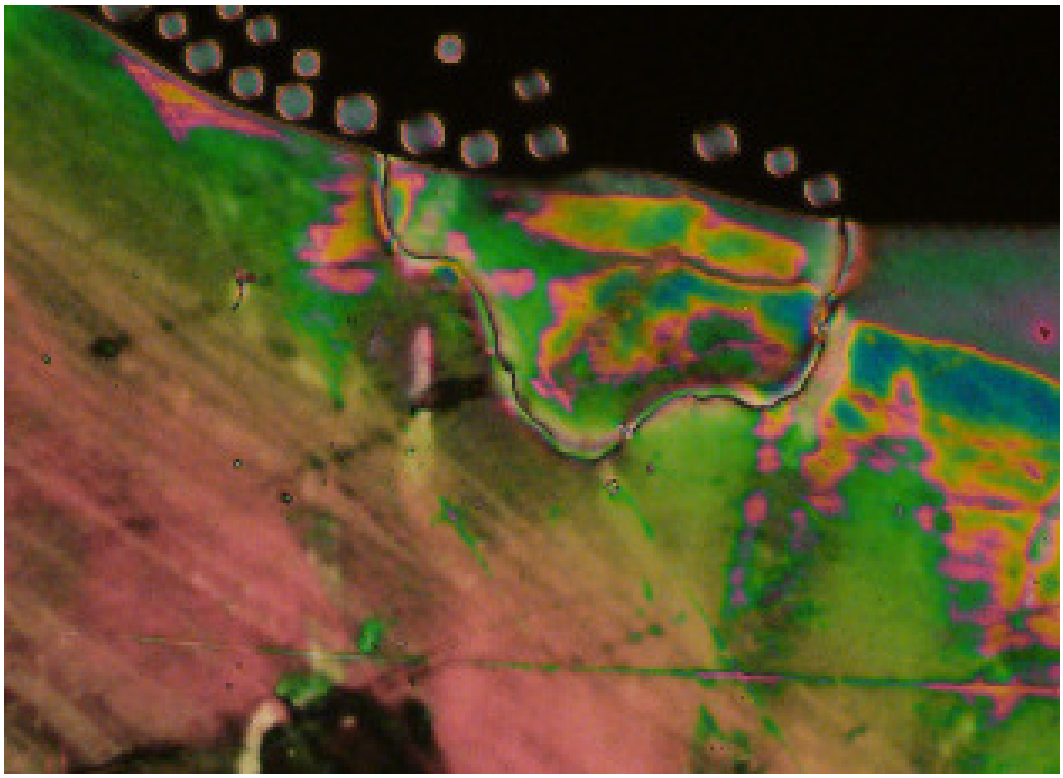

S74. Nematic mesophase texture by POM upon cooling of **10c** at 252 ◦C.

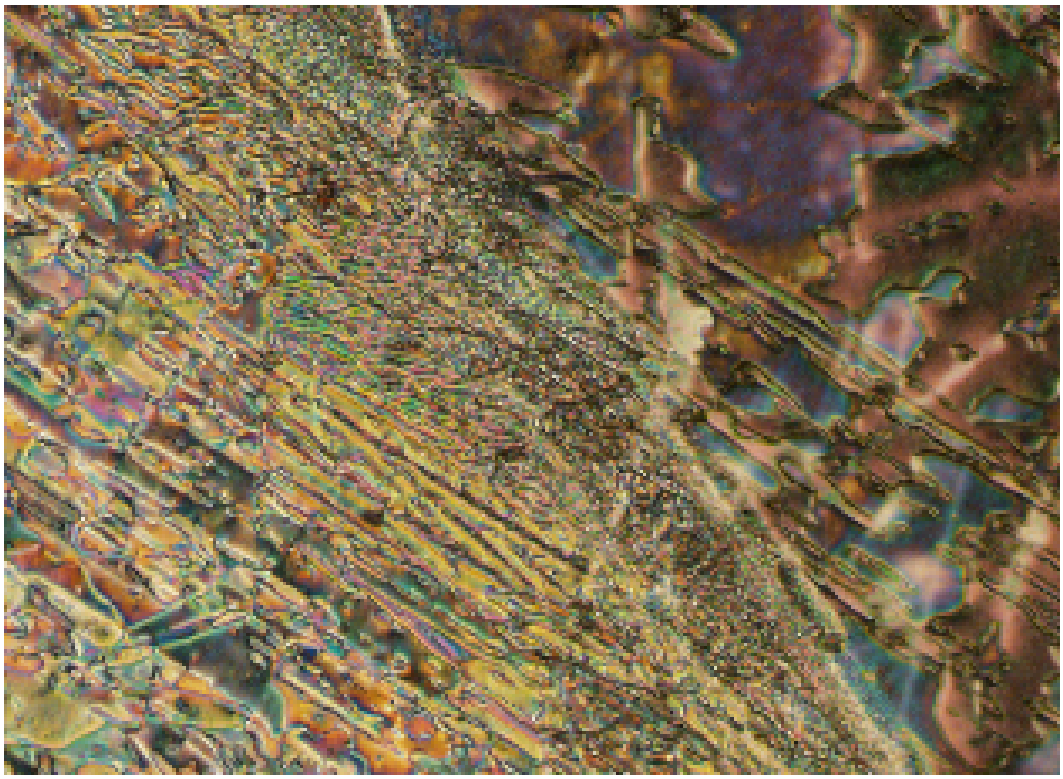

S75. Transition between nematic and SmC mesophase by POM upon cooling of **10c** at 140 ◦C.

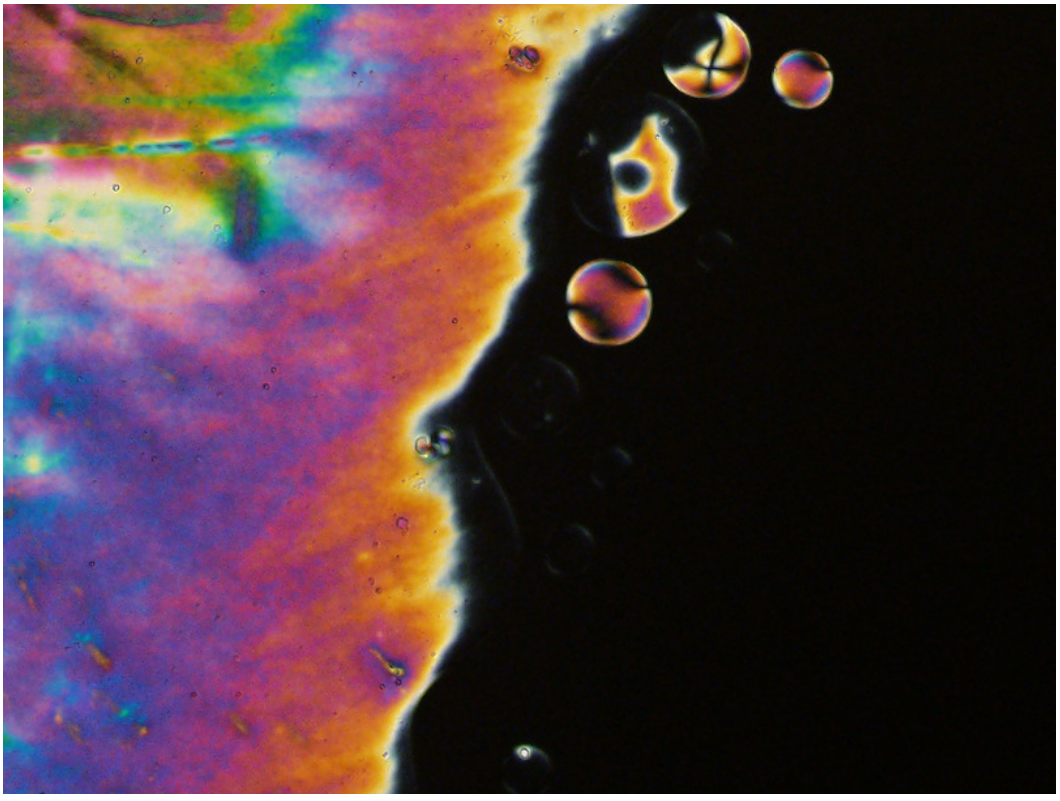

S76. Nematic mesophase texture by POM upon cooling of **10d** at 254 ◦C.

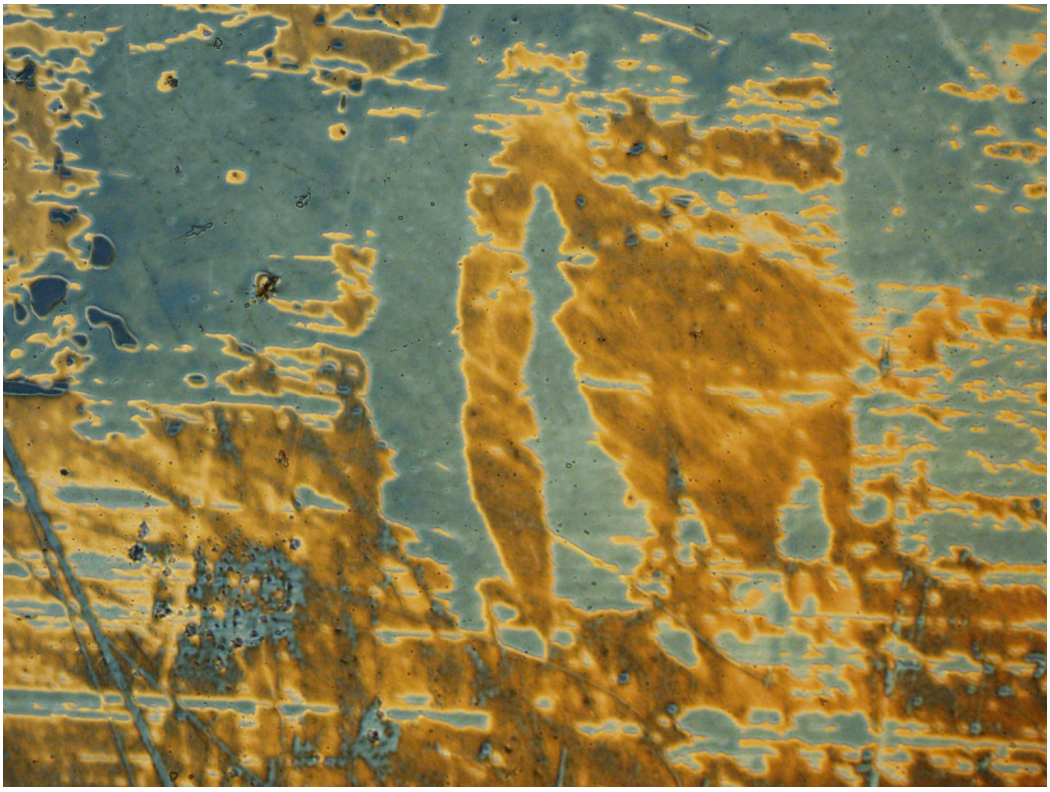

S77. SmC mesophase (marble texture) by POM upon cooling of **10d** at 175 ◦C.

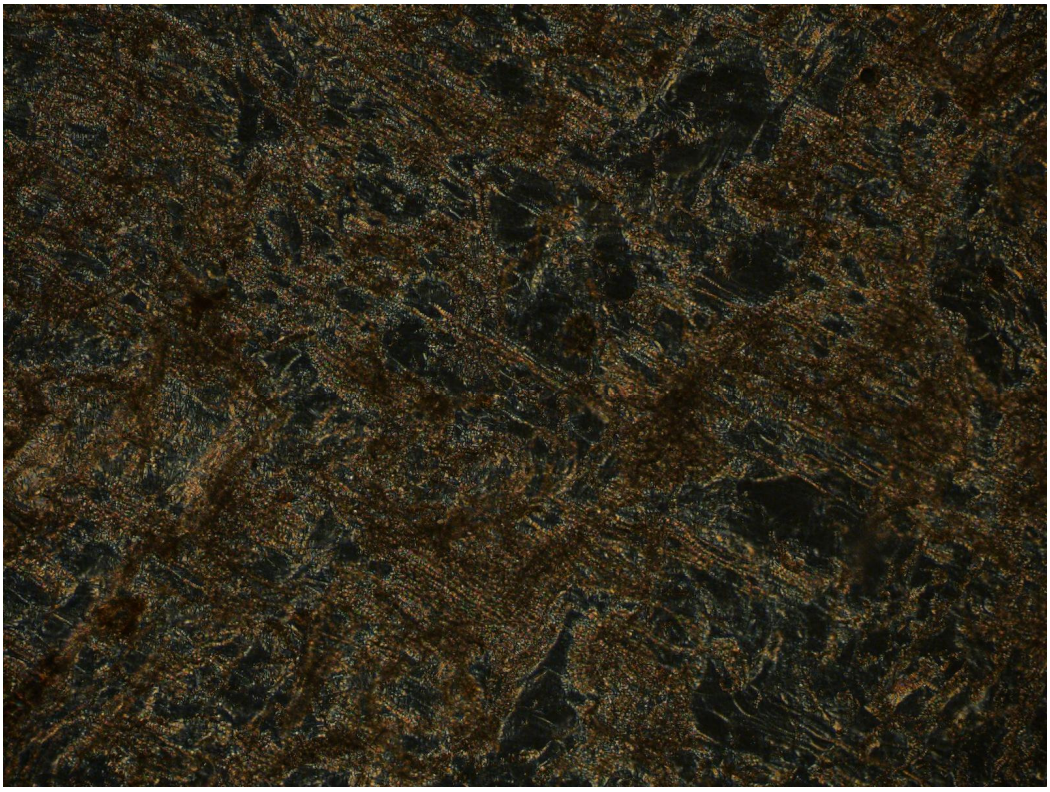

S78. SmA mesophase (fan-shaped/homeotropic texture) by POM upon heating of **10e** at 250 °C